THE MORPHOLOGY AND ABSOLUTE DIAMETERS OF GALAXIES

by

DAVID LAZAR BLOCK, M.Sc.

A thesis submitted to the
Department of Astronomy
University of Cape Town
for the degree of
Doctor of Philosophy

The original work contained in this thesis is that of the candidate alone, except where otherwise specifically indicated.

Signed by candidate

Signature removed

ABSTRACT

This is the first time to the author's knowledge that a catalogue of galaxy photographs has been prepared on a *uniform physical scale*. Of the many interesting aspects which result from such an investigation, we mention here the fundamentally new appreciation both of the diversity of spiral arm texture, and in the range of the intrinsic diameters of galaxies, particularly the spirals.

Small, high surface brightness spiral galaxies form an important subgroup; these present a saturated or predominantly saturated image on the SRC IIIa-J Survey. An intercomparison of their appearance on the J-film copies and those of the "Quick Blue" Survey shows an inner morphology often indicative of substantial differential rotation effects.

One of our galaxies in the sample shows significant signs of warping; the spiral has no bright, close companions.

Also of note are faint, featureless outer envelopes in some of the spirals, and galaxies with faint outer spiral arms whose pitch angles are significantly different from those of the central inner region.

Further results are discussed in chapter 3 onwards.

A by-product of this investigation is the identification of the largest known (type b) barred spiral.

ACKNOWLEDGEMENTS

The idea for the investigation came at the suggestion of my supervisor, Dr. A.P. Fairall. Words cannot describe the assistance and guidance he was always ready to provide, and I do wish to thank him most sincerely for the many stimulating and thought provoking discussions I was privileged to have.

Special thanks are also due to

- the Director of the South African Astronomical Observatory, for the use of the U.K. Schmidt IIIa-J film copies
- Professor G. Tammann, for selflessly devoting many hours of his time in discussions, suggestions, and in viewing the photographs; also for his generosity in placing at my disposal prepublication data from the forthcoming "Revised Shapley Ames Catalogue".
- Dr. V. Rubin for an important preprint relating in part to the intrinsic sizes of galaxies.
- Dr. W.K. Huchtmeier for his prepublication photograph of the HI distribution around M83.
- Dr. M. Tarenghi for a 4-m film copy of NGC 6872.
- Professor G.F.R. Ellis, for enabling me to lecture in the Department of Applied Mathematics whilst concurrently conducting research in the Department of Astronomy.
- Dr. K. Petterson for discussions on spiral structure.
- Dr. L.A. Balona for his invaluable assistance at the computer.
- Mr. C. Fowle, and Mr. C. Tomlinson, for their work in "seeing the thesis to press".

and last, but by no means least, Penny Dobbie for her unusual skill in typing the manuscript.

TABLE OF CONTENTS

Page

A. CHAPTER ONE

INTRODUCTION 1

CHAPTER TWO

UNCERTAINTIES IN THE DETERMINATION OF THE INTRINSIC DIAMETERS OF GALAXIES 8

2.1 The Value of the Hubble constant 8

2.2 Inclination effects on the diameters and optical luminosities of galaxies 22

2.3 Foreground Galactic Extinction 24

2.4 Velocities used in preparing the photographs . 25

CHAPTER THREE

THE LINEAR DIAMETERS OF GALAXIES AS A FUNCTION OF VARIOUS PARAMETERS 28

3.1 Absolute magnitude and Surface Brightness 28

3.2 Luminosity Class 35

3.3 Hubble Type 51

3.4 Maximum Rotational Velocity 52

3.5 Pitch angle, and Winding Angle 53

B. PHOTOGRAPHING GALAXIES ON A UNIFORM LINEAR SCALE: A SELECTION FROM THE U.K. Schmidt IIIa-J Survey

CHAPTER FOUR

Preparation of the Photographs 60

CHAPTER FIVE

THE SPIRALS: TYPES c to O/a 63

5.1 The type bc, c Spirals 65

5.1.1 Saturated Images on IIIa-J Survey 66

5.1.2 Massive Arms 70

5.1.3 Medium Arms 72

5.1.4 Weak Arms 74

5.1.5 Type bc, c Galaxies with two distinct spiral components 76

5.2 Spirals of type ab, b 95

5.2.1 Saturated Images on IIIa-J Survey 96

5.2.2 Massive Arms 99

5.2.3 Medium Arms 100

5.2.4 Weak Arms 102

5.2.5 Edge-On 103

5.2.6 Some Individual Cases 113

5.3 The type O/a, a Spirals 118

CHAPTER SIX

GALAXIES OF TYPE cd AND LATER 124

6.1 Type cd, d

6.1.1 Saturated Image 124

6.1.2 Massive Arms 125

6.1.3 Medium Arms 125

6.1.4 Weak Arms 126

6.2 Type Magellanic 127

CHAPTER SEVEN

THE ELLIPTICALS AND LENTICULARS

7.1 The Ellipticals 134

7.2 The Lenticulars 139

CHAPTER EIGHT

8.1 Gravitationally Interacting Systems 143

8.2 Galaxies with Uncertain Classifications/ No RC2 Classification 150

8.3 Galaxies with a high surface brightness disk and faint outer spiral arms 156

8.4 Two Southern Galaxies with predominant, elliptically shaped nuclei 161

C. OTHER SELECTED SAMPLES ON A UNIFORM LINEAR SCALE

CHAPTER NINE

ScI GALAXIES FROM THE PALOMAR OBSERVATORY SKY SURVEY 163

CHAPTER TEN

A MONTAGE OF IIIa-J AND "QUICK BLUE" SURVEY PHOTOGRAPHS 175

CHAPTER ELEVEN

MISCELLANIA

11.1 The Danver Spirals: A Comparison 185

11.2 A Montage of Some Well Known Galaxies 185

11.3 Galaxies from the Fairall Survey 190

D. AN OVERVIEW

CHAPTER TWELVE

CONCLUSIONS 195

E. REFERENCES 211

TABLES

Table 1
Fundamental calibrators in the Local Group, and the NGC 2403 - M81 Group 12

Table 2
Galaxies with a small range in intrinsic diameter but a large range in absolute magnitude 32

Table 3
Type c, Luminosity Class I, I-II Spirals from the "Revised Shapley Ames Catalogue" 37

Table 4
Type c, Luminosity Class III Spirals from the "Revised Shapley Ames Catalogue" 43

Table 5
Type Sc, SBc Spirals from Danver, with measured Pitch Angles, and Winding Angles 56

Table 6
List of Southern Galaxies Photographed from Film Copies of the U.K. Schmidt IIIa-J Survey, I 203

Table 7
List of Southern Galaxies Photographed from Film Copies of the U.K. Schmidt IIIa-J Survey, II 208

Table 8
Danver Spirals, with known Apparent Magnitudes and Distance Moduli (or v_o) 209

CHAPTER ONE

INTRODUCTION

It is curious to find that one of the most fundamental questions one may ask in extragalactic astronomy has met with surprising neglect. The question is simply:

"What are the ranges in the linear diameters of spiral galaxies?"

If one then turns to the standard reference work "Galaxies and the Universe" (published in 1975), one finds only one section of a page dealing with the upper limits.

What has happened is clear, and is well summarised by Baade (1951). Hardly had the extragalactic nature of the spirals been established, and provisional data for a few of the nearest galaxies been obtained, when the first redshift-magnitude diagram appeared, and the direction of inquiry was swung into understanding *the large scale structure of the universe.*

"Thus, it was assumed that the galaxies as a group were sufficiently homogeneous to justify the introduction of a standard model which would permit us to compute the changes in bolometric brightness caused by the redshift... Altogether there are good reasons to believe that solution of the cosmological problem is much more difficult than was thought some 15 years ago".

[Baade (1951)]

Reading through the recent essay by Ellis (1979), one could not agree more with Baade's statement.

Asked of the representative size of a large (Sb) spiral, many an astronomical student today would quote that

of M31. In fact, prior to the detailed work of Sandage and Tammann in "Steps Toward the Hubble constant" (1974a-d, 1975a-b, 1976), this viewpoint was (and sometimes still is) prevalent in the literature; Baade himself once remarked that

"the largest system in the Local Group, and one of the largest in the universe, is the Andromeda spiral".

[Baade (1963)]

For ellipticals, the range is known to be very large. From the dwarf dE class [recognised as such around 1940; c.f. Baade (1944) and Wilson (1955)], one moves to the giant/super-giant cD systems, introduced by Matthews, Morgan and Schmidt (1964) to describe a galaxy with the nucleus of a giant elliptical, surrounded by an extended, slowly decreasing surface brightness envelope. Their measurable extent ranges from about 100 kpc - for NGC 4073 - to over 2 Mpc for the cD galaxy in Abell 1413 (Oemler (1976)), and they constitute by far the largest galaxies known.

In the case of spirals, the range has been thought to be far more restricted, M31 and M101 being considered as typically large spirals within Hubble types b and c. Holmberg (1975) gives the following upper limit for his sample:

E-S0 systems : ~39 kpc (57 kpc)

Sa, Sb galaxies : ~45 kpc (65 kpc)

Sc galaxies : ~37 kpc (54 kpc)

[Holmberg's figures were based on a Hubble constant of H_o = 80 km s^{-1} Mpc^{-1}; the figures in parentheses give the corresponding values for our adopted value of 55 km s^{-1} Mpc^{-1}].

Curiously enough, never before to the author's knowledge has a programme been undertaken with the specific aim

of preparing a large sample of galaxy photographs on a uniform linear or physical scale. All atlases thus far - the magnificent "Hubble Atlas" by Sandage (1961), for example - contain photographs where the emphasis is on overall morphology rather than morphological features on a linear scale; this is natural enough, since the Hubble Atlas shows definitively, by means of the illustrations, the Hubble classification scheme, first proposed by Hubble in 1926. But how far do the diameters of galaxies extend? - moreover, what effect do their sizes have on their overall morphological appearance? Are some intrinsically small spirals contained in a faint surrounding optical envelope, and is this envelope featureless, or are there inherent signs of spiral structure?

Most important, what is the range (on a linear and not angular scale) of spiral arm texture? M33 is a good example where, on an angular scale, the arms appear "massive", yet on a uniform physical scale they are not massive at all. While galaxy diameters can be computed theoretically, *it is only possible to investigate the above question when seeing galaxies "side by side" on a uniform linear scale.*

The ideally suited survey for our purposes from which to photograph galaxies is the U.K. Schmidt IIIa-J Survey, reaching a limiting magnitude of B = 23^m, two magnitudes fainter than either the Palomar Observatory Sky Survey (POSS), or the "Quick Blue" survey of the European Southern Observatory.*

* The U.K. 1.2m (48-inch) Schmidt telescope is, in most respects an exact copy of that at Palomar, but the fainter limiting magnitude is made possible by the use of sensitized IIIa-J emulsion [Cannon (1976), Tritton (1978)]

Each survey plate measures 356 mm x 356 mm, equivalent to a field of view of 6.5 x 6.5 degrees; 606 fields are required for a coverage of the southern sky south of -20°. The number of plates in the ESO B Survey is exactly the same, except that the overlap between fields is less, as each plate measures 300mm x 300 mm.

In comparison, the two-colour [O=blue, E=red] Palomar Observatory Sky Survey contains 935 areas, each 6 x 6 degrees, covering the entire northern sky, and the southern sky down to -30°. [The Whiteoak Extension (in red only) extends further south down to -42°]

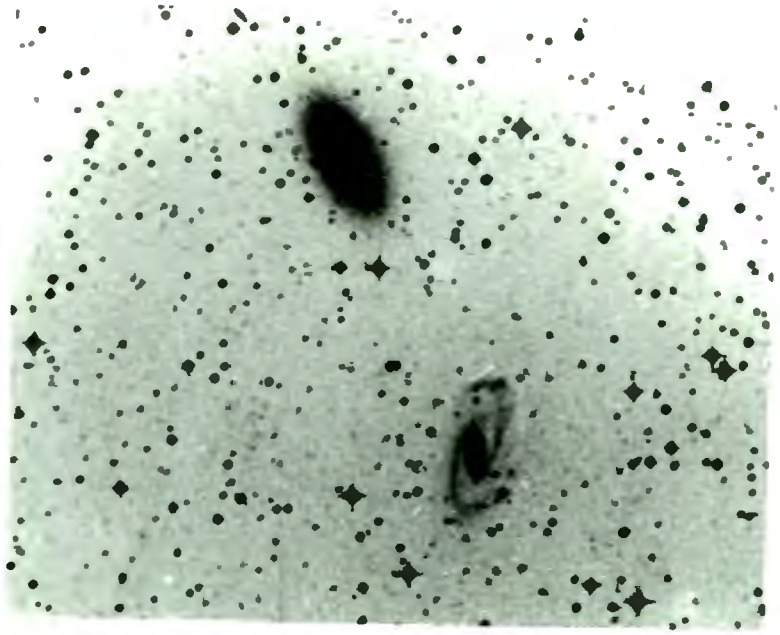

F51 AND NGC 6673—UNIFORM ANGULAR SCALE (ABOVE) AND LINEAR SCALE (BELOW)

UNIFORM LINEAR SCALE

0 10 20 30 40 50 kpc

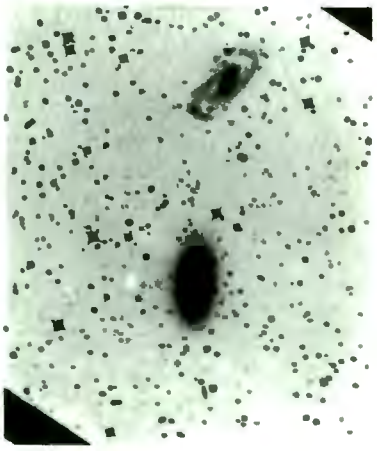

ELLIPTICAL NGC 6673

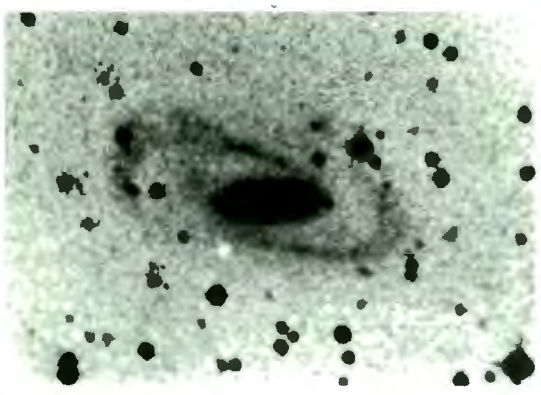

F 51

Plate 1

The limiting surface brightness (for extended objects) on the IIIa-J film copies is ~25.5 - 26.0 B mag arcsec^{-2} (Hawarden (1979)); the plate scale is 67.1 arcsec mm^{-1}.

Photographs from the U.K. Schmidt survey are presented in chapter 5 onwards; in all cases, the degree of enlargement is matched to the galaxy redshift. A Hubble constant of 55 km s^{-1} Mpc^{-1} is assumed throughout.

Thus, a galaxy with a redshift of z = 0.016 is enlarged four times as much as one with a redshift of z = 0.004; the technique is well illustrated in the accompanying plate 1, which is galaxy no. 186 in a paper by Fairall (1979b); without redshift data, one might be under the impression that the photograph represents a physical pair - a large elliptical accompanied by a spiral. However, the elliptical (NGC 6673) has a redshift of z = 0.004, whereas the spiral (F-51; also illustrated by Fairall is a Seyfert galaxy with a redshift of z = 0.014. Printing these on a uniform linear scale clearly shows the spiral to be much larger in physical size.

For this investigation, galaxies were selected primarily from the "Second Reference Catalogue of Bright Galaxies" (RC2; de Vaucouleurs, de Vaucouleurs and Corwin (1976)), with the prerequisites that the galaxies had measured redshifts (those with uncertain velocities, indicated in the RC2 by means of an asterisk, were almost always excluded), and that they were accessible on the preliminary J Survey, or shipments 1-6, these being the available shipments at the time of the investigation. Another particularly valuable source of redshift data were the 719 optical redshifts published by Sandage

(1978). For many of the Danver (1942) spirals, redshifts were kindly communicated to the author by Professor Tammann. Redshifts used in chapter eleven are from the spectroscopic surveys of Fairall (1979a-b).

The galaxies seen from chapter 5 onwards have redshifts in the range $z \in [0.004, 0.030]$. The lower limit was placed to minimize the effect of random motions on the diameters, while the upper one was chosen (rather arbitrarily) to ensure that distant galaxies were not over-enlarged i.e. to still have well defined resolution. Error estimates from the velocities used in printing the photographs are discussed in chapter two.

The vast range in the morphology, surface brightness and linear sizes of galaxies within various Hubble types is remarkable; this is also seen for hitherto assumed "ScI standard candles" used in mapping the global Hubble flow [chapter nine].

Surprisingly, we also find that very large spiral galaxies [such as UGC 2885] are not restricted to be of type c; an outcome of the present program is the identification of the largest known type b galaxy NGC 6872, with a corrected diameter of well over 200 kpc.

Such spirals play an important role in placing constraints on models of galaxy formation; in enormous galaxies like UGC 2885, the outer parts have rotated fewer than ten times in the age of the universe, but "*UGC 2885 is an attractive two-armed spiral with a regular velocity field. This implies that a well ordered global pattern must be established soon after galaxy formation; it cannot be the product of smoothing introduced by many differential rotations*" [Rubin,

Ford and Thonnard (1980)].

On the other end of the scale, we find that several intrinsically small galaxies in our sample show signs of having undergone very differential rotations, a result which ties in well with those rotation curves presented by Rubin, Ford and Thonnard.

Spirals of type c to O/a are discussed in chapter five; galaxies of type cd and later in chapter six, and remaining interesting individual subsections in chapter eight.

CHAPTER TWO

UNCERTAINTIES IN THE DETERMINATION OF THE INTRINSIC DIAMETERS OF GALAXIES

2.1 The value of the Hubble constant

Following the work of Sandage and Tammann cited earlier (1974a-d, 1975a-b, 1976), we assume that the Hubble flow is

(i) linear

(ii) isotropic

and

(iii) characterized by a global value H_o.

Comparative intrinsic diameters can then be evaluated independent of the actual value of the Hubble constant; in the following presentation, we shall assume a value of H_o given by

$$H_o = 55 \text{ km s}^{-1} \text{ Mpc}^{-1};$$

for any other value of H given by $H'_o = h \times 55 \text{ km s}^{-1} \text{ Mpc}^{-1}$, all linear diameters will simply scale according to

$$D_{new} = \frac{D(\text{evaluated with } H_o = 55)}{h}$$

An interesting point to note at this stage is that one does not specifically require a Friedmann-Le Maitre-Robertson-Walker universe in order to obtain a linear form of Hubble's law for $v \ll c$.

The result holds in any cosmological model, as will be briefly discussed below, following the exposition by Ellis (1971); adopting the classical cosmological continuum approach, at each point of space-time, there is a unique vector field u^a representing the average velocity of matter,

which is normalized, so that

$$u_a u^a = -1$$

[summation over repeated Latin indices being implied, from 0 to 3].

Using normalized comoving coordinates, defined so that

$$u^a = \delta^a_o$$

we introduce a 3 + 1 splitting of space-time via the projection tensor

$$h_{ab} = g_{ab} + u_a u_b .$$

h_{ab} then projects any vector A^a into the rest space of an observer moving with 4-velocity u^a.

Splitting the relative position vector (spacelike)

$$\eta^a_\perp = h^a{}_b \eta^b$$

of two neighbouring particles A and B into a magnitude $\delta\ell$ and a direction n_a i.e.

$$u^c n_c = 0$$

with the normalization

$$n_c n^c = 1$$

one obtains

$$\frac{(\delta\ell)^\cdot}{\delta\ell} = \sigma_{ab} n^a n^b + \frac{1}{3}\theta \qquad (2.1)$$

where $\theta = u^a{}_{;a}$, and $\sigma_{ab} = \sigma_{(ab)}$ is the (symmetric) shear tensor determining possible distortion arising in the fluid flow.

The isotropic part of the expansion is determined by θ, (the volume expansion). Also, we may define a representative length ℓ by the equation

$$\frac{\dot{\ell}}{\ell} = \frac{1}{3}\theta \qquad (2.2)$$

In a Friedmann-Le Maitre-Robertson-Walker (FRW) universe, the shear is zero

$$\sigma_{ab} = 0 \qquad (2.3)$$

and furthermore, $\ell(t) = R(t)$, so that (2.1) yields, upon using (2.2) and (2.3),

$$\frac{(\delta\ell)^{\cdot}}{\delta\ell} = \frac{\dot{R}}{R}$$

- the usual linear (and isotropic) form of Hubble's law in a FRW universe.

To summarise, we see that while a necessary consequence of a FRW universe model is a linear Hubble law (also Block (1974), equation (1.8)), the converse does not necessarily follow: one does not need a homogeneous and isotropic matter and energy distribution (i.e. a FRW universe) to obtain a linear Hubble relationship.

Alternatives to the FRW universe models are discussed by Ellis, in his essay "The Homogeneity of the Universe" (Ellis (1979)).

A priori, if one had no means of determining extragalactic distances, one would impose two conditions on the extragalactic distance scale:

(i) that our Galaxy, and M31, should not be excessively large when compared to other spirals

(ii) that the Hubble constant obtained would accommodate all available age determinations*; [in realistic FRW

---

* The oldest objects in our Galaxy are the globular clusters, with the metal poor ones having ages of the order of $14 - 16 \times 10^9$ years (Demarque and McClure (1977)); determinations of the age of the universe from radioactive elements based on the Rhodium-Osmium chronometer yield lower limits of $11 - 18 \times 10^9$ years (Hainebach and Schramm (1976)).

models, with the deceleration parameter $q_o > 0$ and the usual energy conditions

$$\mu + p > 0$$

and

$$\mu + 3p > 0,$$

the upper limit is H_o^{-1} years (c.f. Ellis (1971)].

The first condition (i) places upper and lower limits on H_o; if the value is too high, our Galaxy will dominate the sizes of Sb spiral galaxies, while if it is too low, our Galaxy and M31 will be dwarfed by other Sb spirals. Tammann (1976) finds these limits to be

$$40 \leq H_o \leq 75 \text{ km s}^{-1} \text{ Mpc}^{-1},$$

with a "best" value of $H_o = 60 \pm 15$ km s^{-1} Mpc^{-1}.

These values are of course obtained without recourse to an accurate calibration of the extragalactic distance scale, to which we now turn.

Table 1 lists the 11 fundamental calibrators in the Local Group, and the NGC 2403 - M81 group, whose distances are known from Cepheids (the actual number of galaxies whose distances are known from Cepheids is 13, but we exclude M31 and M81 on account of their early Hubble types).

One immediately notes from the diameters of the 11 calibrators* that dwarf and extreme dwarf systems are over-represented; *"great care has to be applied to avoid the ensuing falsification of the distance scale. A direct comparison between the distance indicators nearby and those far out*

---

* A point we do wish to mention here is that not all galaxies with, for example, luminosity class V (i.e. "dwarf" galaxies) are in fact intrinsically small: two good examples are DDO 28 and DDO 29 - both type V - but with (Holmberg) diameters of the order of 40 kpc (Fisher and Tully (1975); Table 1).

Table 1

Fundamental Calibrators in the Local Group, and the NGC 2403 - M81 Group

Galaxy (1)	$(m-M)^{o}$ (2)	r(Mpc) (3)	log D_{25} (4)	D_{25} (kpc) (5)
LMC	18.59	0.052	3.81	9.74
SMC	19.27	0.071	3.45	5.80
M33	24.56	0.817	2.79	14.61
NGC 6822	23.95	0.616	2.01	1.83
IC 1613	24.43	0.769	2.08	2.68
NGC 2403	27.56	3.25	2.25	16.76
NGC 2366	27.56	3.25	1.88	7.15
NGC 4236	27.56	3.25	2.27	17.55
IC 2574	27.56	3.25	2.09	11.60
Ho II	27.56	3.25	1.88	7.15
Ho I	27.56	3.25	1.55	3.34

Notes to Table 1:

The corrected distance moduli $(m-M)^{o}$ for the calibrators - listed in col. 2 - are from Sandage and Tammann (1974a: table 2). The logarithm of the apparent major diameters (in 0!1) - to a limiting isophote of 25 mag arcsec^{-2} - are from the RC2 (1976); using these apparent diameters and the distances in col. 3, we compute the linear diameter (in kpc) for each calibrator in col. 5.

would require a comparison of incomparable quantities" *(Tammann (1976))*.

Tammann illustrates this by noting that if the HII regions of IC 1613 were compared to those of M101 (with a diameter over 50 kpc), the latter would have a distance underestimated by a factor of ten.

In their "Steps toward the Hubble constant", Sandage and Tammann used the above 11 galaxies to calibrate the brightest blue ($B-V < 0^m.4$) and red ($B-V > 2^m.0$) stars and largest HII regions. They found the linear dimensions of the HII regions to increase steeply with the luminosity of the parent galaxy (fig. 9 in ST 1974a); two galaxies with the same angular size for their HII regions would not, in general, lie at the same distance.

[In this regard, it is interesting to note that Arp (1973), in discussing Stephan's Quintet, makes the remark that

"There the identical size and appearance of the HII regions in two of the component galaxies, NGC 7320 and NGC 7318, show that from this criterion they must be at the same distance".

Not a valid argument!]

To circumvent the above difficulty, the linear diameter (in parsecs) of the mean core plus halo diameters of the first three largest HII regions $\langle D_H, D_C \rangle_3$ were calibrated with the luminosity class of the parent galaxy.

Using the Local Group and the M81-NGC 2403 group data, Sandage and Tammann obtained their calibration equation:

$$\langle D_H, D_C \rangle_3 = -96.5(\pm 14.4) L_C + 557(\pm 60)$$

$$\sigma(\Delta D/D) = 0.24 \qquad (2.4)$$

Since the fundamental calibrators only span the lower range of luminosity classes, the diameter calibration had to be extrapolated by 1.5 luminosity classes from M33 (II-III) to luminosity class I. Using M101 and its five companions NGC 5204, NGC 5474, NGC 5477, NGC 5585 and Ho IV enables a fit of the latter to the local calibrators as well as automatically extending the calibration to luminosity class I; the point is whether the extrapolation is linear or not. If it is linear, then at a distance of 7.2Mpc*, M101 has abnormally large values for its first three largest HII regions†; Sandage and Tammann justify this on the independent grounds *"that M101's HII regions do appear more conspicuous than the HII regions in other comparable galaxies - this is especially true of the outlying region NGC 5471 which has been catalogued as a separate galaxy on many occasions"*.

Kennicutt (1979) has argued that the HII region diameters of M101 are not exceptionally large, and that *"one should adopt an HII region calibration which is forced to pass through the one data point [M101] which we have for ScI galaxies"*. His "minimum" calibration is the least squares fit to the Local Group and M81 group [analogous to the work of Sandage and Tammann (1974a)], whereas Kennicutt's

---

* In paper III (Sandage and Tammann (1974c)) a major effort was made to determine the distance to the M101 group, which they found to be 7.2 ± 1 Mpc, or $(m-M)^{\circ} = 29.3 \pm 0.3$.

† At the above distance to M101, its three largest HII regions give $\langle D_H, D_C \rangle_3 = 575$ pc, whereas from (2.4) for a type I galaxy the calibration extrapolates to $\langle D_H, D_C \rangle_3 = 460$ pc.

"maximum" calibration (c.f. fig. 5 of his paper) is the one forced to pass through M101 at the luminosity class I end, and the Ir V galaxies at the other end. His "best" regression fit lies somewhere in between, representing a least squares solution to the Local Group and M81 group and M101 group.

That 7.2 Mpc is an upper limit to the distance of M101 is discussed in a paper by Capaccioli and Fasano (1980).

Adopting the Sandage Tammann (ST) calibration (2.4), distances to 39 late-type (Sc-Sd-Sm-Ir) field galaxies were determined from the sizes of their HII regions (ST 1974d); thus

$$r(pc) = \frac{206265 \langle D_H, D_C \rangle_3}{\langle \theta_H, \theta_C \rangle_3} \qquad (2.5)$$

Combining the derived distances* with the galaxies apparent magnitudes yielded their absolute magnitudes, and hence a calibration of luminosity classes in terms of absolute magnitude; the shape of the $M_{pg}^{o,i}$ versus L_c plot being shown in fig. 5 of Sandage and Tammann (1974d).

Adopting $M_{pg}^{o,i} = -21.25$† for ScI, these galaxies were used to map the Hubble flow beyond any possible local velocity anomaly. From an unbiased distance-limited sample, a value for H_o of 56.9 $\pm$ 3.4 km s^{-1} Mpc^{-1} was obtained (Sandage

---

* In view of the large range in diameters within, for example, the Sc I group (Chapter 3.2), distances derived from luminosity classes in this way must be treated with caution. For example, NGC 5236 = M83 is one of the smaller type I spirals, and one might therefore expect that its HII regions are intrinsically not as large as in a bigger parent type I galaxy - i.e. that the representative $\langle D_H, D_C \rangle_3$ = 460 pc for ScI's is in this case an overestimate, resulting in a distance to M83 which is too large. In ST (1974d), the distance computed to M83 using (2.5) is 8.9 Mpc, compared to Tammann's (1977) estimation of ~6.5 Mpc to the NGC 5128 group.

† The large scatter in absolute magnitude, surface brightness and diameter within every luminosity class (as discussed in Chapter 3) necessitates a reconsideration of this result; a preliminary analysis (Tammann, Sandage and Yahil (1979c)) shows that as far as the distance scale is concerned, their result on the velocity field will still be valid.

and Tammann, paper VI, 1975b).

The point here is that if a magnitude limited sample - obtained by working to the limiting threshold of the telescope - is used to find the Hubble constant, the discrimination against intrinsically fainter objects can become very severe. In an apparent magnitude limited sample, the bias - if the luminosity function of the galaxies has a finite width - is in favour of those intrinsically bright galaxies drawn from the high luminosity end of the distribution, which, even though at large distances, still fall within the apparent magnitude limit of the sample.

In contrast, a distance-limited sample reflects the relative frequency of objects of a given class of all different luminosities - provided it is sufficiently large and still complete for the faintest objects - and hence also their true mean absolute magnitude $\bar{M}$.

Accordingly, the Malmquist bias (Eddington (1914), Malmquist (1920)) has to be considered; under idealized conditions*, the mean absolute magnitude $\bar{M}'$ of the magnitude limited sample is $1.38\sigma^2$ brighter than the mean absolute magnitude $\bar{M}$ of the distance-limited sample. (Here σ is the standard deviation - signifying the true dispersion in the absolute magnitudes of the objects). Thus, ideally

$$\bar{M}' = \bar{M} - 1.38\sigma^2 .$$

---

* These are that the apparent magnitude sample (e.g. the galaxies contained in the "Revised Shapley-Ames Catalogue", with a catalogue limit of 13.2) be complete - in practice, one introduces a completeness function f(m) (c.f. fig. 6 in Sandage, Tammann and Yahil (1979a)), that the luminosity function be Gaussian, and that the space density be constant.

Distance indicators with large intrinsic dispersion are most vulnerable to the Malmquist effect. As an illustrative example, we might consider the ScI's, which have been used as distance indicators or "standard candles" in the past. With the recently found dispersion of $\sigma(M)\sim 1^m$ (c.f. table 3, chapter 3), neglect of Malmquist bias will incorrectly assume that the most distant objects are of average luminosity (when compared to nearby ScI's), and hence a systematic underestimate of distance will result.

Examples where the distances would be severely underestimated would be NGC 309 and NGC 5230, two distant high luminosity Sc(r)I and Sc(s)I spirals respectively, with absolute magnitudes, corrected for both foreground galactic absorption and inclination, of $M_{B_T}^{o,i} \approx -23.0$ [$H = 55$ km s^{-1} Mpc^{-1}].

As noted earlier, we shall be adopting a linear Hubble flow with a Hubble constant of 55 km s^{-1} Mpc^{-1}; values twice as large have been proposed in the literature.*

The most deviating, independent distance scale from that of Sandage and Tammann is the one by de Vaucouleurs (c.f. de Vaucouleurs and Bollinger (1979)). As tertiary distance indicators, de Vaucouleurs (1979a-b) uses isophotal diameters D_o and total apparent corrected B magnitudes B_T^o.

Defining a composite luminosity index

$$\Lambda_c = (L_c + T)/10 \qquad 0<\Lambda_c<2$$

---

* Apart from claims that the local velocity field is nonlinear, there have also been suggestions by Hawkins (1962) and Segal (1975) that even the global flow is nonlinear (in fact parabolic); Sandage, Tammann and Yahil (1979a) show how such a conclusion can incorrectly be reached, neglecting the observational bias caused by a luminosity function that is broader than is encompassed by the apparent magnitude limit of the sample (in this case, the RSA).

[L_c here is the "corrected luminosity index", and T has the range (for spirals and type Im)

	SO/a	Sa	Sab	Sb	Sbc	Sc	Scd	Sd	Sdm	Sm	Im
T =	0	1	2	3	4	5	6	7	8	9	10]

de Vaucouleurs (1979a) finds that for $|\Lambda_c - 1| \leq 0.65$, his calibrating galaxies satisfy

$$\log D_\ell = a_1 + b_1(\Lambda_c - 1) \qquad (2.6)$$

with

$$\langle a_1 \rangle = 4.18 \pm 0.04$$

$$\langle b_1 \rangle = -0.60 \pm 0.05$$

where D_ℓ is the linear diameter (in parsecs).

If a galaxy of intrinsic diameter D_ℓ subtends an angle D_o at a distance r (in pc), then

$$D_o = \frac{206265 D_\ell}{r}$$

(D_o in seconds of arc), or alternatively,

$$D_\ell = \frac{D_o r}{34377.5}$$

with D_o in tenths of a minute of arc (as in the RC2 (1976)).

The distance modulus of the galaxy

$$\mu \equiv 5 \log \frac{r}{10}$$

is then simply

$$\mu = 5 \log D_\ell - 5 \log D_o + 17.68$$

If instead of D_ℓ, we use the <u>mean</u> diameter as determined by (2.6), so that

$$\mu = 5[4.18 - 0.60(\Lambda_c - 1) - \log D_o] + 17.68 \qquad (2.7)$$

(c.f. equations (5) and (6) in de Vaucouleurs (1979a)), then (2.7) <u>can only hold with a considerable degree of scatter</u>.

In fact, rewriting (2.6) slightly as

$$\log D_\ell = \log D_\ell(1) - 0.60(\Lambda_c - 1)$$

we see that $D_\ell(1)$ is the linear diameter of a galaxy with corrected index $\Lambda_c = 1$, so that using

$$\langle \log D_\ell(1) \rangle = 4.18 \pm 0.04$$

is equivalent to the assumption that all galaxies with $\Lambda_c = 1$ (e.g. type III; c.f. NGC 598, classified in table 1 of de Vaucouleurs (1979a) as type III, has $T = 6$, $L_c = 4$ and hence $\Lambda_c = 1$) have approximately the same intrinsic diameter.

Analogously, he finds with the same constraint $|\Lambda_c - 1| \leq 0.65$

$$M_T^o = c_1 + d_1(\Lambda_c - 1) \qquad (2.8)$$

with

$$\langle c_1 \rangle = -19.15 \pm 0.12$$

$$\langle d_1 \rangle = 3.0 \pm 0.15$$

so that the distance modulus, derived using (2.8), is

$$\mu_o = B_T^o - M_T^o$$

$$= B_T^o(1) + 19.15 \qquad (2.9)$$

where

$$B_T^o(1) \triangleq B_T^o - 3.0(\Lambda_c - 1).$$

Rewriting (2.8) as

$$M_T^o = M_T^o(1) + 3.0(\Lambda_c - 1),$$

the assumption is once again that all galaxies with $\Lambda_c = 1$ (e.g. ScIII) have approximately the same absolute magnitude of -19.15.

In a comparison of the Sandage and Tammann, and de Vaucouleurs distance scales, Tammann, in Tammann, Sandage and Yahil (1979c) computes $M_{B_T}^o$

(i) using B_T^o and $\log v_o$ (for a sample of 328 galaxies as given in de Vaucouleurs (1979b)) and assuming a constant value of $H_o = 50$ km s^{-1} Mpc^{-1}.

(ii) using B_T^o and the distance moduli of the galaxies as derived from the above tertiary distance indicators [(2.7) and (2.9)]. Also computed was $M_{B_T}^o$ for those Shapley-Ames galaxies with $v_o > 5000$ km/s, using (for such velocities) the asymptotic value of $H_o = 90$ km s^{-1} Mpc^{-1}, as proposed by de Vaucouleurs (1979b).

The results are shown in figure 12 of Tammann, Sandage and Yahil (1979c).

In the first instance, plotting the absolute magnitudes (as computed in (i)) against log v_o demonstrates a well defined increase of the maximum luminosity and log v_o, with the upper limit of $M_{B_T}^o$ being well represented by a Schechter type luminosity function (Schechter (1976)).

In the second case (where the absolute magnitudes are computed as prescribed in (ii)), the corresponding plot of absolute magnitude and log v_o shows that with $v_o < 5000$ km s^{-1}, no spiral can exceed the absolute magnitude of NGC 224=M31 by $0^m.4$, while over the entire v_o range, the luminosity function drops off sharply at $M_{B_T}^o \approx -21^m$.

Of the two possibilities - either a well defined luminosity function - or one with a sharp cut-off point, the first is certainly the more plausible. It is evident that in using the above two tertiary distance indicators, one underestimates the luminosity/diameters of the more distant spirals, and the resulting distance moduli have been subject to strong Malmquist bias.

We have discussed the various steps in the calibration of the extragalactic distance scale at considerable length, as it is only with this at hand that accurate inferences of

of the diameters of galaxies can be made.

2.2 Inclination effects on the diameters and optical luminosities of galaxies

The problem of the effects of inclination on the observed magnitudes and diameters of galaxies is well discussed in a paper by Tully (1972); in that investigation, spiral galaxies in the Virgo cluster were plotted in an (apparent magnitude m_{pg}, apparent diameter d_m) plane, using photographic magnitudes m_{pg} and photometric diameters d_m from Holmberg (1958).

The separation between face-on ($b/a > 0.5$) and edge-on ($b/a \leq 0.5$) spirals could be accounted for in essentially two different ways:

(a) either the apparent magnitudes have to be corrected, in the sense that the path length through the disk of a galaxy increases as the ratio of its major to minor axis becomes larger, resulting in a greater degree of intrinsic absorption.

or

(b) the apparent diameters of the edge-on systems are too large, due to the increased path length through the galaxy in the line of sight.

Whichever correction is used will remove the discrepancy between face-on and edge-on systems in the (m_{pg}, d_m) plane; the first correction corresponding to a vertical move upwards for the edge-on systems to brighter apparent magnitudes ($\theta = 90^{\circ}$ for the arrow in fig. 1 of Tully (1972)), while the second corresponds to a move in the horizontal direction parallel to the d_m axis ($\theta = 0^{\circ}$), decreasing the diameters for inclined systems.

If both corrections are applied, the amplitude of each has to be reduced, and it is here where the simultaneous calibration of the two corrections is difficult.

With regard to (a), Holmberg (1958) showed that a correction of the form

$$\Delta m_i = A_i(\sec i - 1) \qquad (2.10)$$

was required to account for intrinsic absorption, the coefficient A_i dependent on galactic type.

For Sc galaxies,

$$A_i = 0.28$$

while for classes Sa and Sb, Holmberg (c.f. table 9) found

$$A_i = 0.43$$

[In (2.10), $i = 0^{\circ}$ for face-on systems; otherwise we would have $\Delta m_i = A_i$ (cosec i - 1)].

Pertaining to (b), Heidmann, Heidmann and de Vaucouleurs (1972) suggest a correction to diameters of the form

$$\log D(0) = \log D - \gamma \log R \qquad (2.11)$$

with $\gamma \approx 0.2$, and where D(0) is the corrected major diameter corresponding to the observed major diameter D; R is the ratio of major to minor diameters.

It is the form (2.11) which is used by de Vaucouleurs, de Vaucouleurs and Corwin (1976) in the "Second Reference Catalogue of Bright Galaxies" - the value of γ used there is 0.235, compared to $\gamma = 0.4$ in the "Reference Catalogue of Bright Galaxies" (de Vaucouleurs and de Vaucouleurs (1964)).

In considering the two corrections (a) and (b), Tully (1972) concluded that if the full internal absorption correction is made as prescribed in (2.10), then there is no evidence that a significant diameter correction has to be made.

Concluding this section, it is appropriate to note that both corrections can be problematic, if the spiral arms of the galaxy do not lie in the same plane (for example, the warped optical plane of NGC 598=M33 - Sandage and Humphreys (1980) - also the distorted HI isovelocity contours of the southern galaxies NGC 300 and NGC 5236=M83 (Lewis (1968)), and the model for M83 comprising concentric rings lying in different planes (Rogstad, Lockhart and Wright (1974); fig. 8).

2.3 Foreground Galactic Extinction

The effect of foreground galactic extinction is responsible for decreasing the (optical) apparent diameters of galaxies at low galactic latitudes, as discussed, for example, by Reiz (1941).

The proper form for this correction is still uncertain; Rubin, Ford and Thonnard (1980) note that the corrections in the RC2 (1976), of the form

$$\log D_o = \log D(0)_{25} + (0.12 - 0.007T)A_B \qquad (2.12)$$

(where A_B is the galactic absorption, in magnitude in the B passband) are adequate for galaxies only with little extinction; instead they adopt

$$\log R^{o,i} = \log R(25) - 0.07 \log a/b - \log (1 - A_B/3.35) \qquad (2.13)$$

as formulated by Burnstein and Heiles (1979).

Their justification for using this form comes from the fact that if (2.13) is used for galaxies at values of low $|b|$, then the radii out to 25 mag arcsec^{-2} lie outside the image detectable on the POSS prints, and beyond the last detected emission knots, which is reasonable.

However, with the smaller RC2 corrections, Rubin, Ford and Thonnard find that the corrected radius often lies within the optical image and is smaller than the radius of the last detected emission - a more unlikely proposition.

2.4 Velocities used in preparing the photographs

In printing the sample of galaxy photographs, heliocentric velocities v were used in all cases, except where otherwise specifically noted, where the then standard correction of

$$\Delta V = 300 \sin(\ell)\cos(b) \text{ km s}^{-1} \qquad (2.14)$$

determined by Humason and Wahlquist (1955) was applied.

[This differs from the new solution by Yahil, Tammann and Sandage (1977):

$$\Delta V = -79\cos(\ell)\cos(b) + 296 \sin(\ell)\cos(b) - 36 \sin(b)$$

which, although close to the conventional value, differs from (2.14) by significant amounts in certain directions; the maximum deviation being

$$\pm 87 \text{ km s}^{-1}$$

in the directions

$$\ell = 3^{\circ}\ , b = 24^{\circ}$$

$$\ell = 183^{\circ}, b = -24^{\circ}$$

and which would be important for very nearby galaxies with small redshifts].

As mentioned in the introduction, our sample comprises galaxies with redshifts in the range

$$z \in [0.004, 0.030]$$

corresponding to recessional velocities of

$1200 \leqslant v \leqslant 9000$ km s^{-1} *

Working with redshifts instead of velocities, (2.14) amounts to a change in redshift of

$$z = 0.001 \sin(\ell)\cos(b)$$

(c.f. Sandage (1975a)), so that, in modulus,

$$|\Delta z| \leqslant 0.001$$

Working to a given isophote, the (major) diameter of a galaxy with specified velocity w km s^{-1} and apparent major diameter α (in minutes of arc) may be computed from [(3.14)]

$$D = 0.29\frac{w\alpha}{H_o} \text{ (kpc)}$$

Using the heliocentric velocities v for the photographs,

$$D \text{ (on original photographs)} = 0.29\frac{v\alpha}{55} \text{ kpc}$$

If the velocities corrected to the centroid of the Local Group were used,

$$D(\text{with } v_o) = 0.29\frac{v_o\alpha}{55} \text{ kpc}$$

Differences in the galaxy diameters will thus scale as v/v_o. For example, suppose a galaxy has an observed heliocentric velocity corresponding to $z = 0.004$, whereas its true velocity corresponds to a redshift of $z = 0.003$ (for nearby galaxies, any random motions can be particularly important). Then the ratio

$$\frac{\text{Printed diameter}}{\text{True diameter}} = \frac{1200}{900}$$

$$= 1.33$$

so that, in this instance, the printed diameter is 33% larger than the actual diameter. (This is the well known result

---

* The lower limit of v can actually be taken as 1050 km s^{-1}, giving $z = 0.0035$, which when rounded off to 3 decimals gives $z = 0.004$. Similarly the upper limit can be increased to 9149 km s^{-1}.

that for nearby galaxies, any velocity errors or random motions can produce a gigantic change in the linear diameter).

Consider now, toward the middle range of our redshift interval, NGC 6872 ($v = 4737$ km $s^{-1} \equiv z = 0.016$, $v_o = 4589$ km $s^{-1} \equiv z = 0.015$). Then

$$\frac{\text{Printed diameter}}{\text{True diameter}} = \frac{4737}{4589}$$

$$= 1.03$$

- the printed diameter is 3% larger than the actual diameter as determined by v_o.

The conclusion is that the percentage errors in diameter scale down rapidly with increasing redshift distance.

Particular care has to be taken for galaxies in gravitationally bound systems, such as the Virgo cluster (chapter eleven). Observed redshifts can fail to be accurate indicators of distance in such cases

(a) due to our infall velocity <u>toward</u> the Virgo cluster, as discussed by Tammann, Sandage and Yahil (1979c, 1980); the infall velocity vector has a magnitude of $\sim$280 km s^{-1} (Tammann (1980))

(b) motions within the cluster itself, amounting to some hundred km s^{-1}.

For the Virgo cluster, all galaxies are printed with

$\langle v_o \rangle = 1100$ km s^{-1}

(ST, paper IV, 1974d).

CHAPTER THREE

THE LINEAR DIAMETERS OF GALAXIES AS A FUNCTION OF VARIOUS PARAMETERS

3.1 Absolute Magnitude and Surface Brightness

The degree of correlation to be expected from any absolute magnitude-diameter relationship necessarily depends on the variation of surface brightness of the galaxies included in the regression analysis.

For example, using Holmberg's (1964) and Liller's (1960, 1966) photometric data of spirals and ellipticals in the Virgo cluster, Heidmann (1967) found that the intrinsic luminosity of a galaxy, L, was related to its linear major diameter D (up to some fixed isophote) by an equation of the form

$$L \propto D^{q} \tag{3.1}$$

where the dependence of q was on galaxy type:

q = 1.9 for ellipticals

q = 2.8 for spirals.*

Heidmann (1969b, 1970) then obtains the distance modulus of a galaxy in terms of its apparent magnitude and apparent diameter:

$$(m-M)_o = \frac{m_{pg}^{o,i}}{1-q/2} + \frac{2.5q}{1-q/2} \log a(0) + K \tag{3.2}$$

---

* Further evidence for the validity of (3.1) [with $q \neq 2$] was found by Heidmann (1969a) using elliptical, SO and SBO galaxies in the Coma cluster; subsequent work by Heidmann, Heidmann and de Vaucouleurs (1972) showed that the best value of q in (3.1) for spirals is

$q = 2.6 \pm 0.1$

Extending his luminosity-diameter relation to the van den Bergh (1966) dwarf galaxies, Heidmann, in Balkowski *et al.* (1974) found (3.1) to be valid over a 9 magnitude range.

In (3.2), $m_{pg}^{o,i}$ is the apparent (photographic) magnitude in the Holmberg (1958) system* [corrected for foreground galactic absorption and inclination], a(O) (in minutes of arc) is the apparent major Holmberg diameter corrected to face-on orientation, and K is a constant (c.f. Heidmann (1969b) equation (2)).

Calibration of K is possible by using spirals in the Local Group and the M81-NGC 2403 Group where the corrected apparent magnitudes, diameters and distance moduli are known. Sandage and Tammann (1974c, p. 239) find a value for K of 86.06 ± 0.77.

The proposition in (3.1) is thus that the linear diameter of a galaxy is a function of only two parameters: its absolute magnitude, and its type (i.e. whether spiral or elliptical).

We show that such a generalization cannot be true by taking as a particular example the well known high surface brightness spiral NGC 5236 = M83, which is intrinsically small [with a diameter of only 20 kpc - based on a distance to the NGC 5128 group, of ~6 Mpc (Tammann (1977)] but nevertheless very bright [its absolute magnitude (in the B_T system of the RC2 (1976)), corrected for internal absorption and foreground galactic extinction, is $\approx -21^m$ - Sandage and Tammann (1980) "Revised Shapley Ames Catalogue" (RSA)†].

---

* The limiting isophote in that analysis is 26.5 mag (pg) per square second of arc.

† Our magnitudes have to be reduced from those of the RSA by 0.21 of a magnitude, since our adopted Hubble constant is $H_o = 55$ km s^{-1} Mpc^{-1}.

The "face-on" diameter of M83 (to a surface brightness of 25 mag arcsec^{-2}) is 10!96 [log D(0) = 2.04 (RC2, 1976)]. In the Holmberg system, log a(0) can be obtained from log D(0) by adding 0.19 to that logarithm (Heidmann, Heidmann and de Vaucouleurs, 1972); thus log a(0) = 2.23, or a(0) = 16!98. We need log a(0) [with a(0) in arcmin] for substitution into (3.2). Hence

For M83: log a(0) = 1.23

Its apparent magnitude is m_{pg} = 8.11*, which we correct for intrinsic absorption using (2.10), with a value for type c spirals in that equation of 0.28; i.e.

$$A^i_{pg} = 0.28\ (\sec i - 1)$$

($i = 0^o$ corresponding to face-on orientation).

Using the formula of Holmberg (1946),

$$\cos^2(i) = 1.042(b/a)^2 - 0.042 \qquad (3.3)$$

we find that for log R = 0.04 as given in RC2, a/b = 1.10†; substituting the inverse of this into the above equation yields an inclination of $i = 24^o.75$.

Hence $A^i_{pg} = 0^m.03$; furthermore, from (3.9), the correction for foreground galactic absorption is $0^m.12$ for $b = 31^o.97$ - thus, $m^{o,i}_{pg} = 7^m.96$.

---

* This is the value used by Sandage and Tammann (1974d, Table 2); the parentheses in that paper indicate that the galaxy was not studied by Holmberg, and so an equivalent magnitude was computed using

$$m_{pg} = B(0) + 0.149(B-V)(0) - 0.22$$

[in the notation of the "Reference Catalogue of Bright Galaxies" (hereafter RC1) by de Vaucouleurs and de Vaucouleurs (1964)]. "*For most galaxy types (B-V)(0) is very close to and for many purposes practically identical with the total or asymptotic colour* $(B-V)_T$". - col. 19 of the RC1.

The value of (B-V)(0) for M83 as listed in the RC1 is 0.72; improved values have recently been published by Talbot, Jensen and Dufour (1979): $(B-V)_T$ = 0.66.

† a = major diameter, b = minor diameter

Substituting the above values for $m_{pg}^{o,i}$ and log a(O) with q = 2.6 in (3.2) yields a distance modulus of M83 exceeding 32^m i.e. beyond the Virgo cluster!

What we have illustrated is how completely falsified distances can be obtained from a diameter-luminosity relationship if proper account is not taken of surface brightness variations.

Another form of the (M,D) relation has been determined by Holmberg (1975):

$$M = -6.00 \log D_H + 7.14 \qquad (3.4)$$

where D_H (in parsecs), is the absolute major diameter in the Holmberg (1958) system to a limiting surface brightness of 26.5 mag arcsec^{-2}, and M is the absolute photographic magnitude.

For M83, we note that the value of a(O) = 16!98 corresponds, at a 6 Mpc distance, to a Holmberg diameter of

$$D_H \text{ (pc)} = 3 \times 10^4,$$

so that the Holmberg absolute magnitude-diameter relation gives an absolute magnitude which is too low by one order of magnitude.

The essential point is that while the correlation between absolute magnitude and diameter found in (3.1) and (3.4) is very high (ρ = -0.97 and -0.96 respectively, where ρ is the correlation coefficient), not all high luminosity galaxies are intrinsically large; they may be small, but have a high surface brightness, such as M83 above, or NGC 6215, as seen in Table 2 on the next page.

Referring to that table within the small interval of 10 $\leq$ D(O) $\leq$ 15 kpc ($\equiv$1.00 $\leq$ log D(O) $\leq$ 1.18 kpc), there is a range in $M_{B_T}^{o,i}$

Table 2

Galaxies with a small range in intrinsic diameter but a large range in absolute magnitude

Galaxy	Type (RSA)	$M_{B_T}^{o,i}$ *	D(O) [kpc]
NGC 2397	Sc(s)III	-19.19	10
NGC 5398	SBc(s)II	-18.95	14
NGC 6215†	Sc(s)I.8	-21.12	14
NGC 1437	Sc(s)II	-20.01	15

of some two magnitudes. Moreover, we see that intrinsically small galaxies need not necessarily have low $M_{B_T}^{o,i}$.

In 1958, Holmberg introduced surface brightness considerations in his classification scheme of galaxies: thus Sc- galaxies (prototypes NGC 5194 and NGC 5457) were those with a "*small, sometimes semistellar nucleus; mean surface brightness about the same as for Sb+; more or less symmetrical, open, and rather pronounced spiral arms; resolution well advanced*" while Sc+ galaxies display "*no prominent nuclear region; mean surface brightness lower than for Sc-; confused, and loosely defined spiral arm system (short arms);*

---

* Here $M_{B_T}^{o,i}$ is the absolute magnitude, corrected for both inclination and foreground galactic absorption, by the precepts in the "Revised Shapley-Ames Catalogue" (RSA). The face-on diameters D(O), in kpc, are computed using the values of D(O) (to a limiting surface brightness of 25 mag arcsec^{-2}) given in the RC2 (1976).

† This spiral is characterized by a very high surface brightness, as is immediately evident on the IIIaJ SRC survey.

high resolution" (Holmberg, 1958, p. 26); examples of type Sc+ being NGC 598=M33 and NGC 2403.

He defined a mean surface brightness by

$$S_o = m^o + 5 \log a \qquad (3.5)$$

where m^o is the integrated photographic magnitude, corrected for galactic absorption (the correction $A_{pg} = 0.25$ (cosec $|b|$ - 1) was applied in his analysis), and a the apparent major diameter - in the Holmberg system - in minutes of arc. Note that S_o here is not corrected for inclination effects.

In terms of absolute magnitude and intrinsic diameter, (3.5) may be written as

$$S_o = M + 5\log D + c, \qquad (3.6)$$

and is a measure of the flux within a circle of apparent angular diameter a corresponding to linear diameter D.

In general,

intrinsic diameter α (corrected absolute magnitude, corrected surface brightness) (3.7)

or, alternatively,

corrected absolute magnitude α (intrinsic diameter, corrected surface brightness) (3.8)

We noted earlier (section 2.2) that the simultaneous calibration for the effects of inclination on the optical luminosity and diameter of galaxies is difficult.*

---

* What one is essentially trying to do is to map from the image plane, with axes apparent magnitude and apparent angle (diameter), to the object plane, with axes intrinsic absolute magnitude, and intrinsic diameter [Ellis (1980)].

Note also that if as in (3.1), $L \propto D^q$,

$$5\log D \propto \frac{-2M}{q}$$

so that from (3.5),

$$\frac{\partial S_o}{\partial M} = 1 - 2/q$$

[equation (9.6) in Heidmann, Heidmann and de Vaucouleurs (1972)].

With $\langle q \rangle = 2.6$

$$\frac{\partial S_o}{\partial M} = 0.23$$

For 36 spirals in the Virgo cluster, Holmberg (1958) obtained the relation

$$M = 2.27\ S_o + \text{constant}$$

implying

$$\frac{\partial S_o}{\partial M} = 0.44$$

i.e. of an increasing surface brightness with increasing absolute magnitude, but carefully noted (c.f. equation (3.6))

"The degree of correlation to be expected between S_o and M apparently depends on the variations in the absolute diameters of the galaxies investigated".

This is well reflected in the very low correlation between absolute magnitude and surface brightness for spirals of a particular luminosity class (e.g. type I, I-II) as discussed in the following section, indicating the large range in intrinsic diameter within that class.

Our principal conclusion in this section is that one can only obtain a tight absolute magnitude - linear diameter correlation (or alternatively, an apparent angular diameter - apparent magnitude correlation) for galaxies having a constant surface brightness.

An example of such a sample would be first-ranked cluster elliptical galaxies; Sandage (1972) finds these galaxies to closely follow the line of constant surface brightness*; in his fig. 3, the solid line has the theoretical slope (c.f. (3.5)) of -5: the data is well fitted by

corrected apparent V magnitude = -5 log (angular diameter) + k,

where the constant k in the diagram has the value of 20.5.

3.2 Luminosity Class

In this section, we present graphs and tabular material illustrating the wide range in

(i) surface brightness

(ii) diameter

and

(iii) absolute magnitude

within a given luminosity class, as classified in the "Revised Shapley-Ames Catalogue" by Sandage and Tammann (1980).†

---

* We refer here to the overall surface brightness being constant for these galaxies; this is of course different to the work of Allen and Shu (1979), who find that the extrapolated central surface brightness of nearly all ellipticals is constant [at 12.0 B mag arcsec^{-2}].

† The luminosity classifications in the RSA are a modification of the precepts of those of van den Bergh (1960a-b), illustrated in the catalogue by photographs which define their system.

The principal standards for Sc I are NGC 5457=M101 and NGC 4321=M100, NGC 598=M33 for Sc II-III, and NGC 2403 for Sc III.

Fractional luminosity classes (Sandage and Dressler (1978)) - such as I.8 for NGC 6215 - indicate that the galaxy can either belong to class I-II or class II; they are not intended to specify that the accuracy of the classification is a tenth of a class.

The spread is indeed remarkable; pertaining to surface brightness considerations, we see below that the spiral NGC 6215 (Sc(s) I.8) has a surface brightness of 21.49 mag arcsec^{-2}, which is 3.74 standard deviations from the mean for type I, I-II systems.

Relating to the diameters, where it has generally been thought that all type I, I-II systems are intrinsically very large, the range is marked: NGC 309 outsizes NGC 5236= M83 by more than four times. The diameter of the former (as computed below) is $\sim$95 kpc, while adopting a distance of $\sim$6 Mpc to the NGC 5128 group (Tammann (1977)) yields a diameter for M83 of 20 kpc.

The range in absolute magnitude within a given class is illustrated in figure 1 of Tammann, Yahil and Sandage (1979b); in their "standard sample" of the RSA ($|b|>30^{\circ}$; and excluding the Fornax cluster and the central 6° of the Virgo region), they find that "*luminosity class I and I-II galaxies of type Sbc and Sc have* $M_{B_T}^{o,i}$ *values that range from -23.2 to at least as faint as -19.5* ($H = 50$ km s^{-1} Mpc^{-1}). *This interval largely overlaps the Sc + Sd + Sm + Im class III - IV galaxies, where* $M_{B_T}^{o,i}$ *varies from -21.4 to -17.3*".

Surface brightness, diameter and absolute magnitude are of course inter-related, as discussed in the preceeding section.

In the following table, we present a representative list of Sc luminosity type I, I-II spirals from data provided by Tammann which is contained in their forthcoming RSA catalogue.

Table 3

Type c, Luminosity Class I, I-II Spirals from the Revised Shapley-Ames Catalogue

	NGC (1)	m (2)	A_B (3)	m^o (4)	log D_{25} (5)	SB (6)	V_o (7)	M^o (8)	D (kpc) (9)
1	157	11.03	0.00	11.03	1.63	23.07	1749	-21.48	39.46
2	214	12.95	0.09	12.86	1.32	23.36	4690	-21.79	51.82
3	237	13.70	0.00	13.70	1.25	23.84	4259*	-20.74	40.06
4	309	12.40	0.00	12.40	1.49	23.74	5786	-22.71	94.57
5	578	11.50	0.00	11.50	1.68	23.79	1675	-20.92	42.40
6	628	9.75	0.05	9.70	2.01	23.64	861	-21.28	46.60
7	877	12.50	0.06	12.44	1.37	23.18	4117	-21.93	51.04
8	895	12.30	0.00	12.30	1.56	23.99	2319	-20.82	44.53
9	908	10.85	0.00	10.85	1.74	23.44	1470	-21.28	42.72
10	1042	11.50	0.00	11.50	1.67	23.74	1360	-20.47	33.64
11	1232	10.50	0.00	10.50	1.89	23.84	1644	-21.88	67.49
12	1337	12.20	0.04	12.16	1.83	25.20	1189	-19.52	42.52
13	1566	10.26	0.06	10.20	1.88	23.49	1178	-21.45	47.26
14	2441	13.00	0.13	12.87	1.35	23.51	3782	-21.32	44.78
15	2776	12.20	0.06	12.14	1.46	23.33	2643	-21.27	40.31
16	2903	9.50	0.06	9.44	2.10	23.83	467	-20.20	31.09
17	2955	13.45	0.04	13.41	1.25	23.55	7027*	-22.13	66.09
18	2967	12.30	0.09	12.21	1.48	23.50	1963	-20.55	31.35
19	2989	13.42	0.17	13.25	1.15	22.89	3869	-20.99	28.90
20	2998	12.65	0.04	12.61	1.48	23.90	4734*	-22.07	75.61
21	3198	10.94	0.00	10.94	1.92	24.43	691	-19.56	30.40
22	3294	12.20	0.00	12.20	1.52	23.69	1566	-20.07	27.43
23	3370	12.28	0.00	12.28	1.49	23.62	1213	-19.44	19.83
24	3512	13.00	0.00	13.00	1.23	23.04	1340	-18.93	12.04
25	3631	11.03	0.00	11.03	1.66	23.22	1245	-20.74	30.10
26	3672	11.66	0.05	11.61	1.61	23.55	1737	-20.88	37.43
27	3756	12.15	0.00	12.15	1.64	24.24	1159	-19.47	26.76
28	3888	13.09	0.00	13.09	1.26	23.28	2541	-20.23	24.46
29	3938	10.91	0.00	10.91	1.73	23.45	838	-20.00	23.80
30	3976	12.24	0.00	12.24	1.59	24.08	2398*	-20.96	49.34
31	4047	13.10	0.00	13.10	1.18	22.89	3426*	-20.87	27.43
32	4100	11.62	0.00	11.62	1.72	24.11	1215*	-20.10	33.72
33	4136	11.58	0.00	11.58	1.61	23.52	434	-17.91	9.35
34	4162	12.25	0.00	12.25	1.40	23.14	2454	-21.00	32.60
35	4321	10.10	0.00	10.10	1.84	23.19	1100	-21.41	40.25
36	4536	10.99	0.00	10.99	1.87	24.23	1646	-21.39	64.53
37	4835	12.53	0.33	12.20	1.53	23.74	1951	-20.55	34.96
38	5012	12.47	0.00	12.47	1.46	23.66	2810*	-21.07	42.86
39	5085	11.94	0.08	11.86	1.53	23.40	1720	-20.62	30.82
40	5161	11.95	0.14	11.81	1.73	24.35	2018	-21.01	57.32
41	5230	12.75	0.00	12.75	1.35	23.39	6755	-22.70	79.98
42	5236	8.20	0.12	8.08	2.05	22.22	337	-20.85	20.00
43	5247	11.10	0.06	11.04	1.73	23.58	1511	-21.15	42.92
44	5301	12.66	0.00	12.66	1.64	24.75	1673	-19.76	38.62
45	5364	11.05	0.00	11.05	1.85	24.19	1349	-20.90	50.51
46	5457	8.20	0.00	8.20	2.43	24.24	396	-21.09	56.37
47	5584	11.95	0.00	11.95	1.52	23.44	1588	-20.35	27.81
48	5669	12.00	0.00	12.00	1.61	23.94	1372	-19.98	29.56
49	5861	12.31	0.08	12.23	1.48	23.52	1805	-20.35	28.83
50	6070	12.35	0.09	12.26	1.56	23.95	2060	-20.61	39.56
51	6215	11.79	0.69	11.10	1.30	21.49	1532(v)	-21.12	16.17
52	6412	12.35	0.12	12.23	1.37	22.97	1650	-20.16	20.46
53	7125	12.84	0.06	12.78	1.50	24.17	2913	-20.84	48.72
54	7309	13.05	0.00	13.05	1.33	23.59	4086	-21.30	46.20
55	7412	11.90	0.00	11.90	1.60	23.79	1686	-20.53	35.50

Remarks

The tabular material presented in each column is discussed in the text.

Fractional type I luminosity classes were generally not included; exceptions to this were NGC 6215 (I.8), which has a high surface brightness appearance on the IIIaJ U.K. Schmidt survey, and the low luminosity I.3 spiral NGC 3294. We also include M83, classified in the RSA as SBc(s) I-II.

Column 1 in table 3 contains the NGC number; the apparent magnitudes (either the total or asymptotic B_T magnitude in the B system of the RC2 when available; otherwise the Harvard photographic magnitudes statistically corrected to the B_T system [$\equiv m_c$ in the RC2]) are listed in column 2; the adopted galactic absorption correction

$$A_B = 0.132\ [\csc|b| - 1] \qquad |b| \lesssim 50^o$$
$$= 0 \quad \text{for } |b| > 50^o \tag{3.9}$$

following the work of Sandage (1973), and Sandage and Visvanathan (1978) [and using a canonical value of 4 for the ratio $R_B = A_B/E_{B-V}$] is computed in column 3; the <u>corrected</u> apparent magnitude

$$m^o = B_T\ [\text{or } m_c] - A_B \tag{3.10}$$

is listed in column 4; we calculate the mean surface brightness (in magnitudes per square arc second) in col. 6, according to

$$SB = m^o + 5 \log (6\ D_{25})$$
$$= m^o + 5 \log D_{25} + 3.89 \tag{3.11}$$

[c.f. eqn. (3.5)], where log D_{25} in col. 7 (in 0!1 from the RC2) is the lograthim of the apparent major isophotal diameter to a limiting surface brightness of 25 mag arcsec^{-2}; in (3.11), we have not made any additional correction for inclination effects. Recessional velocities v_o

(corrected to the centroid of the Local Group using (2.14)) in col. 7 are from the RC2, except for those values marked with an asterisk or underlined, where the redshift data is from Sandage (1978) or Tammann (private communication) respectively.

(Those v_o values given by Tammann are corrected to the centroid of the Local Group using the new solution by Yahil, Tammann and Sandage (1977) - c.f. chapter 2, section 2.4).

The absolute magnitude for each galaxy, corrected for foreground galactic absorption but not for inclination, is computed according to

$$M^o = m^o - 5 \log (v_o/H_o) - 25 \qquad (3.12)$$

and is listed in col. 8 (where we have adopted as usual H_o = 55 km s^{-1} Mpc^{-1}).

Finally, in col. 9, we note that for a galaxy r Mpc away, its intrinsic diameter D (in kpc) up to a limiting surface brightness of 25 mag $arcsec^{-2}$ may be calculated from

$$D = r(6D_{25}/206265)$$

[D_{25} in 0!1]

or in terms of v_o and H_o,

$$D(\text{kpc}) = 2.9 \times 10^{-2} \frac{v_o D_{25}}{H_o} \qquad (3.13)$$

[It is sometimes convenient to write (3.13) as

$$D(\text{kpc}) = 0.29 \frac{v_o D^*_{25}}{H_o} \qquad (3.14)$$

with D^*_{25} in <u>minutes</u> of arc].

The two decimals for each diameter in col. 9 are retained, for computing means and standard deviations, and preventing rounding-off error.

From Table 3, we find that

(a) the mean surface brightness $\overline{SB}$ of the 55 galaxies is

$\overline{SB}$ = 23.62 mag arcsec^{-2}

with a standard deviation of

$\sigma(SB)$ = 0.57 mag arcsec^{-2}

The surface brightness of NGC 6215 is hence 3.74σ from the mean.

(b) the mean absolute magnitude is

$\overline{M}^{o}$ = $-20\overset{m}{.}78$

with a standard deviation of close to nine-tenths of a magnitude:

$\sigma(M^{o})$ = $0\overset{m}{.}88$*

NGC 4136 [Sc(r) I-II] has the lowest absolute magnitude in our table:

M^{o}(NGC 4136) = $-17\overset{m}{.}91$

so that its M^{o} value is 3.26σ from the mean.

(c) The mean diameter of type I, I-II spirals is

$\overline{D}$ = 39.98 kpc

with a standard deviation of

$\sigma(D)$ = 16.55 kpc.

For any given galaxy, its absolute magnitude will depend on <u>both</u> its diameter and surface brightness

---

* From the absolute magnitudes (corrected for both foreground galactic absorption <u>and</u> inclination) available to us from the RSA, we find that for the galaxies listed in Table 3,

$\overline{M^{o,i}_{B_T}}$ = $-21\overset{m}{.}37$ (H_o = 50 km s^{-1} Mpc^{-1})

= $-21\overset{m}{.}16$ (with our value of H_o)

and $\sigma(M^{o,i}_{B_T})$ = 0.90

(section 3.1).

We may thus conclude from (a), (b) and (c) that application of the luminosity criteria still allow for a large range in absolute magnitude, diameter and surface brightness within a given luminosity class.

Also, the overlap in absolute magnitude between classes will depend on diameter and surface brightness: even small magellanic types can have large absolute magnitudes if their surface brightness is high (e.g. the SBmIII spiral NGC 7764).

If the surface brightness, absolute magnitudes and diameters for Sc I, I-II spirals were each normally distributed, one could obtain a $1-\alpha$ confidence interval for each above standard deviation using

$$\frac{(n-1)\sigma^2}{\chi^2_{\alpha/2,n-1}} < \sigma_p^2 < \frac{(n-1)\sigma^2}{\chi^2_{1-\alpha/2,n-1}}$$

where $\chi^2_{\gamma,n-1}$ represents the chi-square distribution with n-1 degrees of freedom (n is the size of the sample), and where σ_p is the "true" (population) standard deviation (Freund (1971)).

For a confidence interval of $1-\alpha = 0.99$, one then obtains, using (a), (b) and (c) above,

$$0.46 < \sigma_p(SB) < 0.75 \text{ mag arcsec}^{-2}$$
$$0^m.70 < \sigma_p(M^O) < 1^m.16$$
$$13.23 < \sigma_p(D) < 21.85 \text{ kpc}$$

with values of $\chi^2_{\gamma,\nu}$ from the Biometrika Tables for Statisticians (1954).

$$[\chi^2_{\alpha/2,n-1} = \chi^2_{.005,54} = 84.50,$$

$\chi^2_{1-\alpha/2,n-1} = \chi^2_{.995,54} = 30.98]$.

The type III spirals

Analogous to table 3, table 4 contains a list of 26 Sc type III spirals from the RSA. Here we find

(a) the mean absolute magnitude for type III spirals is

$\overline{M}^o = -19.45$

with a standard deviation of

$\sigma(M^o) = 1^m.03$

(b) the mean surface brightness is

$\overline{SB} = 23.60$ mag arcsec^{-2}

with a standard deviation of

$\sigma(SB) = 0.60$ mag arcsec^{-2}

(c) the value of the mean diameter is

$\overline{D} = 21.69$ kpc

with

$\sigma(D) = 9.94$ kpc

The tabular material in tables 3 and 4 is presented diagrammatically in figures 1 to 6.

Casting one's mind back on photographs of classic, well known galaxies such as M83 and M101, the viewpoint has often been that these represented "giant" or even "super-giant" spirals in the rank of galaxy sizes.

Our immediate conclusion from figure 1 is that:

Not all type I, I-II galaxies are intrinsically large - a point we have already noted; they may be small, and have a high surface brightness (esp. M83 and NGC 6215), or they may be small, and have a low surface brightness.

Table 4

Type c, Luminosity Class III Spirals from the "Revised Shapley-Ames Catalogue"

	NGC (1)	m (2)	A_B (3)	m^o (4)	log D_{25} (5)	SB (6)	v_o (7)	M^o (8)	D (kpc) (9)
1	701	12.90	0.00	12.90	1.40	23.79	1838	-19.72	24.42
2	949	12.55	0.23	12.32	1.44	23.41	785	-18.45	11.43
3	1518	12.30	0.05	12.25	1.48	23.54	810	-18.59	12.94
4	2397	12.93	0.21	12.72	1.35	23.36	1027	-18.64	12.16
5	2403	8.85	0.14	8.71	2.25	23.85	179	-18.85	16.84
6	2541	12.25	0.11	12.14	1.82	25.13	606	-18.07	21.18
7	3320	12.93	0.00	12.93	1.35	23.57	2367	-20.24	28.03
8	3445	12.80	0.00	12.80	1.21	22.74	2078	-20.09	17.82
9	3495	12.42	0.00	12.42	1.66	24.01	837	-18.49	20.23
10	3547	13.20	0.00	13.20	1.34	23.79	1414	-18.85	16.36
11	3556	10.65	0.00	10.65	1.92	24.14	772	-20.09	33.96
12	3917	12.40	0.00	12.40	1.69	24.74	1041	-18.99	26.97
13	3949	11.40	0.00	11.40	1.47	22.64	745	-19.26	11.63
14	3995	12.80	0.00	12.80	1.44	23.89	3381	-21.14	49.25
15	4027	11.65	0.07	11.58	1.47	22.83	1463	-20.54	22.84
16	4298	12.07	0.00	12.07	1.50	23.46	1042	-19.32	17.43
17	4420	12.71	0.00	12.71	1.35	23.35	1602	-19.61	18.97
18	4605	10.96	0.00	10.96	1.74	23.55	286	-17.62	8.31
19	4647	11.91	0.00	11.91	1.48	23.20	1286	-19.93	20.54
20	4808	12.56	0.00	12.56	1.43	23.60	679	-17.90	9.67
21	5088	13.17	0.04	13.13	1.43	24.17	1324	-18.78	18.85
22	5480	12.89	0.00	12.89	1.26	23.08	1928	-19.83	18.56
23	6207	12.15	0.07	12.08	1.48	23.37	1066	-19.36	17.03
24	1087	11.55	0.00	11.55	1.54	23.14	1844	-21.08	33.82
25	1421	11.95	0.05	11.90	1.56	23.59	2067	-20.97	39.69
26	5653	12.90	0.00	12.90	1.26	23.09	3642	-21.20	35.05

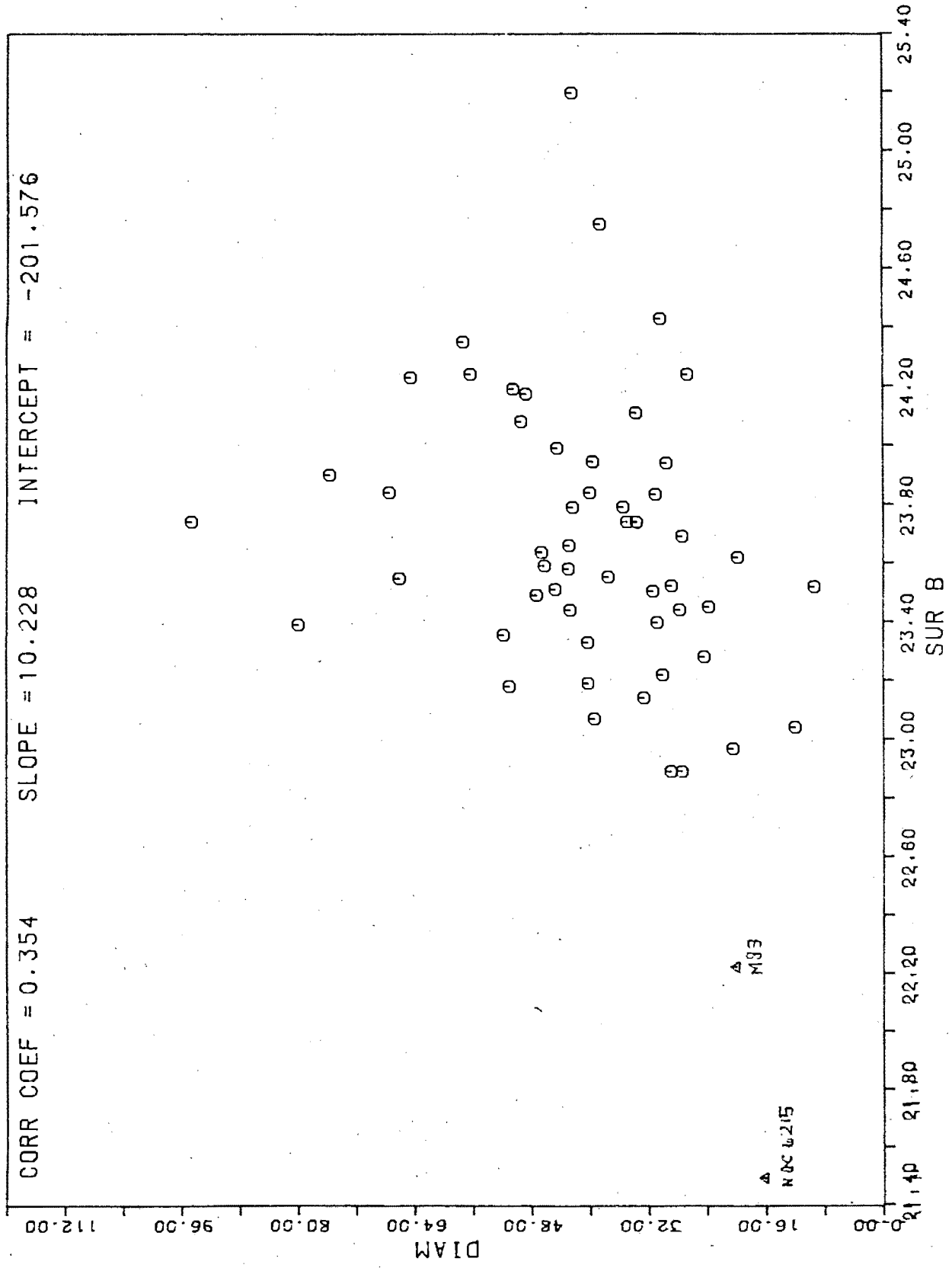

Figure 1. The 55 luminosity class I, I-II spirals listed in table 3 (from the RSA) are plotted here in a (diameter, surface brightness) plane. Both the large range in intrinsic size and surface brightness is evident.

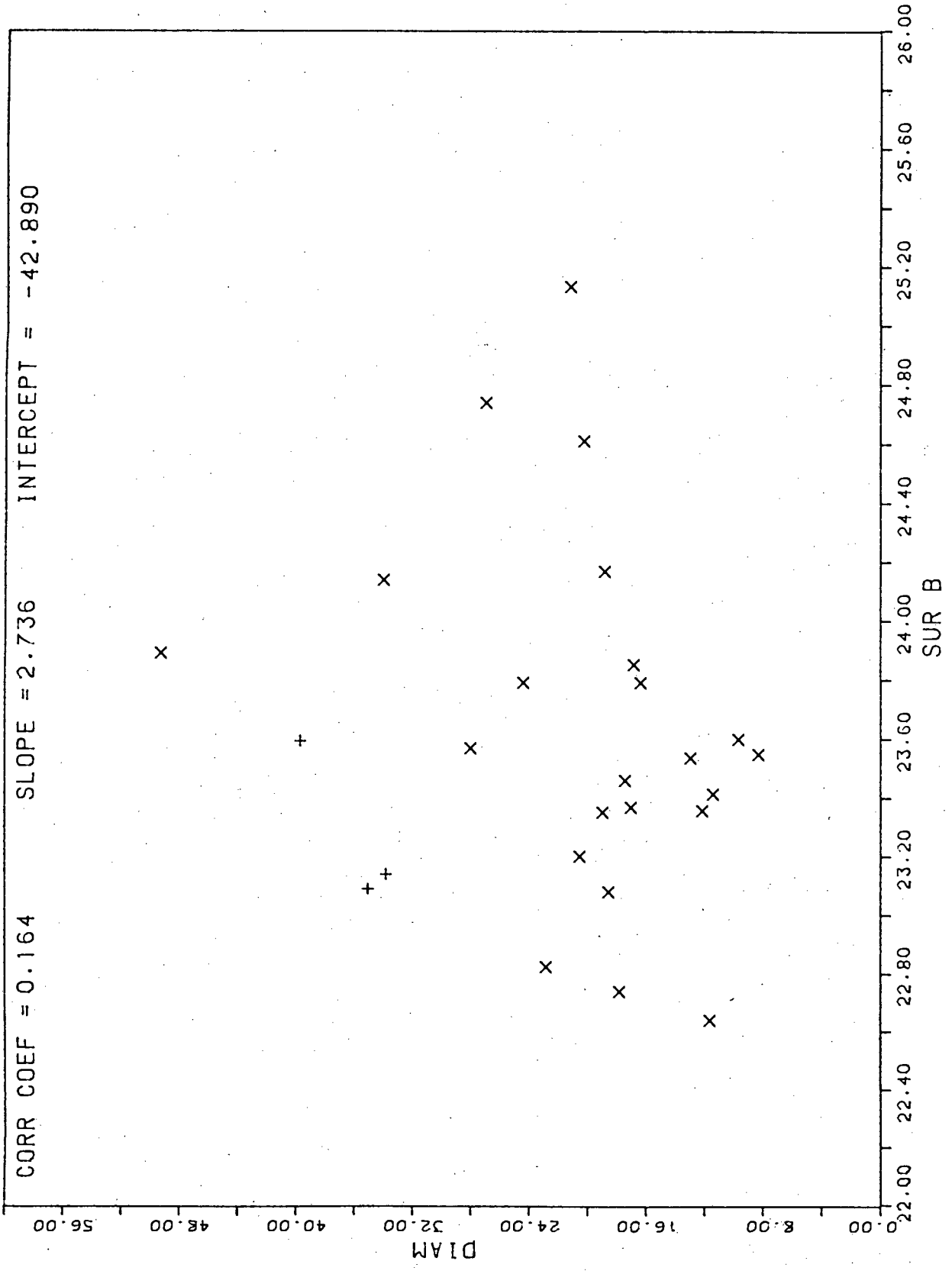

Figure 2. Identical to figure 1, except that the representative sample in this diagram are RSA luminosity class III spirals. Galaxies plotted are listed in table 4; the three + signs denote NGC 1087 (III.3), NGC 1421 (III:) and NGC 5657 (III pec).

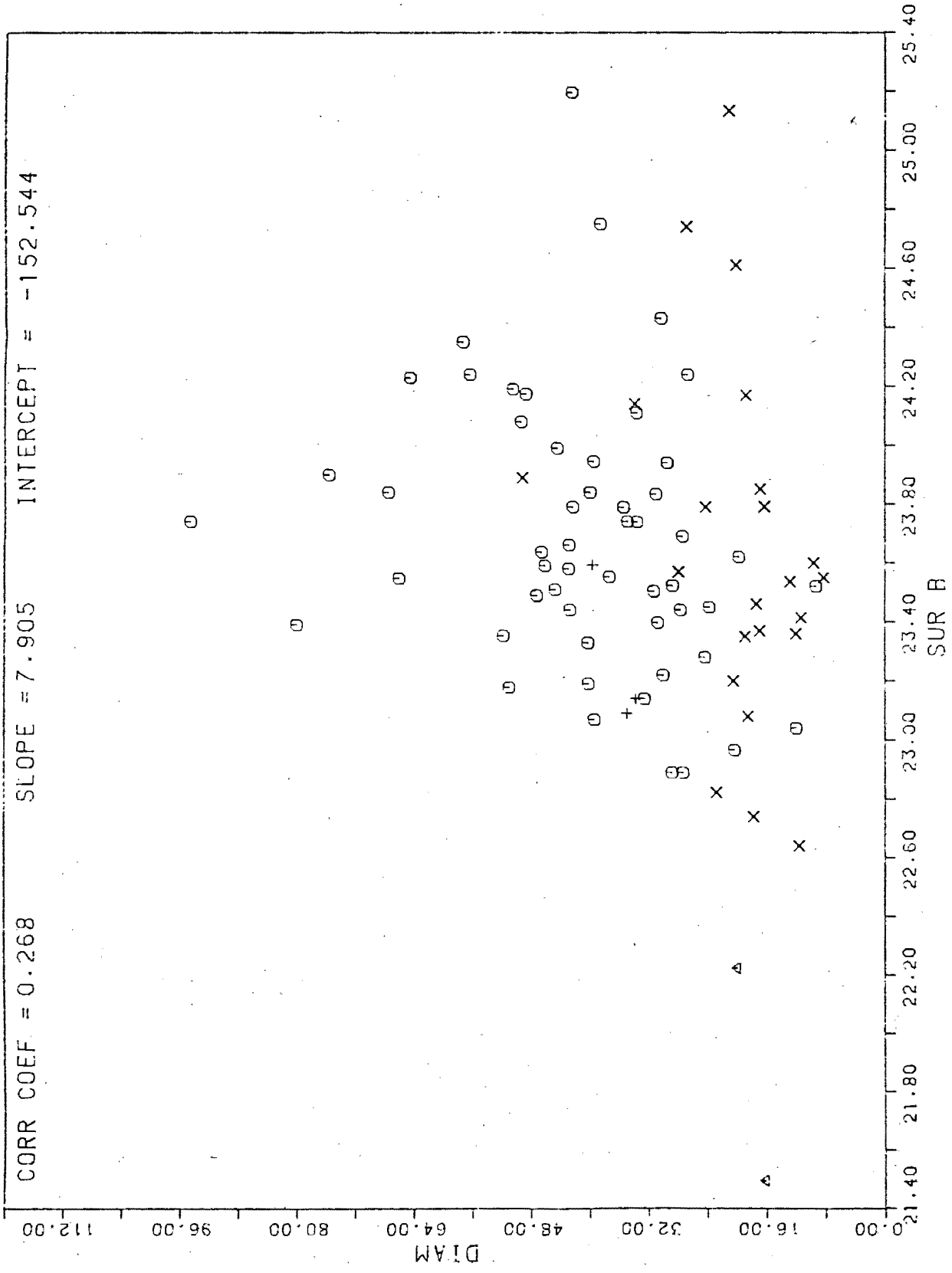

Figure 3. The figure comprises all those galaxies listed in tables 3 and 4, i.e. a composite of luminosity class I, I-II and type III spirals. While the class III generally populate the lower domain in this diagram, the overlap is worthy of note.

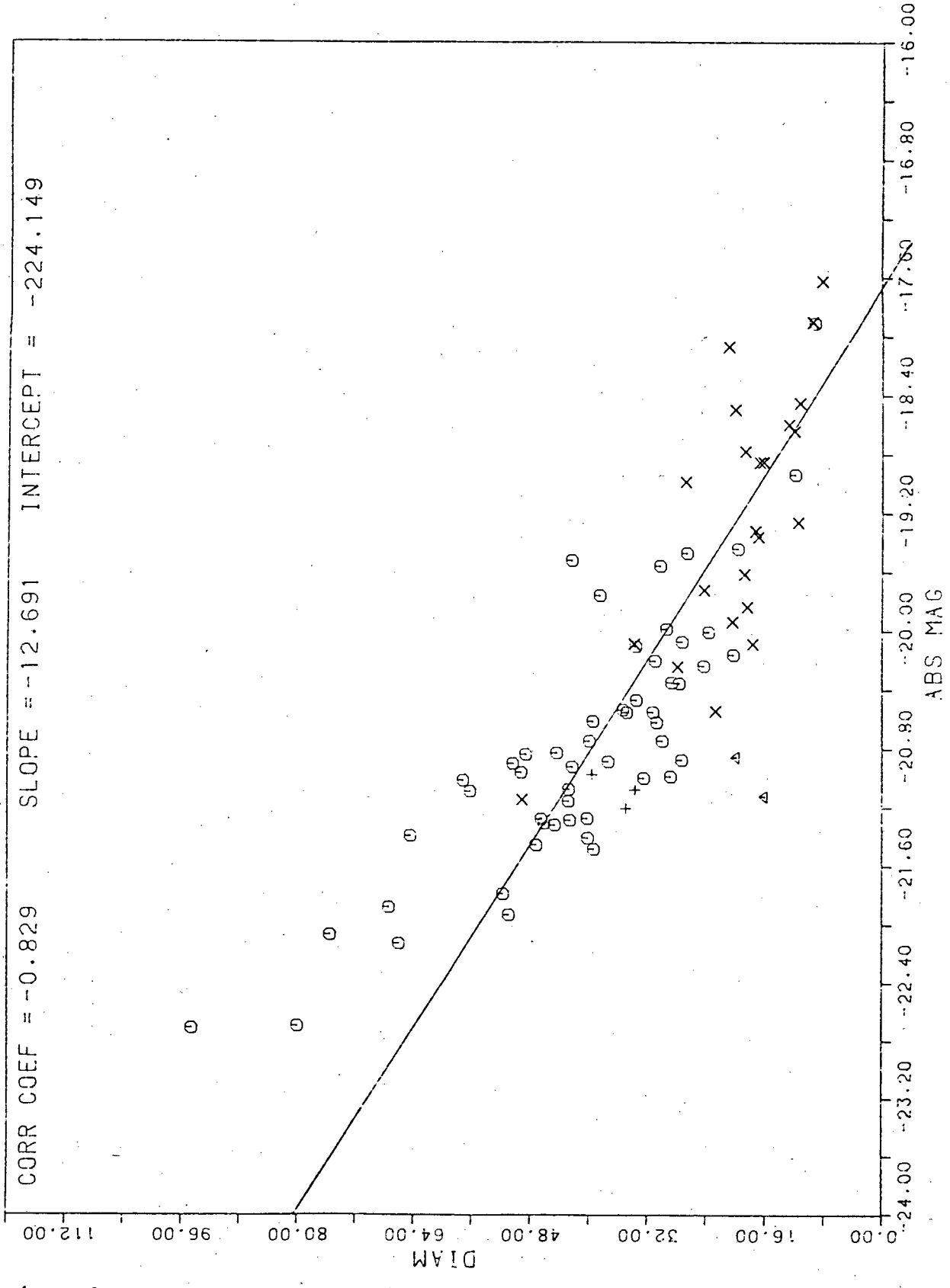

Figure 4. Galaxies from tables 3 and 4, as seen in an (intrinsic diameter, absolute magnitude) plot. While the correlation coefficient is high, within a small range of diameter there can be a large range in absolute magnitude.

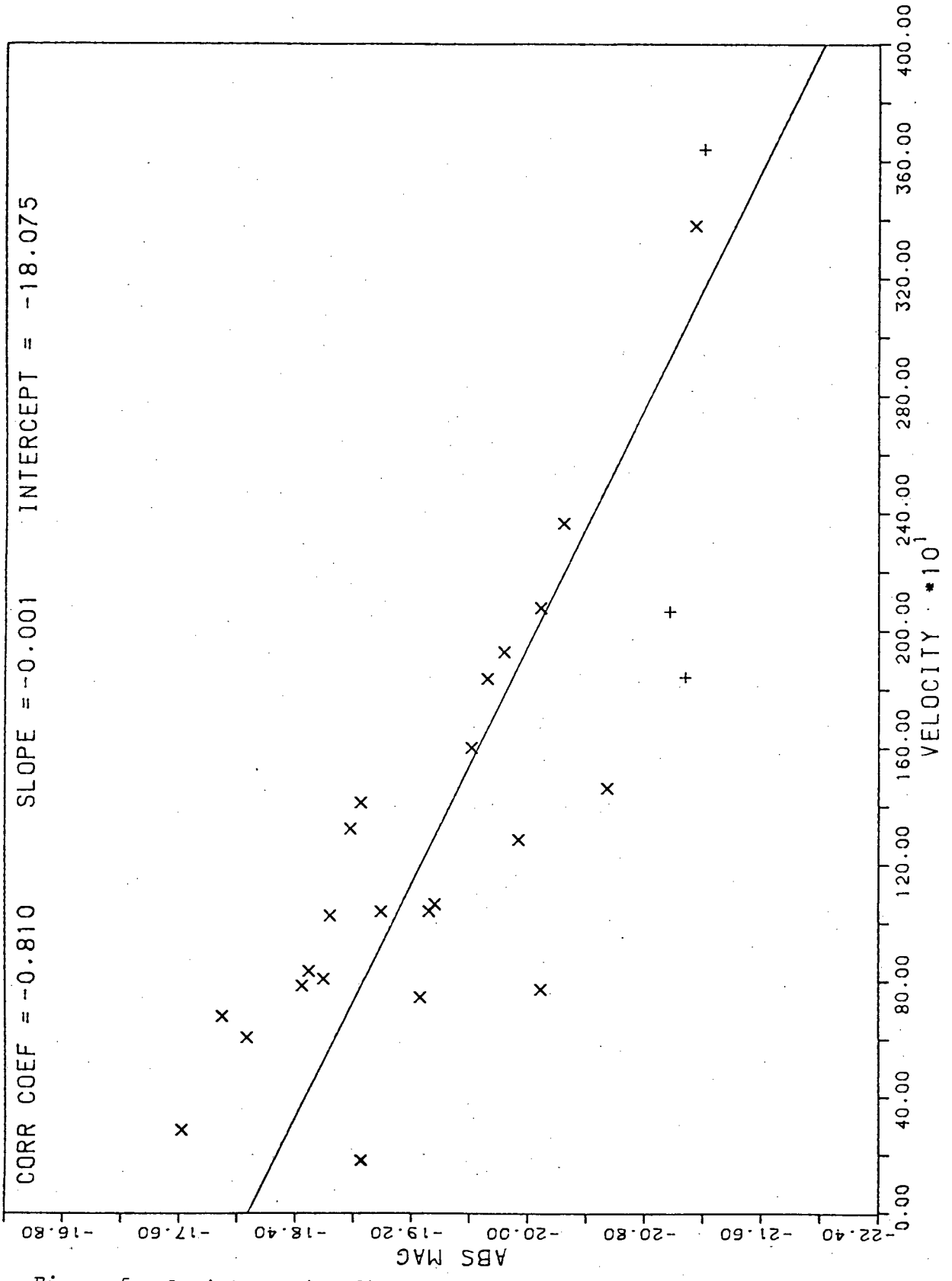

Figure 5. An interesting diagram, clearly showing (for type III spirals) the increase of absolute magnitude with increasing v_o.

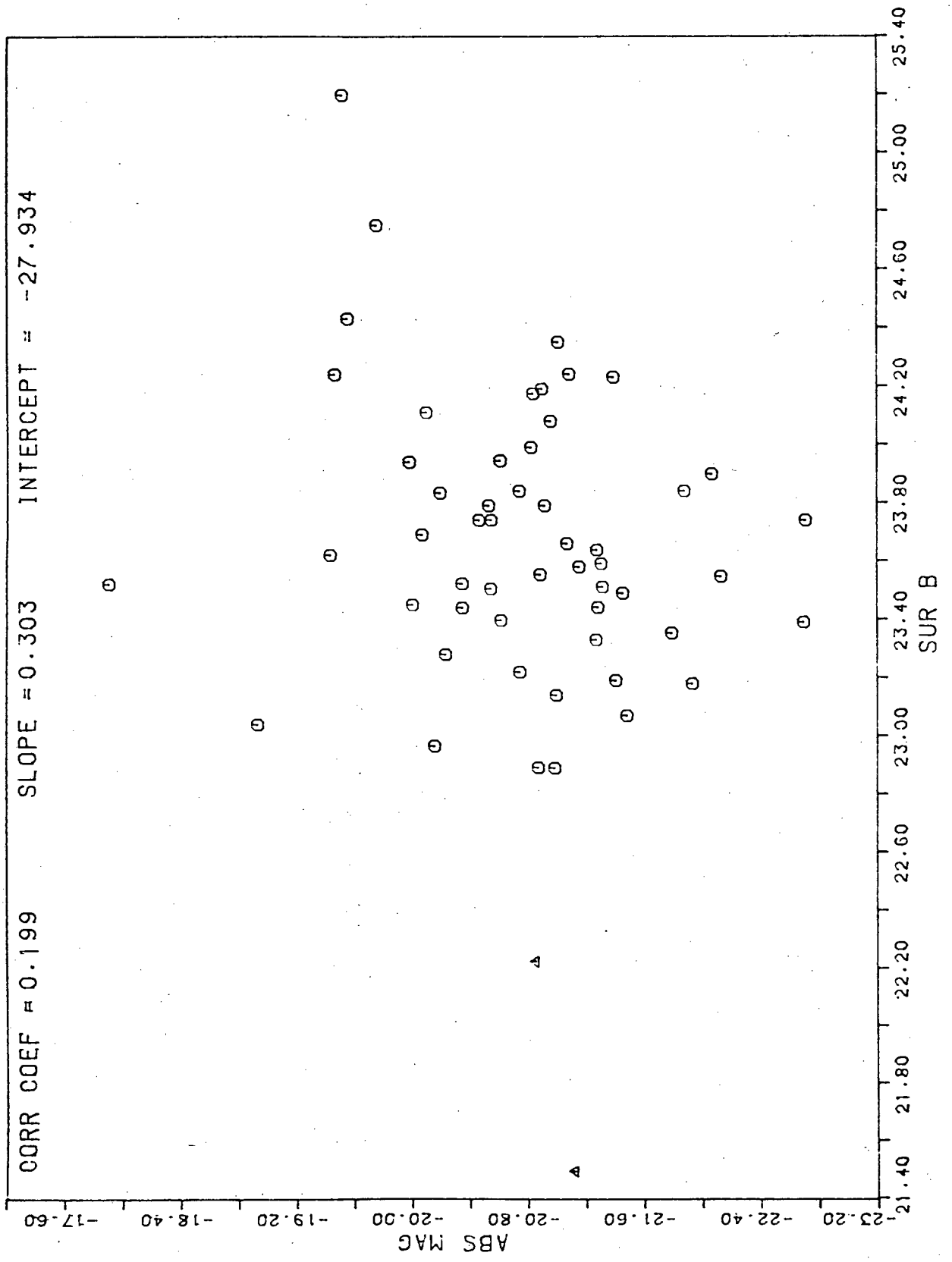

Figure 6. That there is no visible correlation between absolute magnitude and surface brightness for type I, I-II spirals (table 3) - the triangles represent the high surface brightness spirals M83 and NGC 6215 - is indicative of the large range in intrinsic diameter within the class.

Parallel conclusions can be drawn for the type III systems (fig. 2); in the combined plot of type I, I-II and luminosity class III spirals (fig. 3), one does notice that the type III galaxies, while still having a large range in intrinsic diameter, populate the lower region in the (diameter, surface brightness) plane.

An interesting diagram in fig. 5, where we have used the Sc III spirals from table 4 in an (absolute magnitude, velocity) plot; the increase of absolute magnitude with v_o is clear, as to be expected with galaxies drawn from a magnitude-limited sample with a broad luminosity function (c.f. Sandage, Tammann and Yahil (1979a)). The value of the correlation coefficient in fig. 5 is high - $|\rho| = 0.81$.

It is unfortunate that the original hopes and potential of the van den Bergh scheme - of finding "standard candles" on the basis of morphological appearance - are now dimmed; the luminosity criteria do not for example, distinguish intrinsically large type I, I-II galaxies from intrinsically small ones, and still allow for a range of more than 2 magnitudes per square arcsec in surface brightness (figs. 1 and 2). The scatter about the regression line in the (diameter, absolute magnitude) diagram (fig. 4) is hence considerable.*

---

* That there is no recognisable correlation between surface brightness and absolute magnitude (e.g. fig. 6 for type I, I-II spirals) is simply a reflection of the large range in intrinsic diameter within the class (c.f. the remarks in section 3.1 and equation (3.6)).

3.3 Hubble Type

The remarkable feature of the Hubble classification is that if one uses the three well known morphological criteria:

(i) openness of the spiral pattern;

(ii) the apparent ratio of the central bulge to the exponential disk;

(iii) the degree of resolution of the arms into luminous stars;

[Hubble (1926), (1936); Sandage (1961, 1975a)]

one finds that the change in stellar content follows the same order as the form sequence: for both ordinary and barred spirals, in the order Sd to Sa, one can enumerate these as:

(a) decreasing absolute luminosity for the brightest stars in the spiral arms;

(b) a decreasing percentage of mass in the form of dust and gas;

(c) a decreasing number of spiral arm HII regions, and

(d) increasing red (B-V) and (U-B) colours.

However, from our foregoing discussions, and from the photographs in chapter 5 onwards, it is apparent that one cannot decide whether a spiral of a specific Hubble type is large or small; "supergiants" may be intrinsically bright, but still physically small; "dwarfs" may be dwarfs in luminosity, but not in diameter (c.f. footnote on page 11 of chapter 2).

The situation is very much analogous to that for ellipticals; one cannot, for example, when inspecting two E3's on a photographic plate, decide which one has the

larger absolute diameter - unless of course one has redshift data, but this then takes one in a direction away from using only morphological characteristics, to requiring information of both a qualitative as well as quantitative nature.

The beauty of the Hubble scheme lies most surely in its simplicity; but if we are to gain a deeper understanding of spiral galaxies and their formation, an appreciation of both the vast range in spiral arm texture (as classified in chapter 5) and linear diameter is called for.

3.4 Maximum Rotational Velocity

In 1977, Tully and Fisher found a very high correlation* between the maximum rotational velocity of a galaxy V_{max}, and the galaxy's Holmberg radius R_H (limiting isophote = 26.5 mag arcsec^{-2}).

The calibrating galaxies used were of <u>different</u> Hubble types; their resulting log R_H, log V_{max} relation has a much less steep slope than that determined by Rubin, Ford and Thonnard (1980) for 21 type Sc galaxies.

The particular emphasis is that:

V_{max} is not only a function of <u>Hubble type</u> (Brosche (1971); Roberts (1978); figure 5 in Rubin, Ford

---

* fig. 2 in their paper; it is assumed that the width ΔV of the 21 cm profile measures twice the peak of the rotation curve.

and Thonnard (1978)) but on the variation of linear diameters within that Hubble type

- for Sc's:

$V_{max} = 150 \pm 25$ km s^{-1} for galaxies with radii of 10 kpc rising to

$V_{max} = 300 \pm 60$ km s^{-1} for galaxies with radii of 70 kpc.

[These values are based on $H_o = 50$ km s^{-1} Mpc^{-1}, and come from Rubin, Ford and Thonnard (RFT - 1980)].

As a result of this, a biased relation between log R_H and log V_{max} can be found if galaxies of various Hubble types (and varying radii) are used; the early type spirals having substantially higher values of V_{max} (as a function of radius) than the later types (e.g. Sc's).

"For an Sc to have V_{max} as high as that for an Sa or Sab galaxy, the Sc galaxy must be enormous".

[RFT (1980), c.f. their figure 8].

Once again, the importance of intrinsic diameter comes to the fore; when grouping galaxies according to linear radii, one can expect correlations which would not otherwise be found if the galaxies were grouped according to luminosity class, as the luminosity criteria do not bin galaxies into specific diameter groups, as discussed in section 3.2.

3.5 Pitch Angle, and Winding Angle

We commence this section by referring to the work of Danver (1942), who found (using empirical rectification) that the arms of spiral galaxies could be well described by

logarithmic spirals, these being characterized by the fact that the angle between the radius vector and the tangent to any point on the spiral is a constant.

The equation for a logarithmic (equiangular) spiral may be written*

$$r = r_o e^{\chi\psi} \qquad (3.15)$$

where r and ψ are polar co-ordinates, and the pitch angle μ is given by

$$\tan \mu = \frac{c}{\chi},$$

with $c = \left(\frac{\pi}{180}\right) \log e$

We set out to investigate whether any correlation existed between

(a) pitch angle and linear diameter, in the sense that given any logarithmic spiral of a specific length, one way to increase the distance from the asymptotic point (the nucleus) to the outermost point of the spiral would be to decrease the value of the pitch angle; this then would correspond to the spiral following a more open pattern.

(b) winding angle and linear diameter: do the spiral arms of large Sc galaxies, for example, generally wind round the nucleus a greater number of degrees than small Sc's?

---

* This equation [3.15] was recently used by Sandage and Humphreys (1980) for the spiral arms of M33; their figure 3 shows the resulting face-on (rectified) appearance when the arms for that galaxy are brought to the same plane.

Our results for those type c spirals with measured pitch angles and winding angles as determined by Danver are presented in figures 7 and 8, with the individual galaxies being listed in table 5.

(i) From the D-θ_m diagram (fig. 7), one notes that intrinsically large galaxies can still have small values of θ_m, where θ_m is the "maximum" angular winding (i.e. the value of θ for that spiral arm which winds round the nucleus the greatest number of degrees).

(ii) We see from fig. 8 that a parallel conclusion holds: what this diagram reflects is that all the 52 Sc/SBc galaxies plotted (<u>whether large or small</u>) tend to group around the mean value of the pitch angle

$$\langle\bar{\mu}\rangle = 72^{\circ}.81 \equiv 73^{\circ}$$

with a standard deviation of

$$\sigma = 4^{\circ}.99$$

[For each galaxy, $\langle\mu\rangle$ is the arithmetic mean of the pitch angles of the spiral arms identified and measured by Danver].

In Danver's (1942) appendix III, 90 spirals in his list of 98 galaxies have measured values for their pitch angles; the sample encompasses galaxies of different Hubble types. It is indeed remarkable that for this larger sample, we still have (as noted by Danver) a mean (unweighted) value for $\langle\mu\rangle$ of

$$\langle\bar{\mu}\rangle = 73^{\circ}.69$$

with a standard deviation of

$$\sigma = 5^{\circ}.33.$$

Table 5

Type Sc, SBc Spirals from Danver (1942) with Measured Pitch Angles, and Winding Angles

	Galaxy NGC (1)	Classification (RSA) (2)	$\langle\mu\rangle$ (degrees) (3)	θ_m (degrees) (4)
1	300	Sc II.8	66.6	330
2	578	Sc(s) I-II	70.6	340
3	598	Sc(s) II-III	57.5	260
4	628	Sc(s) I	73.1	530
5	877	Sc(s) I-II	74.7	270
6	895	Sc(r) I	69.0	370
7	908	Sc(s) I-II	77.7	290
8	1042	Sc(rs) I-II	75.9	330
9	1058	Sc(s) II-III	71.5	290
10	1084	Sc(s) II.2	74.6	360
11	1087	Sc(s) III.3	78.0	260
12	1090	SBc(s) I-II	77.1	330
13	1232	Sc(rs) I	74.4	410
14	1385	ScIII:	77.4	150
15	2403	Sc(s) III	75.8	520
16	2835	SBc(rs) I.2	71.5	320
17	2903	Sc(s) I-II	71.8	360
18	2964	Sc(s) II.2	76.1	250
19	2997	Sc(s) I.3	75.8	450
20	3184	Sc(r) II.2	69.9	470
21	3198	Sc(rs) I-II	74.5	460
22	3367	SBc(s) II	76.5	340
23	3511	Sc(s) II.8	66.3	120
24	3512	Sc(rs) I-II	75.4	400
25	3513	SBc(s) II.2	69.1	240
26	3756	Sc(s) I-II	78.5	350
27	3893	Sc(s) I.2	75.7	360
28	3938	Sc(s) I	73.2	490
29	4088	Sc(s) II-III/SBc	68.2	330
30	4145	SBc(r) II	74.4	360
31	4254	Sc(s) I.3	72.0	460
32	4303	Sc(s) I.2	72.9	560
33	4321	Sc(s) I	71.6	430
34	4504	Sc(s) II	77.3	360
35	4535	SBc(s) I.3	72.0	230
36	4567	Sc(s) II-III	70.1	270
37	4899	Sc(s) II.8	79.1	360
38	5068	SBc(s) II-III	71.9	360
39	5085	Sc(r) I-II	79.4	340
40	5236	SBc(s) I-II	73.0	360
41	5247	Sc(s) I-II	57.8	260
42	5364	Sc(r) I	80.3	700
43	5457	Sc(s) I	63.5	430
44	5595	Sc(s) II	71.1	330
45	5597	SBc(s) II	80.5	310
46	5676	Sc(s) II	74.7	300
47	5678	Sc(s) II-III	75.8	180
48	6412	SBc(s)/Sc(s) I-II	74.6	380
49	6643	Sc(s) II	75.7	240
50	6946	Sc(s) II	63.5	270
51	7309	Sc(rs) I-II	68.4	180
52	7424	Sc(s) II.3	70.2	340

Notes to Table 5

(i) For each galaxy, $\langle\mu\rangle$ in col. 3 denotes the (arithmetic) mean of the pitch angles of those spiral arms measured by Danver (1942), appendix III.

(ii) θ_m in col. 4 is the "maximum angular winding" - the value θ for that spiral arm which winds round the nucleus the greatest number of degrees.

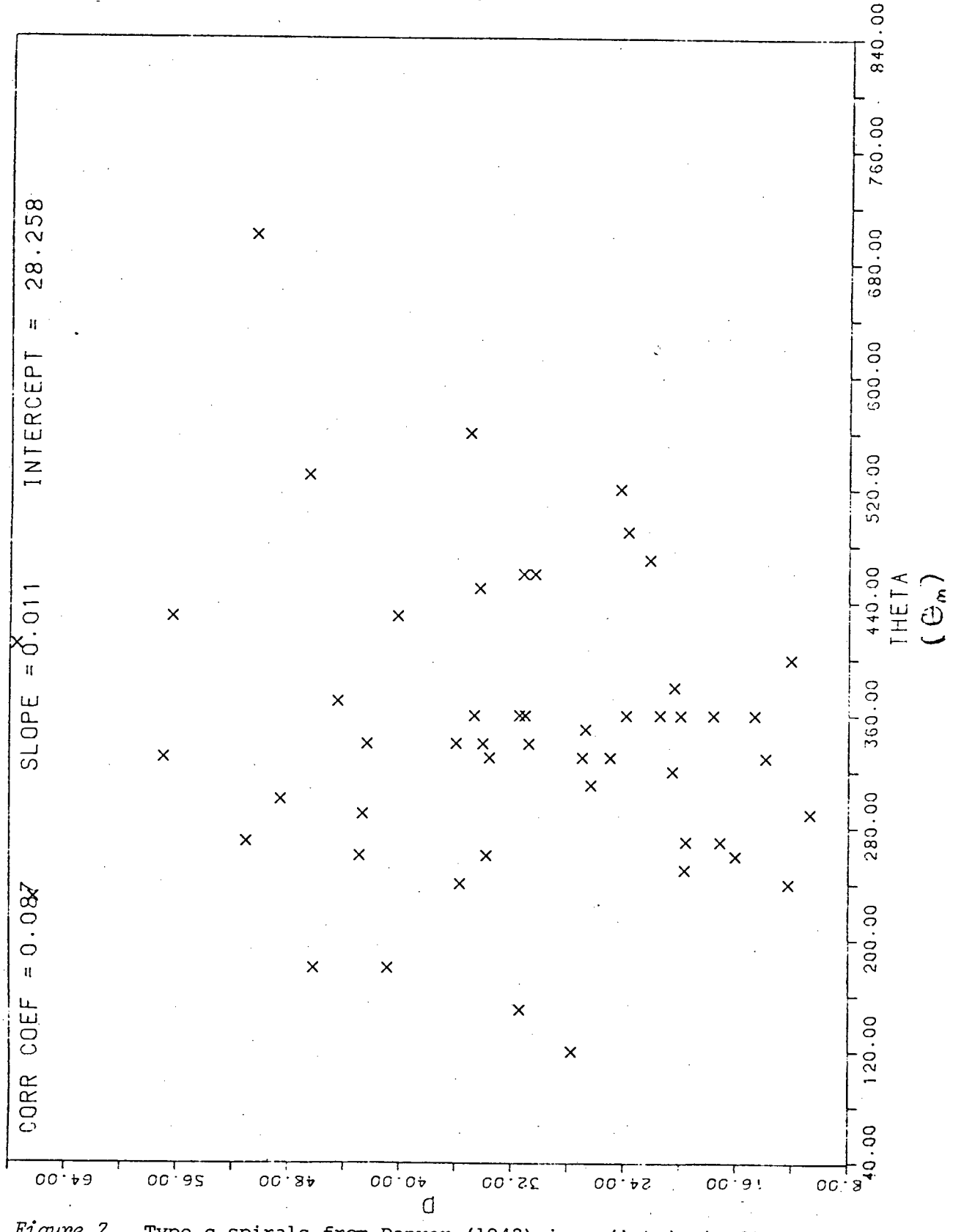

Figure 7. Type c spirals from Danver (1942) in a (intrinsic diameter, θ_m) plot. Individual galaxies are listed in table 5.

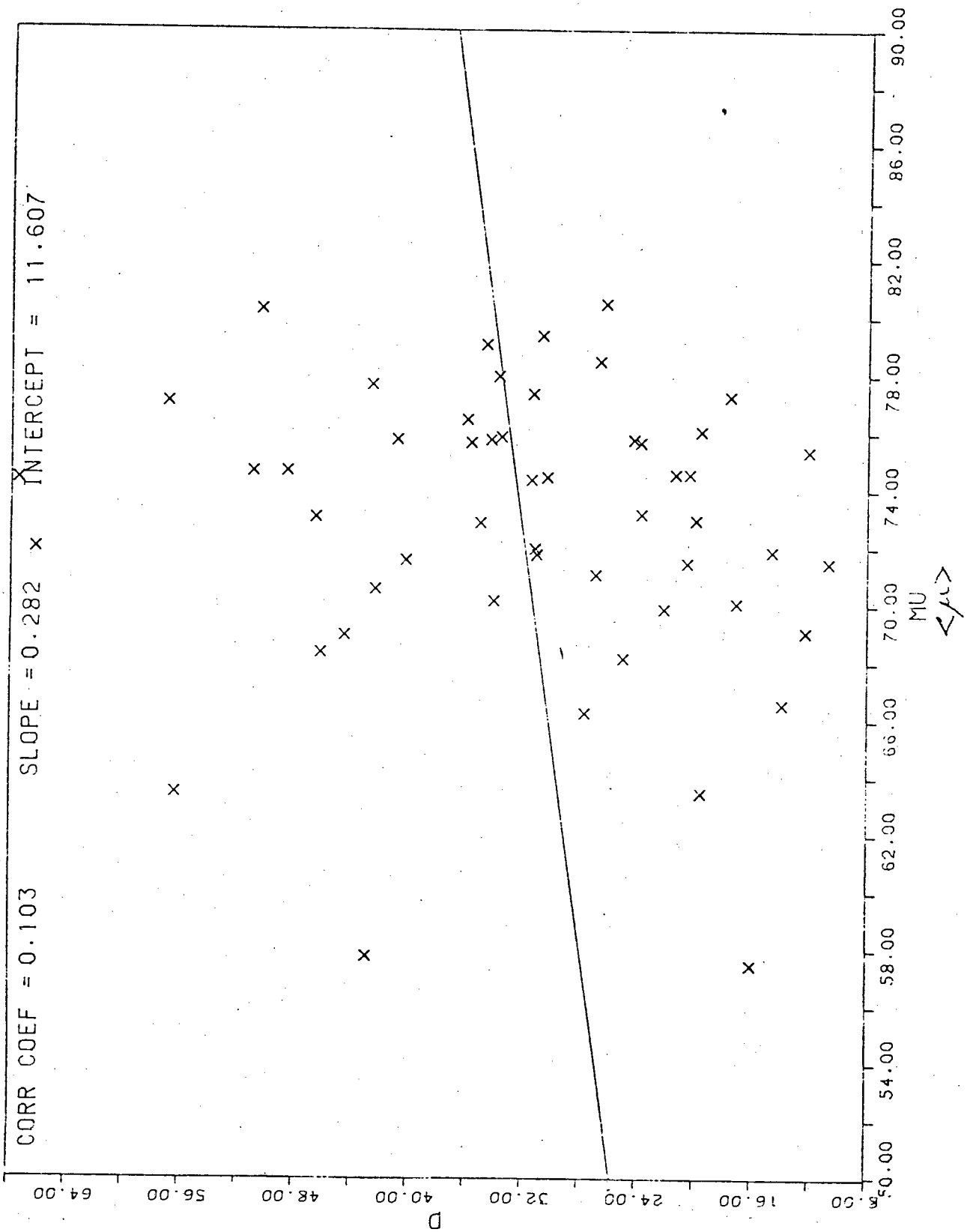

Figure 8. This diagram shows the tendency for both intrinsically small and large spirals to have pitch angles scattered about 73°.

Our conclusions from figures 7 and 8 are simply

"Galaxies are large because they are large!"

- the variation in their size being primarily reflected in a change of the scale factor r_o, and not to any significant degree in pitch angle and/or angular winding.*

As Dr. van den Bergh once commented:

"Galaxies are like people" - to which I add: *"they enjoy independence!"*.

---

* The choice of a logarithmic spiral to represent the form of the arms is not <u>always</u> appropriate [cf. Dzigvashili and Borchkhadze (1970)].

CHAPTER FOUR

PREPARATION OF THE PHOTOGRAPHS

With the availability of the U.K. Schmidt IIIa-J Survey, there was no need to photograph galaxies individually at a telescope.

An excellent example is NGC 6872, where both a U.K. Schmidt film copy and a 105 minute 4-m plate were at the author's disposal. While the latter clearly showed finer detail such as OB associations, the Schmidt copy compared most favourably in revealing tenuous outlying gaseous structure.

It was thus felt that we would rather exercise particular care in obtaining the highest possible quality for each photograph.

With a range in redshift of $z = 0.004$ to $z = 0.030$, the sample was divided into <u>two</u> groups:

(a) <u>Group I</u>:

Those galaxies with redshifts in the range

$z \in [0.004, 0.012)$

were photographed with a frame height of 9mm, using a 75mm lens and light table attached to the Polaroid MP-3 multipurpose system at the South African Astronomical Observatory.

(b) <u>Group II</u>:

Galaxies with redshifts in the remaining interval

$z \in [0.012, 0.030]$

were photographed at a higher magnification - frame height 3mm - employing a 35mm lens, and the same Polaroid MP-3 system.

Calibration of scale between groups (a) and (b) - and in printing the sample - was effected by photographing a mm

ruler at the side of each frame.

In all cases, 35mm fine grain Kodak Panatomic-X film (ASA 32) was used, developed for 5 minutes at 68°F in Acutol FX-14, diluted 1+10. [This well suited developer provides maximum sharpness, definition and resolution with a full tonal range.]

Exposure times (for the IIIa-J Survey) were as follows:

Group I	1s	f11
Group II	4½s	f16

In printing the photographs, it was decided to align the major axis of each galaxy parallel to one of the borders of the photograph; this allows more accurate visual intercomparisons to be made, rather than if the orientations were random.

The adopted printing scale for each individual photograph was 23mm ≡ 10 kpc; the majority of galaxies could then easily be accommodated on 5" x 7" photographic paper, while only the intrinsically large ones required a 10" x 8" format. [An exception was NGC 6872!]

Polyethylene laminated paper Ilfospeed was used, either on a pearl or semi-matt finish. The grade best suited to our purposes was grade 4.

A typical darkroom (printing) run would result in not more than five galaxy photographs; all unacceptable prints were rejected, until an optimum quality was reached.

After exposing each negative (exposure times at the enlarger for varying heights being coordinated with a light sensitive CDS meter), the paper was developed for 1 minute in Ilfospeed Paper Developer, rinsed for 30 seconds in a stop-bath, fixed for 30 seconds in Ilfospeed Paper Fixer, and washed for 2-3 minutes in running water. This process,

as recommended by the manufacturer, results in a print of permanence and completely free of chemicals.

Photographs were mounted individually on cards, so as to enable flexibility in classification, sequencing the galaxies in order of increasing linear diameter, and for use in the intercomparison of IIIa-J and ESO B prints.

Montages of (usually) six photographs were made for binding into this thesis. In making the composite prints, some of the finer detail has inevitably been lost, due to the additional 2-step photographic process and fluctuations in the range in overall density from galaxy to galaxy. Also, because of the number of thesis copies required, it was difficult to exercise the stringent quality control that was applied to the individual photographs.

The author will gladly make available his individual prints to those persons interested.

In the following chapters, the montages are all printed at the same linear scale (as indicated above each plate), so that intercomparisons from montage to montage can be made.

It is important, however, to note that the ellipticals and lenticulars have been printed at a reduced linear scale, to allow a greater number of galaxies to be photographed in an individual montage. The same applies to our montage of ESO (B) and IIIa-J photographs (chapter ten), and in galaxies from the Fairall Survey (chapter eleven). The reduced scale is seen in each plate, to avoid any possible confusion.

CHAPTER FIVE

THE SPIRALS : TYPES c TO O/a

The range in the intrinsic size of spirals, particularly type b and c, is remarkable; when we initially set out the present programme, we expected *a priori* to find only a large range for the ellipticals!

In making the composite photographs, we generally found that spirals of a particular Hubble-Sandage-de Vaucouleurs type could comfortably be grouped into one of four separate classes, according to their appearance on the SRC IIIa-J Survey. These are

(i) those spiral galaxies which present a saturated/predominantly saturated image on the J-Survey; some very high surface brightness spirals (21.5 - 22.5 mag arc sec^{-2}) are included;

(ii) spirals with thick "massive", high surface brightness arms, in NGC 309, of the order of ~7 kpc.

(iii) an intermediate category [medium arms], and

(iv) galaxies which present relatively weak or filamentary spiral arms.

It is important to stress that the terms "massive", "medium" and "weak" depend on comparing galaxies side by side *on an absolute scale;* as one example, we consider the high surface brightness Sc spiral NGC 6215, whose arms are described by Dressler and Sandage (1978) as being "semi-massive"; on an absolute scale however, this galaxy is intrinsically small, and the arms are not at all massive when compared with the massive-armed spirals seen here. This then is where we

deviate from the purely morphological criteria of the van den Bergh scheme (1960a, b).

The measured diameters in this and the following chapters are isophotal major diameters as determined on the photographs [printed using the velocities in table 6]. The limiting surface brightness (for extended objects) on the film copies used from the IIIa-J Survey for the photographs is, as mentioned earlier, about 25.5 B mag arcsec^{-2}.

As a comparison, we also compute the de Vaucouleurs diameter (to 25.0 mag arcsec^{-2}) in column 9 of table 6 for all galaxies photographed with known apparent magnitudes; these are used in our discussion in chapter eleven.

In viewing the selection of photographs from the SRC Survey, it is important to keep in mind our discussions in chapter 2, particularly the effects of inclination for highly inclined systems, and the changes in diameter which random motions can produce. [Also, as we noted in chapter four, the major axis of each galaxy is usually printed horizontally, so as to enable suitable visual diameter comparisons to be made].

5.1 The Type bc, c Spirals

The intrinsically smallest galaxy in this section is NGC 2082, with a diameter of some 7 kpc. Its heliocentric velocity is only 1104 km s^{-1} (table 6), corresponding to a redshift of z = 0.004. Peculiar motions could thus produce a significant change in diameter.

The largest Sc spirals in our sample are NGC 646 (diameter ∿85 kpc) and the Sc I galaxy NGC 309 (diameter ∿90 kpc). NGC 309 is one of the brightest galaxies in the Revised Shapley-Ames Catalogue, with an absolute magnitude in that listing* of -23.04 (H_o = 55 km s^{-1} Mpc^{-1}).

This is still not the upper limit; the largest identified type c spiral is UGC 2885 (Rubin, Ford and Thonnard (1980)). Its uncorrected diameter - to 25.0 mag $arcsec^{-2}$ - is 188 kpc. Using equation (2.13), they find a (corrected) diameter for this galaxy of 244 kpc. Following the analogy used by Rubin, Ford and Thonnard in their paper, we remark that both UGC 2885 and the largest type b spiral NGC 6872 would, if placed at a 20 Mpc distance to the Virgo cluster, subtend angles exceeding 30 minutes of arc, whereas the largest spirals (and ellipticals) in Virgo are 12 arc min [Sulentic (1977)].

The range in morphology for the type bc, c spirals as seen on the J-survey is impressive, and we proceed to discuss each individual section in turn.

---

* Corrected for inclination and foreground galactic absorption.

5.1.1 Type bc, c Spirals - Saturated Images on IIIa-J Survey

The spirals in this group have images on the IIIa-J survey which are predominantly saturated. Their diameters (for type bc, c) range from 7 kpc (NGC 2082) to 47 kpc (NGC 4835).

That these are high surface brightness galaxies is not always reflected in col. 6 of table 6; the value SB computed there is the average surface brightness within a circle of diameter D_{25} seconds of arc. Thus, in the case of NGC 1437 for example, presenting a predominantly saturated image on the J-photograph, one can still find a low overall surface brightness: 23.8 mag arcsec^{-2}. The reason for this is that the diameter out to 25 mag arcsec^{-2} includes a faint outer envelope, resulting in an average surface brightness which is low.

In summary then, we use the term "high surface brightness spiral" for those spiral galaxies with most of their image reaching or almost reaching saturation level on the J-survey.

We begin by considering NGC 6215, classified in the RSA as Sc(s) I.8. It is the highest surface brightness spiral in our entire photographic sample of ellipticals/lenticulars/spirals/irregulars: SB = 21.5 mag arcsec^{-2}. The surrounding envelope probably extends much further than can be seen on the photograph, as this spiral is at a very low galactic latitude ($b = -9^{\circ}.27$).

It is one of the three spirals in this group which could be classed as type M83: NGC 1310, NGC 6215 and of

course M83 = NGC 5236 itself. They are intrinsically small, (all having approximately the same linear diameter), and are of high surface brightness. M83 is the largest, with a diameter on the photograph of ∿22 kpc. [In printing the photograph of M83, we have used the Tammann (1977) distance of 6.5 Mpc]. This value for its (optical) diameter is not particularly large; in the literature, numerous comments have been made to the contrary.*

M83 is unusual in several respects; it is one of the most blue spirals known, having a remarkable (U-B) excess for its value of (B-V) (cf. fig. 2 in Tinsley (1975)), and its (extrapolated) central surface brightness is very high (Freeman (1970), fig. 5). Furthermore, it has been the parent galaxy of 4 supernovae (1923, 1950, 1957, 1968), and also has a peculiar nucleus [Sérsic and Pastoriza (1965, 1967); also Sérsic (1979)]. Moreover, it is perhaps one of the best prototypes of the de Vaucouleurs (1959) class SAB - those transition galaxies which have a definite bar and those which do not.

Magnificent multicolour maps have been produced from the surface photometry conducted by Talbot, Jensen and Dufour (1979). M83 is surrounded by an extensive HI envelope, 6.2 times its Holmberg diameter, and of the order of 200 kpc (plate 6).

Curious outer morphology is evident in NGC 6221; almost the resemblance of some 'bow-wave', with the galaxy

---

* A 'giant galaxy' (Sérsic 1968); a 'supergiant galaxy' (Wood and Andrews (1974)); 'larger than our own' (Moore (1970)).

moving through intergalactic matter. [In the absence of other plate material, it would be hard to believe that one was looking at an Sbc galaxy!]

The smallest type c in our sample is included here - NGC 2082, diameter 7 kpc. Its spiral structure is only clearly evident on the corresponding ESO(B) photograph (plate 49).

[The intrinsically smallest galaxy in which well-defined spiral structure has been observed is the miniature spiral NGC 3928, classified as type E0 in the RC2, but recently shown on a large scale IIIa-J plate to have spiral structure from ∿350 pc to just over 1 kpc (van den Bergh (1980))].

One thus finds spiral structure extending over vast ranges in linear diameter - from the very smallest, to over 200 kpc for the largest. To illustrate the above point, we have have prepared a plate of bc, c galaxies NGC 598 = M33 (Sc(s) II-III), IC 1637 (SA(rs)bc:) and NGC 418 (SB(s) c) placed side by side (plate 5); the range in physical size and spiral arm texture is indeed impressive. [The arms of M33 are then no longer truly massive in an absolute sense (cf. Reynolds (1927)].

NGC 1437, mentioned earlier, is a magnificent type example where the spiral structure terminates abruptly at the boundary of the saturation region - diameter ∿12 kpc - a faint, featureless, surrounding envelope is then seen. The envelope has no distinct sharp edge - it could thus extend as in the case of a floating iceberg.

NGC 1792 and NGC B175 are good examples where the spiral structure on the J-survey is totally saturated, with hints of a faint surrounding envelope. In these two galaxies, the spiral structure is apparent in the outer regions as dust lanes, which one normally only sees closer to the nucleus.

The surface brightness of the central region decreases in NGC 3568 and NGC 4835, so that spiral structure becomes apparent.

NGC 440 shows no detail on the J-photograph, and very little spiral structure on the "Quick Blue" Survey.

The spiral NGC 1511, classified in the RSA as Sc pec, has a faint tail (just above the limiting surface brightness of the photograph) extending to 20 kpc (projected) from the main galaxy. The detectable limiting region of the tail is marked by an arrow.

NGC 7361, with a central high surface brightness core, bears a greater resemblance to a type b galaxy, such as M31 for example. A faint tenuous stretch of gas can be traced from the galaxy to its companion at the upper right.

We conclude this section by remarking that spirals which have saturated/predominantly saturated images on the IIIa-J Survey (such as NGC 6215, NGC 6221 and M83) generally do not have massive, dominating spiral arms.

This ties in nicely with our diameter-surface brightness correlation discussed in chapter 11; the radii of intrinsically small, high surface brightness Sc spirals, for example, will encompass only the initial portion of the common Sc rotation curve by Rubin, Ford and Thonnard; such galaxies will be subject to many rotations, all of them very differential.

5.1.2 Type bc, c-Massive arms

The spirals in this section are characterized by having "massive" arms; there are principally two categories: those spirals where the uniformity of the arms being massive is maintained throughout [type examples are NGC 646, IC 1637, NGC 418 and NGC 7038], and those where the arms become almost abruptly thinner, excellent prototypes here being NGC 6907, and A0112-32, (plate 4).

Their diameters range from ∿13 kpc (A0922-24) to ∿85 kpc (NGC 7038 and NGC 646) and ∿90 kpc (NGC 309; photographed from the POSS O = blue print).

One clearly sees the distinction emphasized by Reynolds (1927) between broad and filamentous spiral arms, by comparing NGC 309 (this section), to NGC 1232 in the next section. The maximum width of the spiral arms of NGC 309 is some 6.5 kpc; in comparison, those of NGC 1232 are thinner by a factor of 1/3 and more.

It is interesting to contrast our photographs of these two galaxies to the photographs on page 32 of the "Hubble Atlas" (Sandage (1961)) - it is really only when "seen in perspective" on a uniform scale that one really appreciates the true difference in spiral arm texture.

Another point to note is how similar morphological patterns can occur on different linear scales; one might, for example, take A0112-32, principally a two-armed spiral with a diameter of 40 kpc, and compare it to the larger and much more massive two-armed galaxy NGC 646 [diameter 85 kpc].

The SB(s)c spiral NGC 418 (diameter ∿60 kpc) - whose arms are similar in texture to those in IC 1637 - bears a

degree of resemblance to M83 - but note the difference in size of 3:1 - once more demonstrating how similar spiral structure can occur on differing scale lengths.

5.1.3 Type bc, c - "Medium" Arms

Here we include those spirals whose arms are neither "massive" nor "weak". Good examples are NGC 5457 = M101, and NGC 1232. The latter galaxy is the largest in this section, with a diameter on the photograph of ∿70 kpc.*

On the intrinsically small side, we have NGC 5398, NGC 406 and A2125-38, with diameters of ∿22 kpc, ∿25 kpc and ∿33 kpc respectively.

An interesting feature of some of these galaxies is the presence of low surface brightness spiral arms which have a pitch angle markedly different from the arms of the main galaxy.

A prototype of such a galaxy would be NGC 4304 (diameter ∿44 kpc); one could well describe the main arms as "giving birth" to the secondary, fainter arms which form a more open spiral pattern. Another example is IC 2580, classified in the RC2 as SB(rs) bc.

Once again, this feature is present in NGC 7329 - a beautiful example of a type r variety in the de Vaucouleurs (1959) scheme. Pertaining to the ring itself, Kormendy (1979) finds that the sizes D of bars, rings and lenses for each morphological type do correlate well with the absolute magnitudes of the parent galaxies M_B, but notes that the form of the correlation

---

* We have printed NGC 1232 at its RC2 heliocentric velocity of 1720 km s^{-1}, corresponding to a redshift z = 0.006. The diameter is not affected if the corrected velocity is used instead; from the RSA, we have for NGC 1232 v = 1782 km s^{-1}, v_o = 1775 km s^{-1}, both of which still give z = 0.006.

5.1.4 Type bc, c Spirals - Weak Arms

The IIIa-J survey is ideally suited for revealing the extent of the weak, faint outlying spiral arms which generally characterize this group: these arms can increase the diameter of the prominent central spiral region by a factor of about 2. As examples, we cite NGC 3059 and NGC 5483, both with overall diameters of the order of 30 kpc; the higher surface brightness inner region measuring in these two galaxies ∿13 kpc and ∿15 kpc respectively. Another good example is A1125-36, where faint spiral arms can be traced to ∿25 kpc on either side of the nucleus, yielding a total diameter of 50 kpc; once again, the more conspicuous central region occupies half this extent.

IC 4721 has a measurable diameter on our J-photograph of at least 65 kpc*; the spiral arms become so tenuous that it is difficult to assign a meaningful isophotal diameter. The de Vaucouleurs diameter is 45 kpc (table 6, col. 9).

We stress here that it is the spiral arms themselves which generally fade to the limiting detectable surface brightness of the survey, and not a surrounding envelope or region which does not have spiral structure.

NGC 5161, diameter ∿65 kpc, provides an illustration of how careful one has to be when assigning luminosity types for inclined systems: the luminosity class as listed in the

---

* IC 4721 is printed assuming v = 2095 km s^{-1}, z = 0.007, which is not the value given in the list of 719 optical redshifts by Sandage (1978). Sandage (private communication) suggests that his published redshift refers not to IC 4721, but to the higher surface brightness elliptical 2:2 to the south. The above value of 2095 km s^{-1} is that determined by Corwin.

RC2 is IV:, whereas Sandage assigns this galaxy the classification Sc(s) I.

Weak but well defined outer spiral arms are present in the SBbc(s) I-II spiral NGC 1187; to a lesser degree in NGC 7059.

The differentiation between a relatively high surface brightness central region and faint outer regions is less marked in NGC 4219 and NGC 1448, but due allowance for inclination effects (particularly in NGC 1448) have to be made. Their (projected) diameters are both of the order of 50 kpc.

5.1.5 Galaxies - Type bc, c - with Two Distinct Spiral Components

The galaxies illustrated here are comprised of two definite and distinct spiral components:

(1) a central region of spiral structure - well resolved on the ESO B Survey - where the surface brightness is very high, and

(2) surrounding spiral arms of very low surface brightness.

The best type example here is NGC 2090; its diameter is ∿90 kpc, more than twice the value of the de Vaucouleurs diameter computed for this galaxy in table 6.

NGC 2369 is reminiscent of the "characteristic shape" of an active spiral as proposed by Fairall (1979b, fig. 1), but once again the central region resolves into spiral structure. The overall diameter (i.e. including the faint arms) is ∿63 kpc.

NGC 7126 in many ways resembles NGC 2090 discussed above; the saturated inner region has a diameter of ∿15 kpc, while the total extent is over 60 kpc.

An another example of this type of galaxy, we include NGC 7531. Its diameter on the photograph is ∿48 kpc; the de Vaucouleurs diameter is ∿29 kpc.

In the above four examples, it is at first sight difficult to believe that one is in fact looking at spirals of type bc and c, with their "prominent bulges" on the IIIa-J Survey.

Galaxies - bc, c - with Predominantly Saturated Images on IIIa-J Survey

NGC	Classification
2082	Sc(s) II-III
2397	Sc(s) III
1437	Sc(s) II*
1310	SA(s) c:
6215	Sc(s) I.8
440	SA(s) bc:
5236	SBc(s) I-II
1511	Sc pec
7361	Sc II-III:
3175	Sc(s) III: pec
6221	Sbc(s) II-III
1792	Sc(s)
3568	SB(s) c:
4835	Sc(s) (I-II)

* Classified in the RC2(1976) as SB(rs) a

Massive armed bc, c Spirals

Galaxy	Classification
A0922-24	SAB(rs)bcp
A1213-34	SB(s)c
A0112-32	SAB(s)c:
A2004-29	SAB(s)c
IC 4366	SA(r)cp
A1018-37	SA(rs)bc?
NGC 6907	SBbc(s) II
IC 1637	SA(rs)bc:
NGC 418	SB(s)c
NGC 7038	Sbc(s) I.8
NGC 646	SA(s)cp
NGC 309	Sc(r) I

Medium Arm Type bc, c Galaxies

Galaxy NGC	Classification
5398	SBc(s) II
406	Sc(s) II
A2125-38	SA(r)c:
6699	Sbc(s) I.2
6754	Sbc(s) II-III
IC2580	SB(rs)bc
6780	Sbc(rs) I-II
5967	Sc(rs)II.2
4304	SBbc(s)II
4852	SAc:
5457	Sc(s) I
2466	SAc:
A1517-36	SB(s)bc:
A0253-27	SA(r)c:
7329	SBbc(r) I-II
7125	Sc(rs) I
IC4837	[SB(s)cdp] Sc(s) II-III
1232	Sc(rs) I

Weak Armed Type bc, c Spirals

NGC	Classification
3059	SBc(s) III
5483	SBbc(s) II
7059	Sc(s) II
1187	SBbc(s) I-II
4219	Sbc(s)(II-III)
1448	Sc(II):
A1125-36	SB(r)bc:
IC4721	SBc(s)II
5161	Sc(s) I

Type bc, c Galaxies with two distinct Spiral Components

Galaxy NGC	Classification	
7531	Sbc(r) I-II	(RSA)
7126	SA(rs)c	(RC2)
2369	Sbc(s) I pec	(RSA)
2090	Sc(s) II	(RSA)

UNIFORM LINEAR SCALE

0 10 20 30 40 50 kpc

TYPE bc,c SPIRALS

SATURATED/PREDOMINANTLY SATURATED IMAGES ON IIIa–J SURVEY

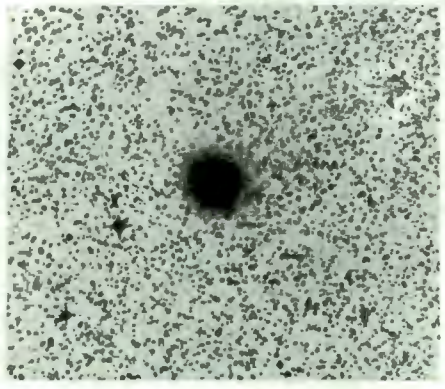

NGC 2082

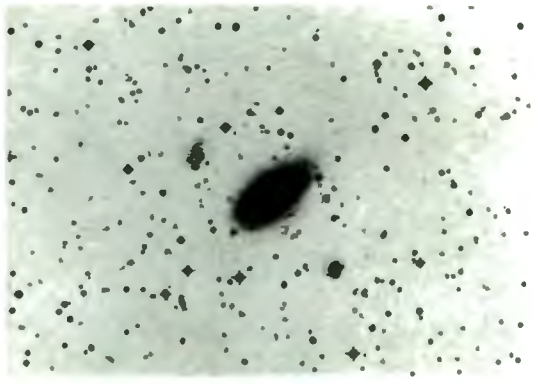

NGC 2397

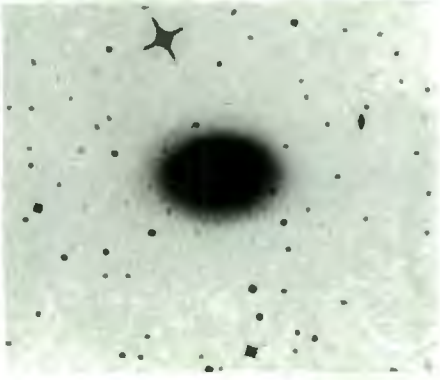

NGC 1437

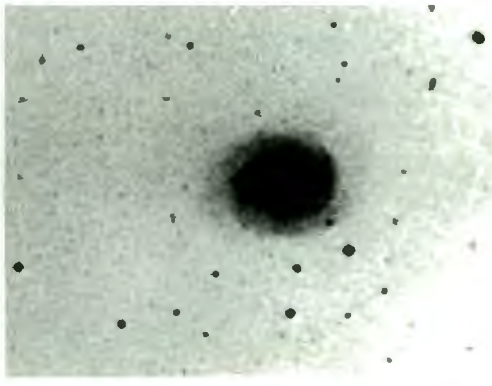

NGC 1310

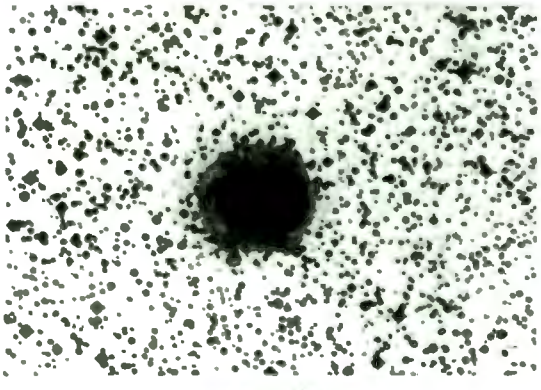

NGC 6215

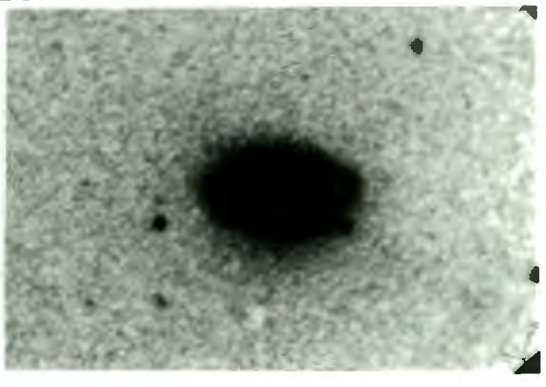

NGC 440

Plate 2

UNIFORM LINEAR SCALE

0 10 20 30 40 50 kpc

TYPE bc,c SPIRALS

SATURATED/PREDOMINANTLY SATURATED IMAGES ON IIIa–J SURVEY

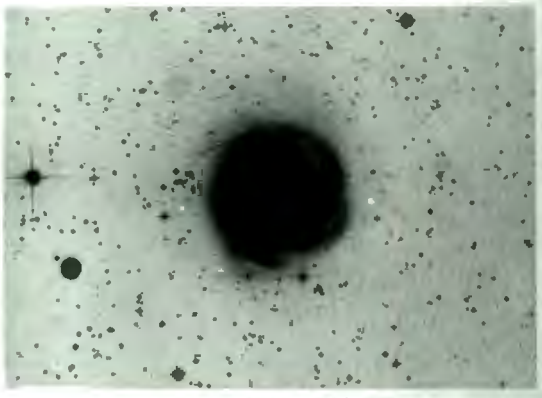

NGC 5236 (M 83)

NGC 1511

NGC 7361

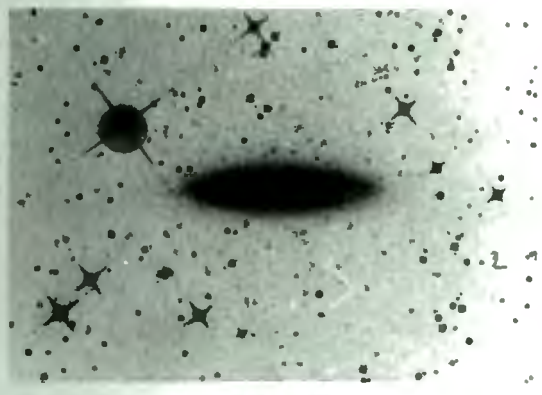

NGC 3175

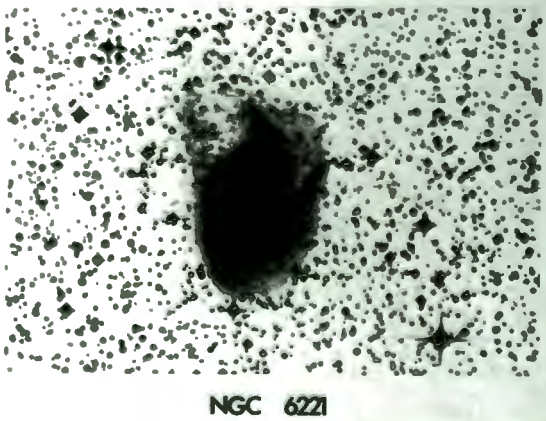

NGC 6221

NGC 1792

Plate 3

UNIFORM LINEAR SCALE

0 10 20 30 40 50 kpc

TYPE bc,c SPIRALS

SATURATED/PREDOMINANTLY SATURATED IMAGES ON IIIa–J SURVEY

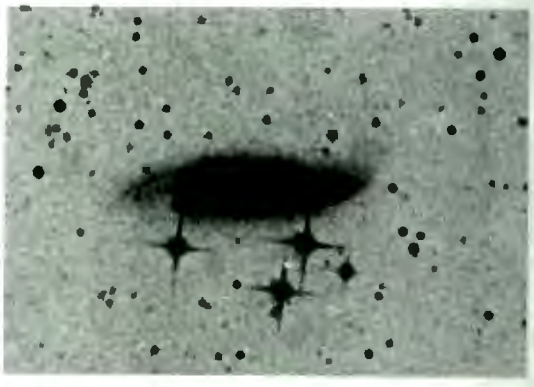

NGC 3568

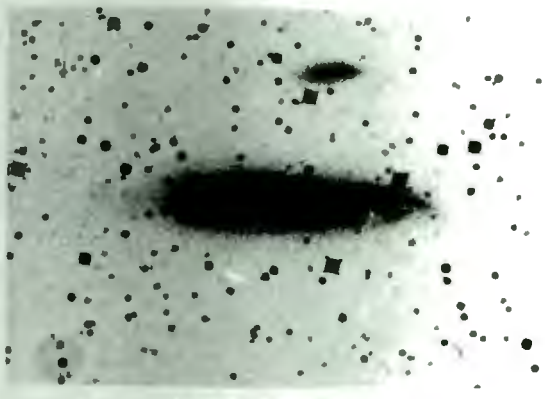

NGC 4835

MASSIVE ARMS

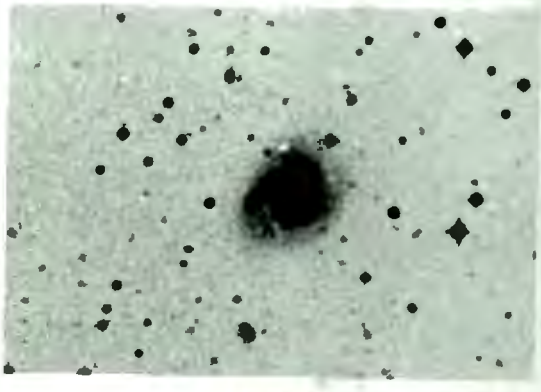

A0922–24

A1213–32

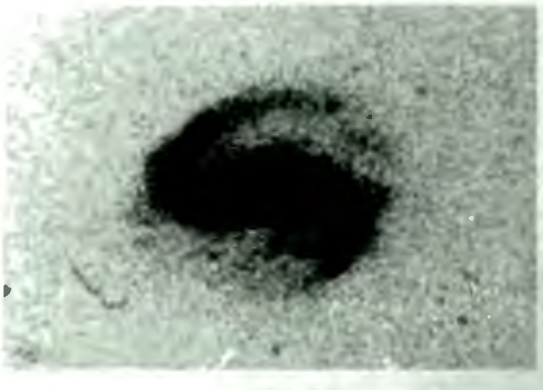

A0112–32

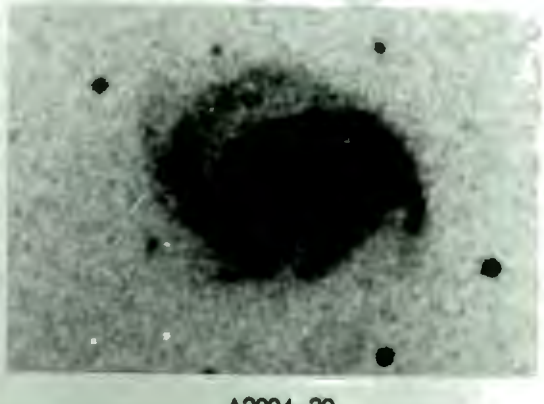

A2004–29

Plate 4

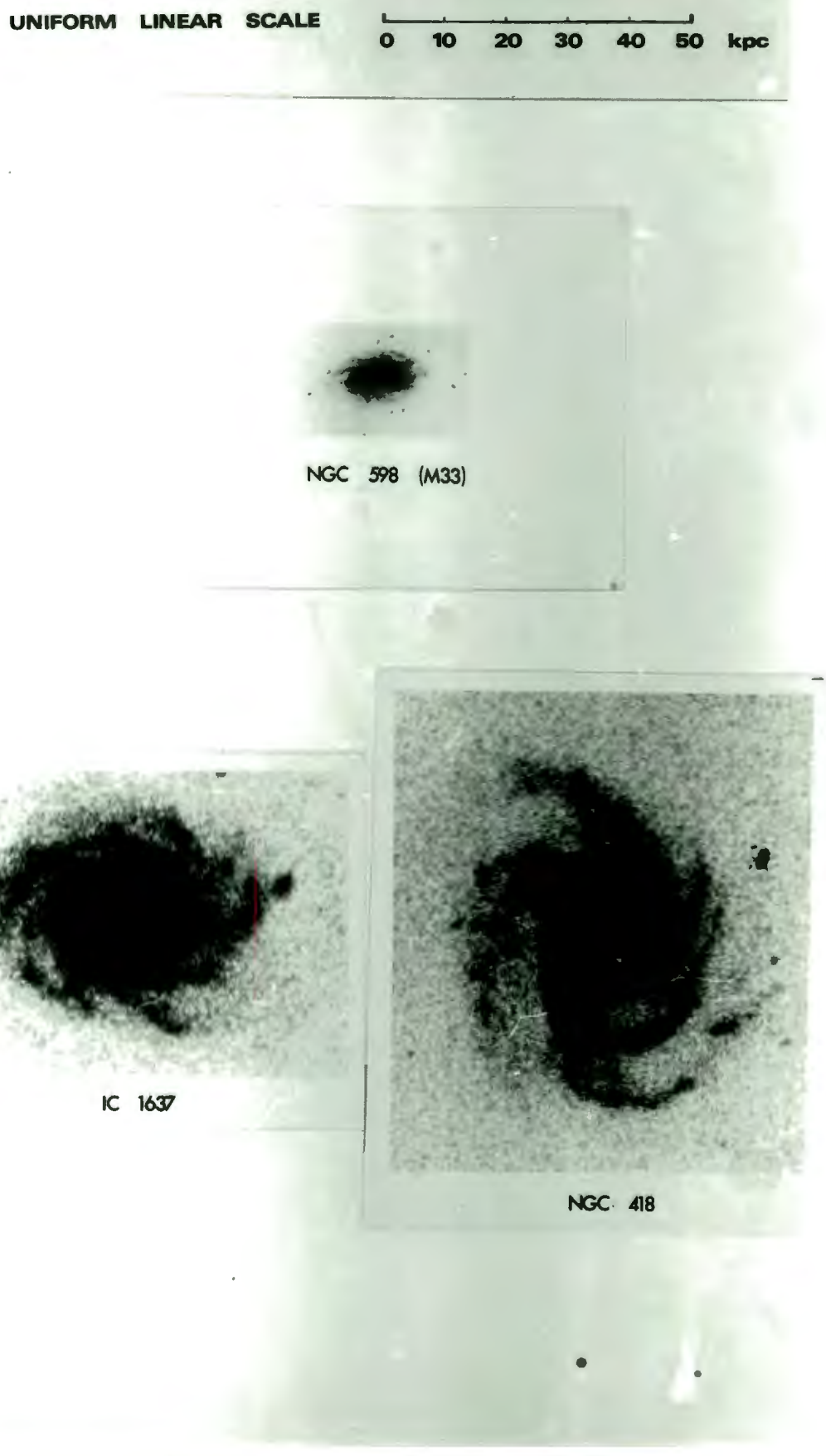
UNIFORM LINEAR SCALE
0 10 20 30 40 50 kpc
NGC 598 (M33)
IC 1637
NGC 418

Plate 5

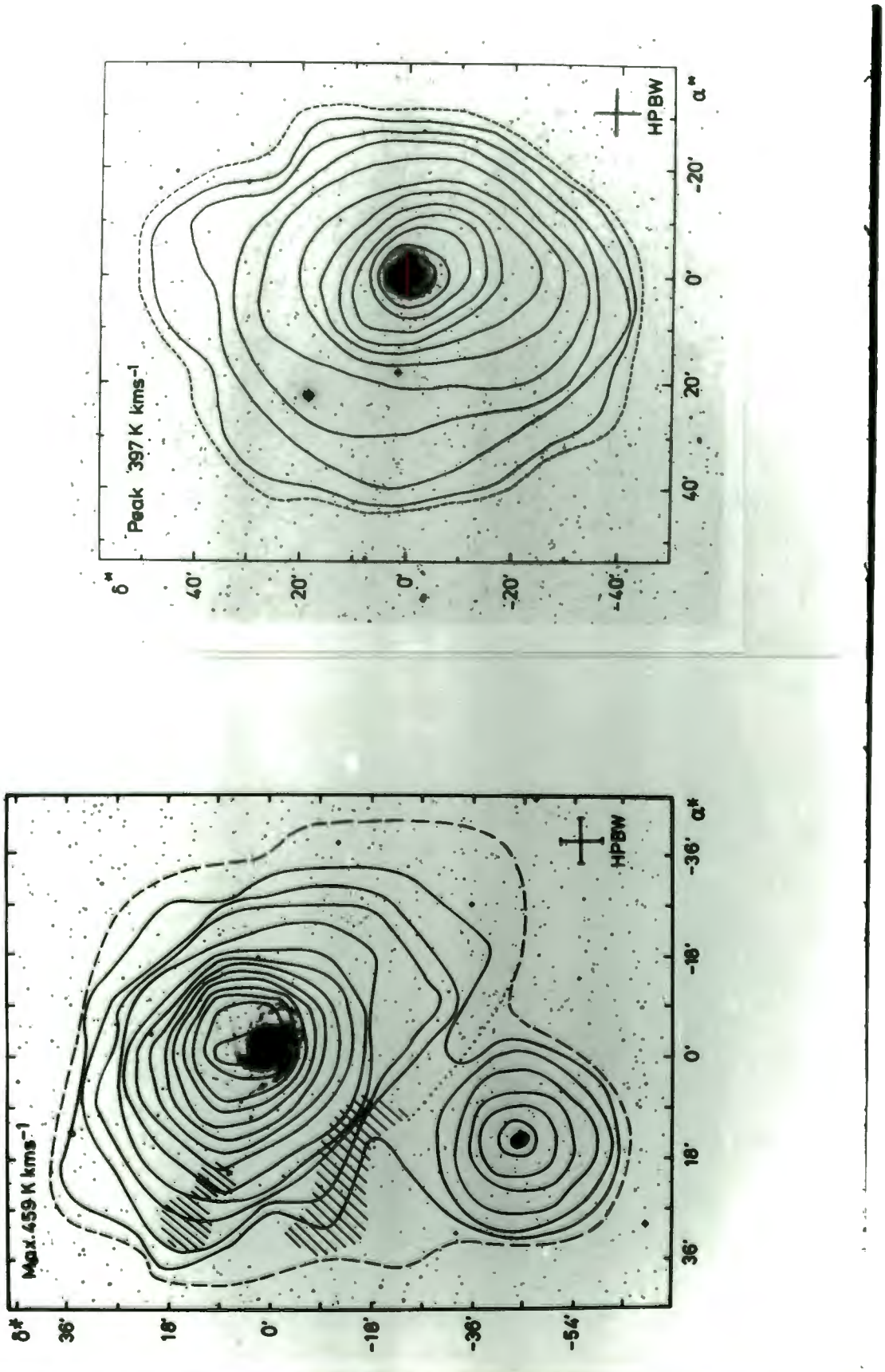
Peak 397 K kms⁻¹
HPBW
δ*
α*
40'
20'
0'
-20'
-40'
Max.459 K kms⁻¹
HPBW
δ*
α*
36'
18'
0'
-18'
-36'
-54'

Plate 6

UNIFORM LINEAR SCALE

0 10 20 30 40 50 kpc

TYPE bc,c SPIRALS

MASSIVE ARMS

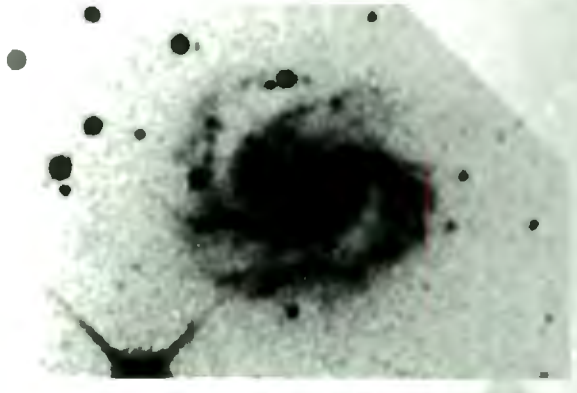

IC 4366

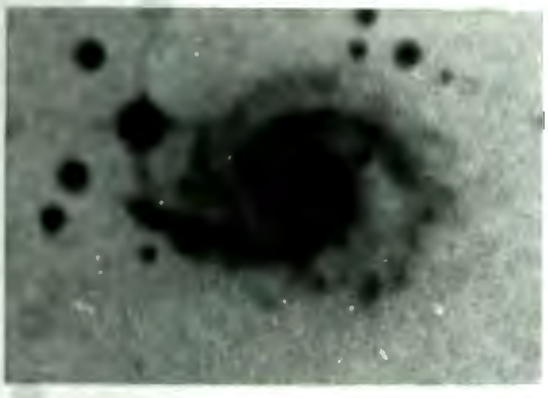

A1018–37

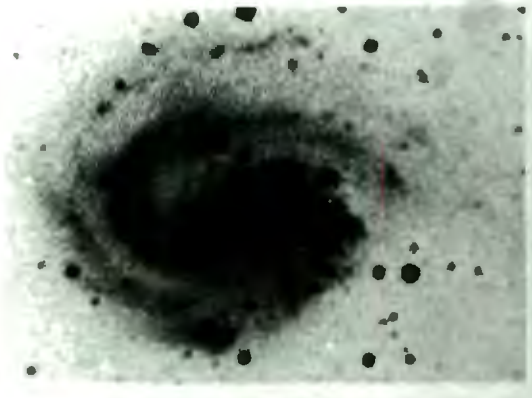

NGC 6907

IC 1637

NGC 418

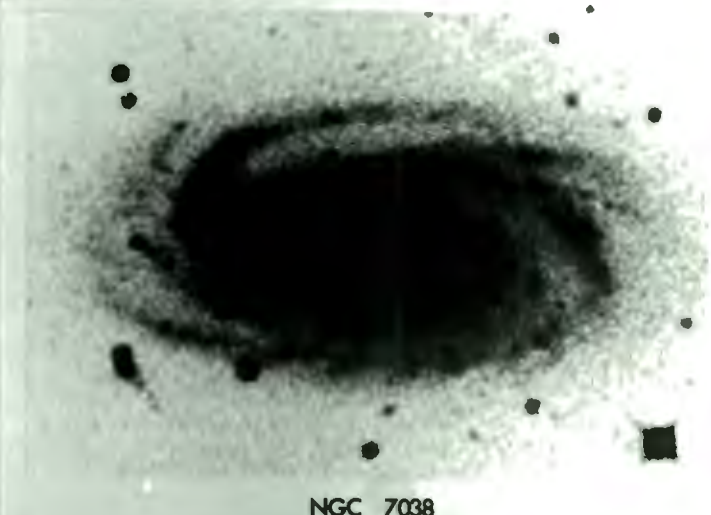

NGC 7038

Plate 7

UNIFORM LINEAR SCALE

0 10 20 30 40 50 kpc

TYPE bc,c SPIRALS MASSIVE ARMS

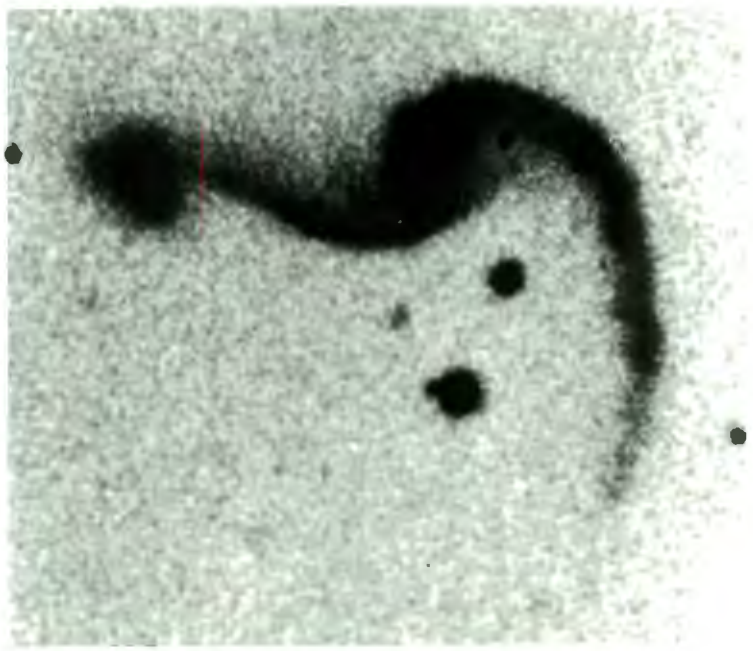

NGC 646

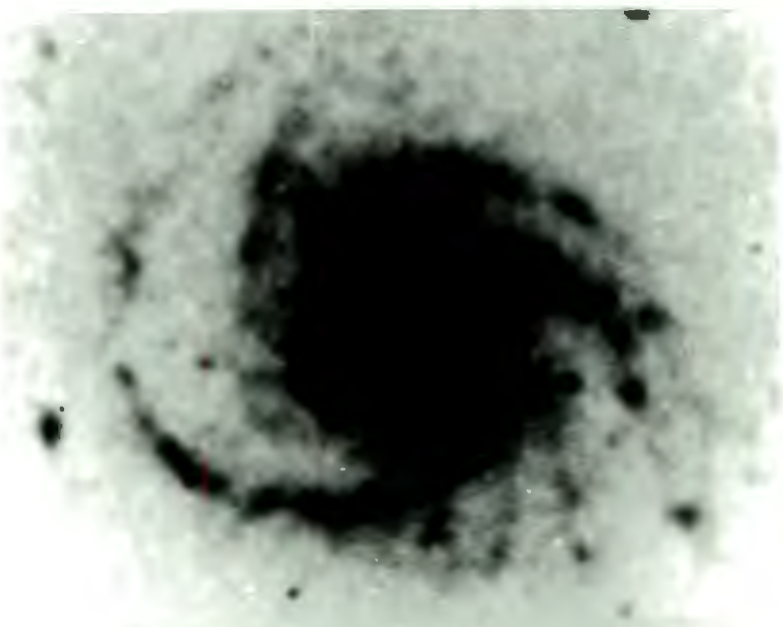

NGC 309

Plate 8

UNIFORM LINEAR SCALE

0 10 20 30 40 50 kpc

TYPE bc,c SPIRALS

MEDIUM ARMS

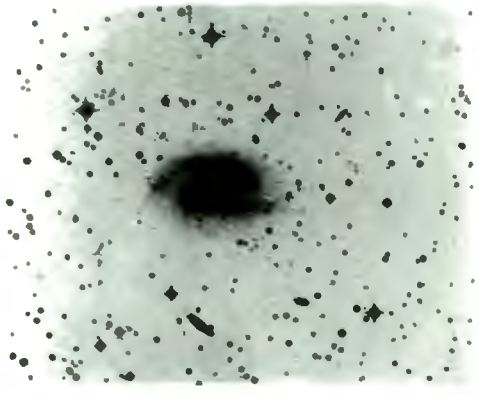

NGC 5398

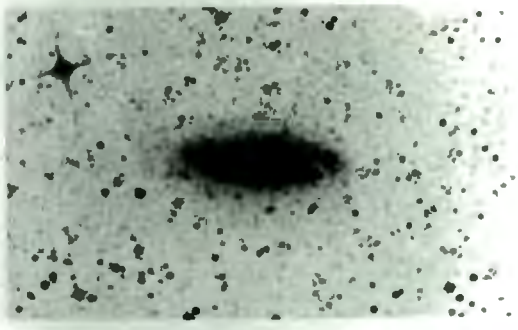

NGC 406

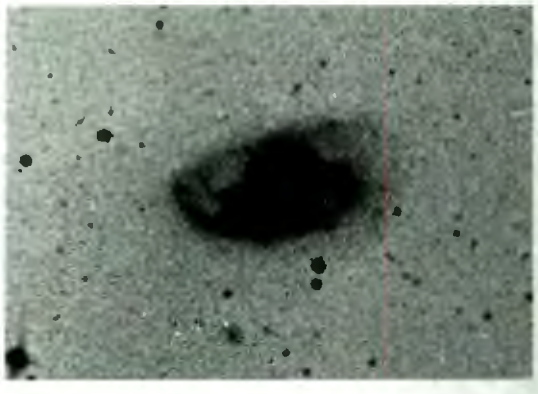

A2125–38

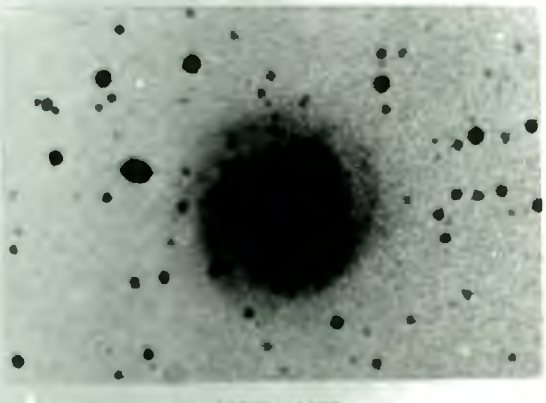

NGC 6699

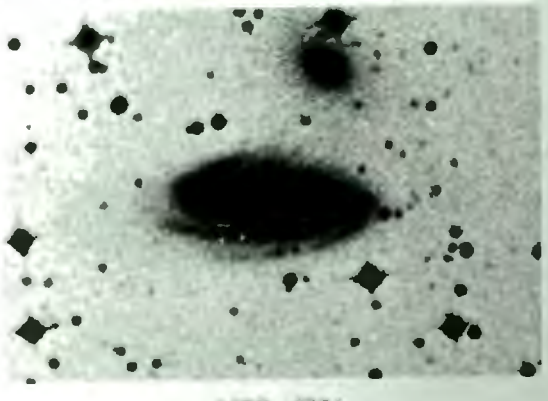

NGC 6754

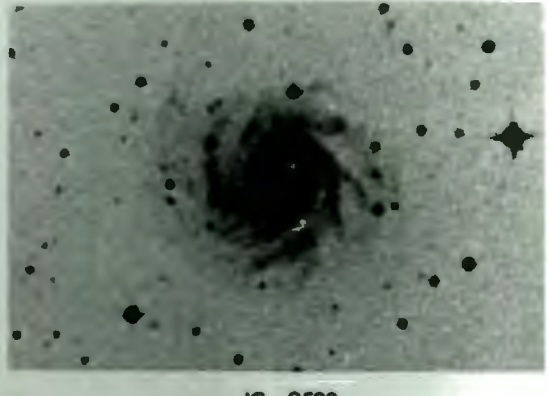

IC 2580

Plate 9

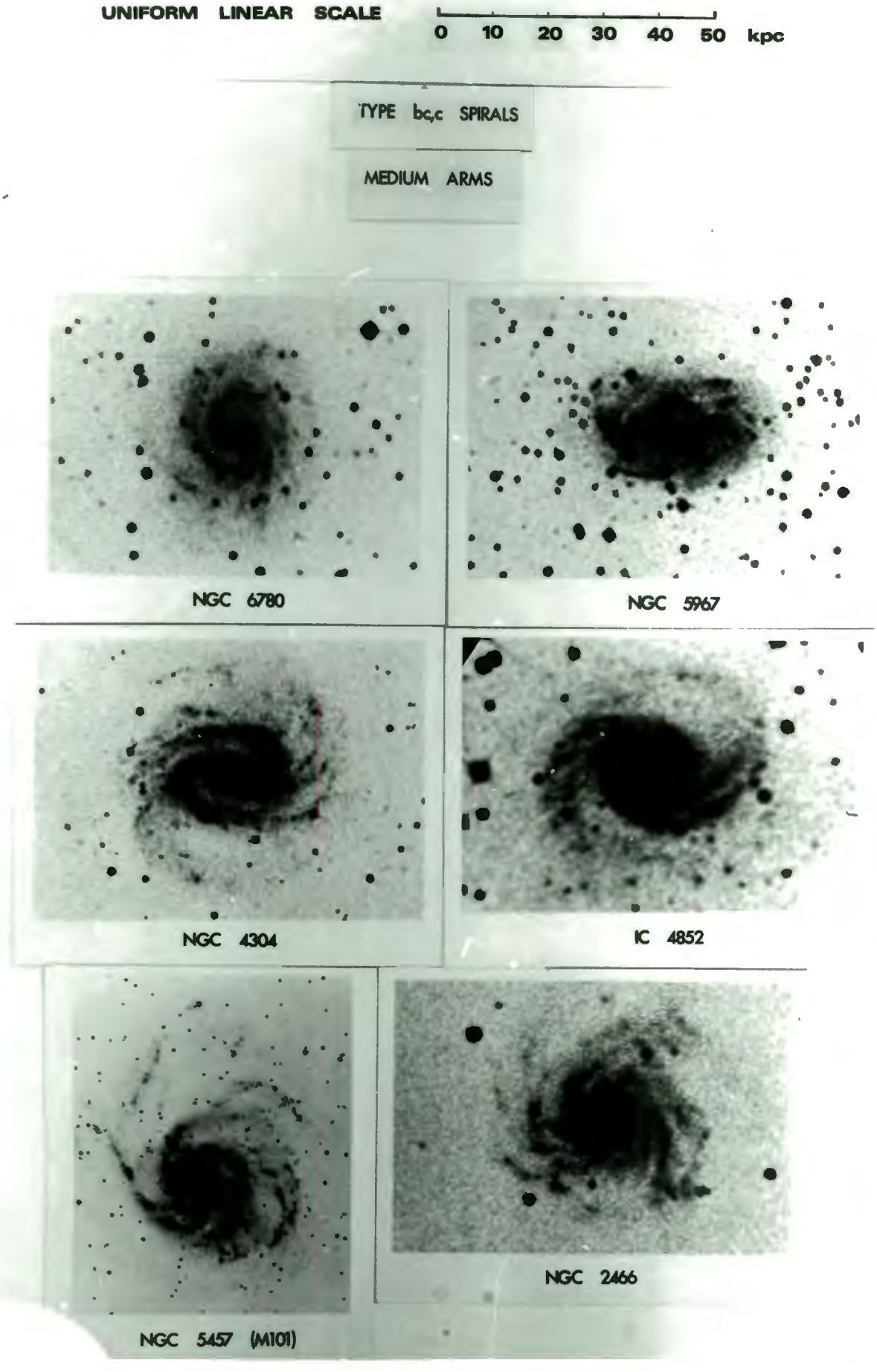
UNIFORM LINEAR SCALE
0 10 20 30 40 50 kpc
TYPE bc,c SPIRALS
MEDIUM ARMS
NGC 6780
NGC 5967
NGC 4304
IC 4852
NGC 5457 (M101)
NGC 2466

Plate 10

UNIFORM LINEAR SCALE 0 10 20 30 40 50 kpc

TYPE bc,c SPIRALS

MEDIUM ARMS

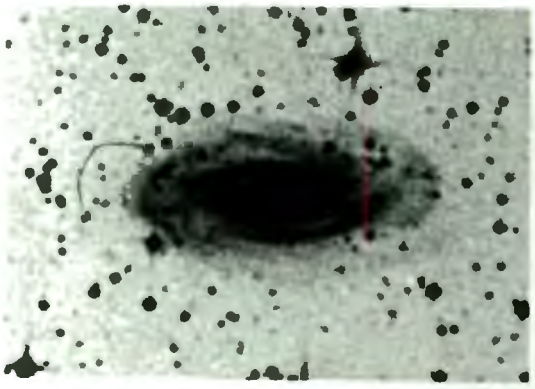

A1517–36

A0253–27

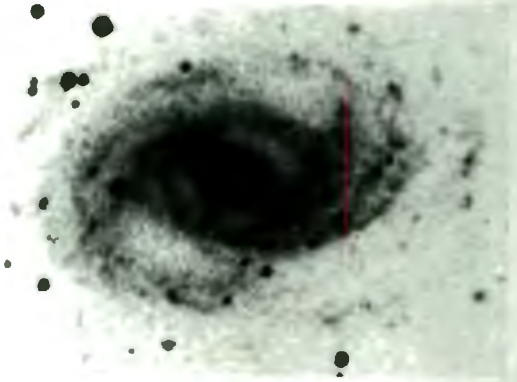

NGC 7329

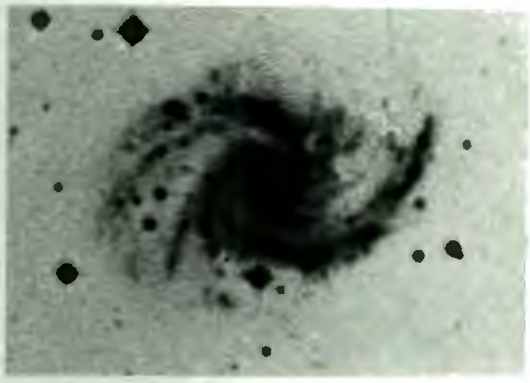

NGC 7125

IC 4837

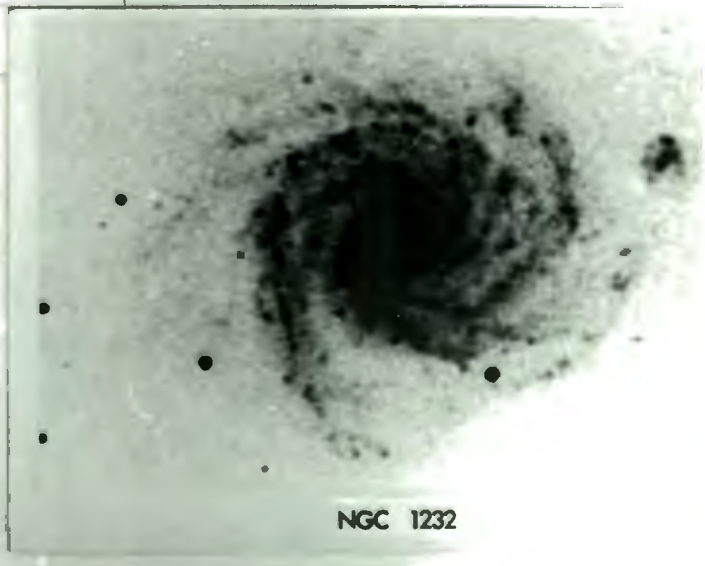

NGC 1232

Plate 11

UNIFORM LINEAR SCALE

0 10 20 30 40 50 kpc

TYPE bc,c SPIRALS

WEAK ARMS

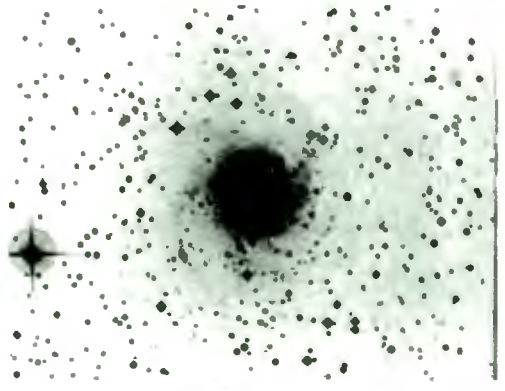

NGC 3059

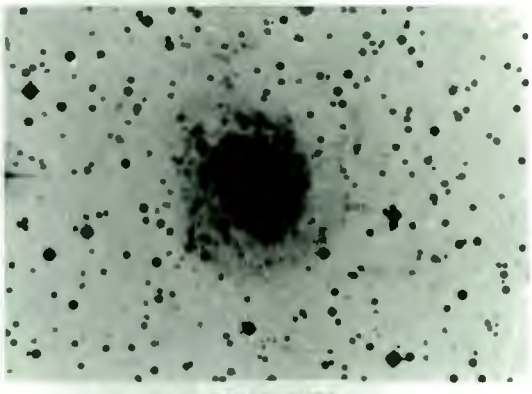

NGC 5483

NGC 7059

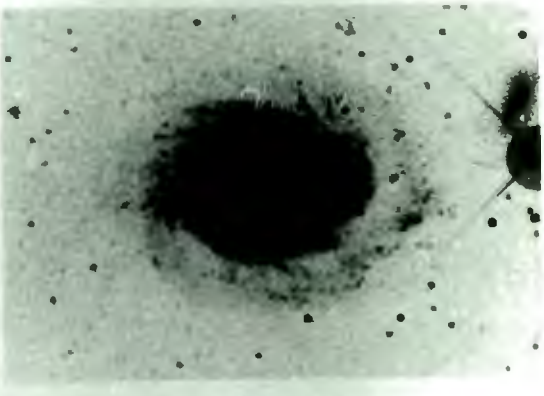

NGC 1187

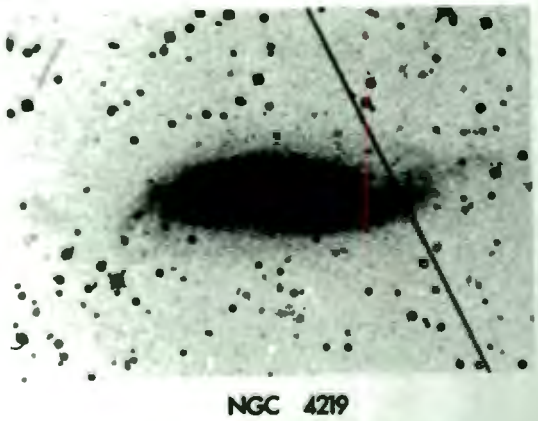

NGC 4219

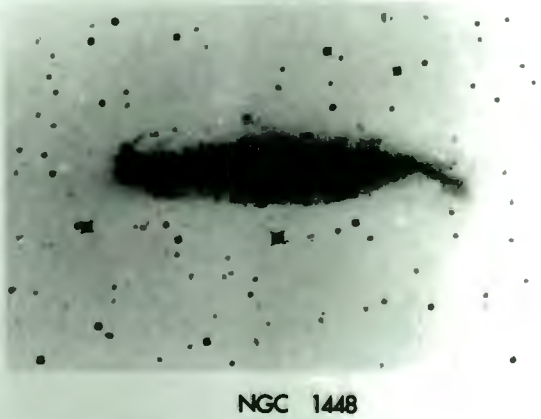

NGC 1448

Plate 12

UNIFORM LINEAR SCALE

0 10 20 30 40 50 kpc

TYPE bc,c SPIRALS

WEAK ARMS

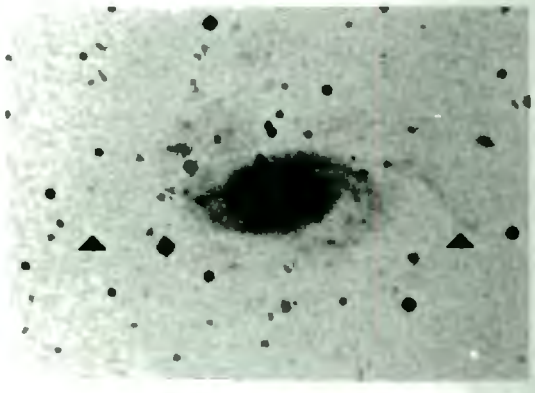

A1125–36

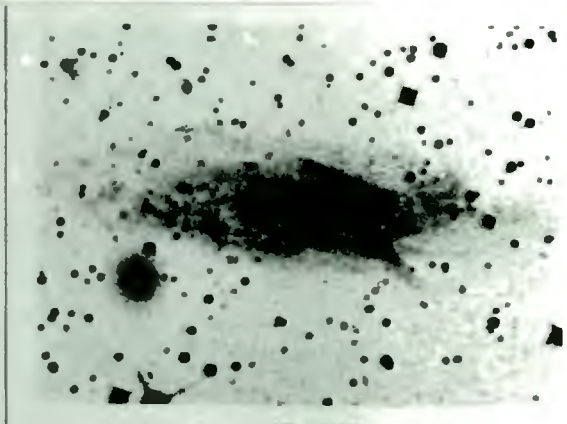

IC 4721

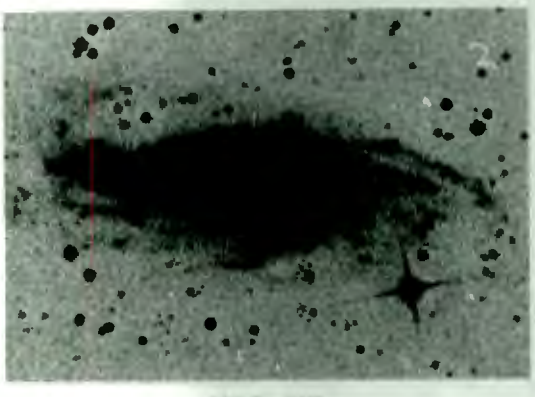

NGC 5161

Plate 13

UNIFORM LINEAR SCALE

0 10 20 30 40 50 kpc

GALAXIES—TYPE bc,c—WITH TWO DISTINCT SPIRAL COMPONENTS

NGC 7531 NGC 7126

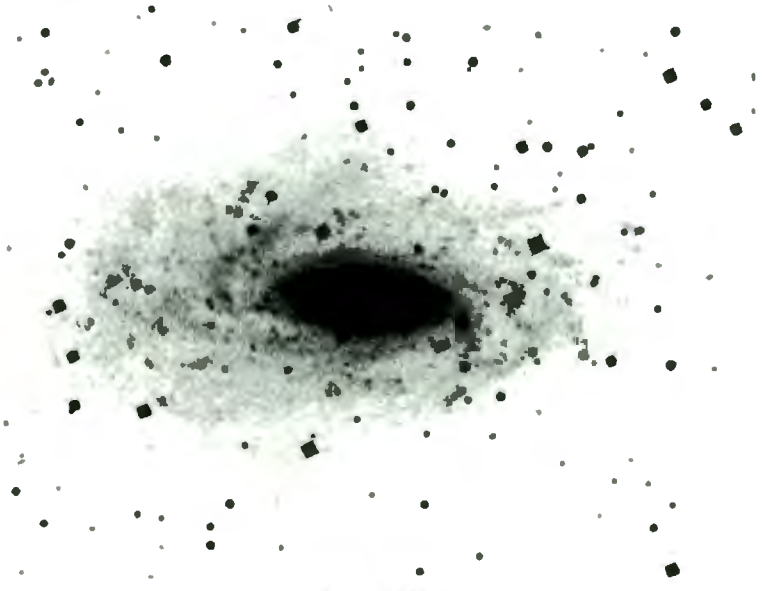

NGC 2090

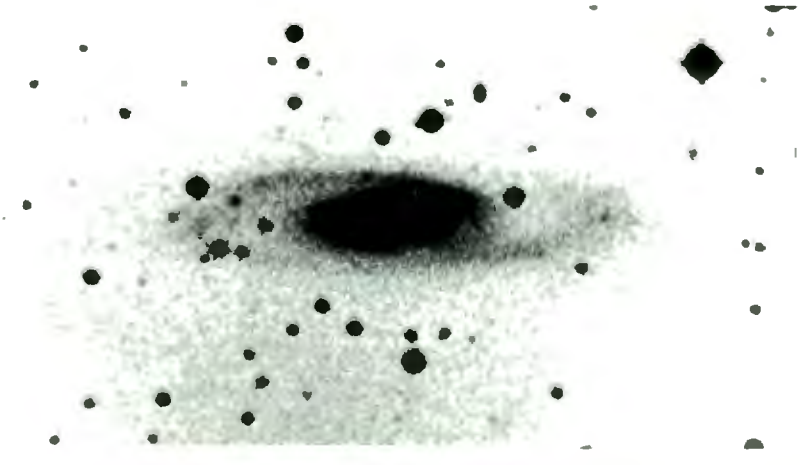

NGC 2369

Plate 14

5.2 Spirals of type ab, b

A surprising result of the present investigation is that the large range in diameters seen in the type c spirals is not restricted to that group - we mention here the b type barred spiral NGC 6872, the largest SB galaxy known (Block (1979)). Thus, we are reminded of the remark made earlier in chapter 3 concerning Hubble types: one cannot on purely morphological grounds decide whether a spiral of a particular Hubble type is large or small.

One also reflects on the general viewpoint concerning the diameters of spirals in the 1960's; that M31 and M101 were representative of typically large galaxies within their respective Hubble types. M31 is illustrated on our scale in plate 55.

As in the previous section, we present our type ab, b spirals in various categories: saturated image, strong "massive" arms, "medium" arms, "weak" arms and also discuss some galaxies which are best described separately.

5.2.1 Type ab, b - Saturated Images on J- Survey

As with the type bc, c spirals, we include in this section those galaxies assigned type ab or b in the RSA or RC2, and whose images are predominantly saturated on the J-survey. Two obvious examples here are IC 4219 and NGC 434. The diameter of the former - the intrinsically smallest within this subgroup - is ∿22 kpc, while the largest, NGC 434, has a diameter on the IIIa-J photograph of ∿52 kpc.

We remarked earlier that some high surface brightness bc, c spirals appeared to be contained in a faint surrounding envelope; here, one sees evidence for this in IC 4219 - note the ragged edge appearance of the spiral arms in that galaxy - and particularly in NGC 6300.

The appearance of NGC 434 on the J- survey is more like a large elliptical than a spiral - even on the ESO B film copy, the spiral structure is poor.*

Finally, we include NGC 3241 (diameter ∿30 kpc) and NGC 5188 (diameter ∿35 kpc) as two less striking examples of this type of galaxy.

---

* The galaxy is assigned class Sab(s) in the RSA, SAB(s) ab in the RC2.

Type ab, b Galaxies with Predominantly Saturated Images on the IIIa-J Survey

Galaxy	Classification
IC 4219	SB(rs)b: p
NGC 3241	Sb(r) II
NGC 6300	SBb(s) II pec
NGC 5188	SB(rs)b: p
NGC 434	Sab(s) (RSA) SAB(s)ab (RC2)

UNIFORM LINEAR SCALE

0 10 20 30 40 50 kpc

TYPE ab,b

SATURATED/PREDOMINANTLY SATURATED IMAGES ON IIIa–J SURVEY

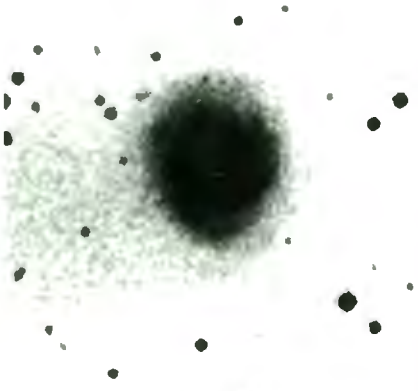

IC 4219

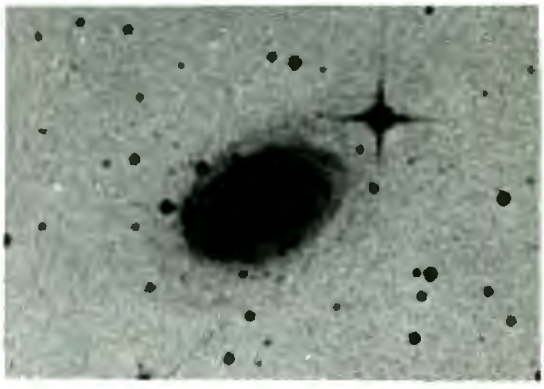

NGC3241

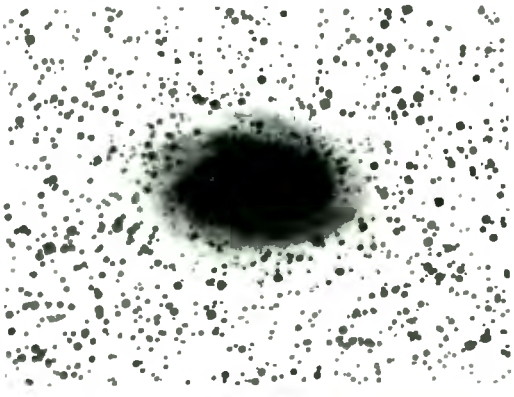

NGC 6300

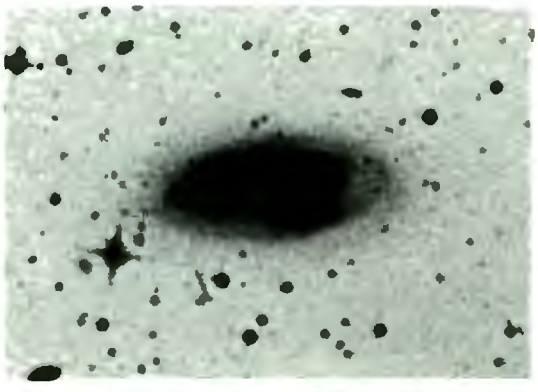

NGC 5188

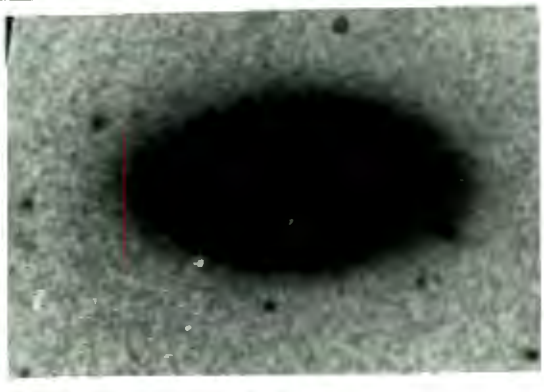

NGC 0434

Plate 15

5.2.2 Type ab, b - Massive Arms

The clearest type example here is SBb(rs) II galaxy NGC 613 (diameter ∿45 kpc), with the massive, high surface brightness spiral arms magnificently portrayed on the IIIa-J photograph.

Another example is NGC 1288, with a diameter of ∿57 kpc. This galaxy, type Sab(r) I-II, has a completely different morphology to that seen in NGC 613, with the arms clearly organized about the nucleus.

NGC 2196 is of de Vaucouleurs type R', NGC 6753 of type R. In both cases, there is a tendency for the outer arms to become fragmentary, particularly in NGC 6753.* On our photographs, NGC 2196 and NGC 6753 have diameters of ∿37 kpc and ∿41 kpc respectively.

---

* It is interesting to compare our photograph of NGC 6753 to that of the type R, class Sa galaxy NGC 1291 in fig. 10 of the "Annual Report of the Director of the Hale Observatories: 1978-1979".

5.2.3 Type ab, b Spirals with Medium Arms

Three of the galaxies in this category are (possible) members of well known southern clusters/groups: NGC 1365 (Fornax cluster), NGC 3312 (Hydra cluster [= Abell 1060]), and NGC 6872 (Pavo Group).

We begin by considering NGC 1365 and NGC 6872. Both have the same Hubble type and luminosity class - SBb(s) I in the RSA for the former, and SBb(s) I for the latter (Sandage (1978)), but their (major) diameters differ by a factor of about 2. In NGC 1365, we see that the spiral arms "curve back" on themselves, while in NGC 6872 the two arms are, at large distances from the nucleus, almost parallel. Thus, for NGC 1365, we find a diameter on the photograph of ∿90 kpc,* while the value for NGC 6872 - from A to B - is more than twice this extent: ∿200 kpc.† NGC 6872 is thus the largest barred spiral known (Block (1979)).

With regard to the inner regions of these two galaxies (besides showing an unmistakable bar on the ESO B film copies), one can say that the nucleus of NGC 6872 is bright and circular, while NGC 1365 has a peculiar "hot-spot" nucleus [c.f. Sérsic and Pastoriza (1965)]. It has been suggested that

---

* For NGC 1365, both the heliocentric and corrected velocities from the RC2 give a redshift of z = 0.005. This agrees with the group recessional velocity of the Fornax cluster as given in table 2 of Sandage (1975b). [The diameter for NGC 1365 of 200 kpc given by Jones and Jones (1980) is incorrect].

† Corrected for inclination and for foreground galactic absorption (following the precepts in chapter 2, section 3 and equation (2.13)), we find, adopting a major to minor diameter ratio of 1.5 as in Block (1979), a corrected diameter of some 220 kpc: of the same order of magnitude - with our value of H_o - as the largest identified Sc spiral UGC 2885 by Rubin, Ford and Thonnard (1980).

NGC 1365 is the source of X-ray emission, but the error box of the OSO 8 satellite observations (Bunner and Sanders (1978)) includes the Seyfert 2 galaxy NGC 1386 (Phillips and Frogel (1980)) and the radio galaxy Fornax A (= NGC 1316).

We noted that some of those galaxies with "medium" arms within Hubble types bc and c were characterised by having low surface brightness spiral arms with different pitch angles to those of the main galaxy. Such could be the case with NGC 1365, although due allowance must be made for inclination effects.

NGC 3312 is classified in the RSA as Sab(r); it has a diameter of ∿48 kpc.* Its rather central position in the Hydra cluster is unusual, as such regions for (relatively) rich clusters as Hydra are almost exclusively the domain of ellipticals.

Returning to the other galaxies included here, NGC 3261 (diameter ∿55 kpc) presents faint outer spiral arms; along the arms, the surface brightness tends to decrease fairly abruptly.

In NGC 2815 (diameter ∿50 kpc), a regular outer spiral arm pattern is seen; the central region is of high surface brightness.

---

* As with any cluster galaxy, care must be taken when interpreting individual galaxy redshifts as distance indicators (c.f. remarks in chapter 2).

5.2.4 Type ab, b - Weak Arms

We discuss the two spirals assigned to this section in turn:

1. NGC 1425

The surface brightness of the central region is high; the spiral arms themselves are thin, patchy and portray a weak spiral structure. NGC 1425 is luminosity class II in the RSA. Its (major) diameter measures ∿57 kpc on the IIIa-J photograph.

2. NGC 7083

This spiral, with a diameter of ∿62 kpc, is assigned type bc in the RC2 (presumably on account of the greater degree of openness in the spiral arm pattern), but type b in the RSA.

The arms are once again patchy; this is particularly evident in one of the arms, where after a decline in surface brightness, the arm thickens for some 10 kpc (projected) and then becomes extremely tenuous and fuzzy.

5.2.5 Type ab, b - Edge-On

The range in linear diameter is impressive - from the smallest (IC 1913, diameter ∿11 kpc*), to IC 4351 and NGC 4565, with diameters of the order of 100 kpc.

The appearance of NGC 1380A on the ESO B Survey very much resembles that of an SOb/c type galaxy in classification scheme proposed by van den Bergh (1976; fig. 2) [a system based on disk-to-bulge ratios]. Its diameter on the J-photograph is ∿20 kpc.

IC 1970 shows a thin outer disk extending to ∿27 kpc. It is assigned type Sb:sp. in the RC2.

IC 4351 (close to edge-on) and NGC 4565† have diameters of ∿96 kpc. Both these galaxies are classified in the RSA as Sb; the latter is illustrated on page 25 of the "Hubble Atlas" (Sandage (1961)) - it is also one of those galaxies in which warped HI planes have been found by Sancisi (1976, 1977).

---

* It would be interesting to obtain a large-scale plate of this galaxy for purposes of a more accurate classification - we remark that on the "Quick Blue" Survey, an almost featureless structure is seen.

† Photographed from the Blue print of POSS, and printed at a redshift of z = 0.004 (v = 1136 km s^{-1}, v_o = 1122 km s^{-1} (RC2)).

Spirals of type ab, b with massive arms

Galaxy	Classification
NGC 2196	Sab(s) I
NGC 6753	Sb(r) I
NGC 613	SBb(rs) II
NGC 1288	Sab(r) I-II

Type ab, b - Medium Arms

Galaxy NGC	Classification (RSA)
3312	Sab(r)
2815	Sb(s) I-II
3261	SBab(s) I
1365	SBb(s) I
6872	SBb(s) I

Spirals Type ab, b - Weak Arms

Galaxy	Classification (RSA)
NGC 1425	Sb(r) II
NGC 7083	Sb(s) I-II

Type ab, b - Edge-on

Galaxy	Classification
IC 1913	SBb? sp (RC2)
NGC 1380A	Sab? sp (RC2)
IC 1970	Sb: sp (RC2)
IC 4351	Sb (RSA)
	SA(s)b: sp (RC2)
NGC 4565	Sb (RSA)
	SA(s)b? sp (RC2)

UNIFORM LINEAR SCALE

0 10 20 30 40 50 kpc

TYPE ab,b

MASSIVE ARMS

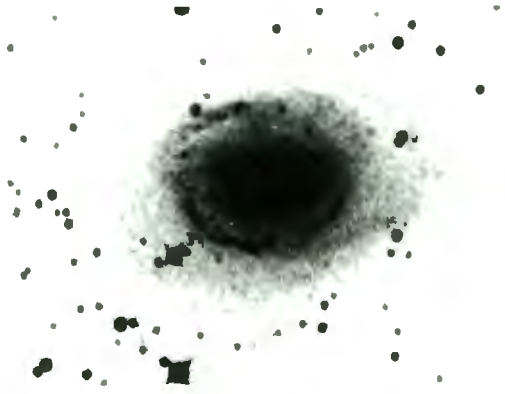

NGC 2196

NGC 6753

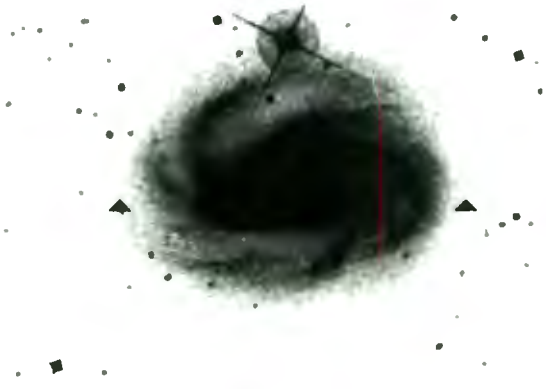

NGC 613

NGC 1288

MEDIUM ARMS

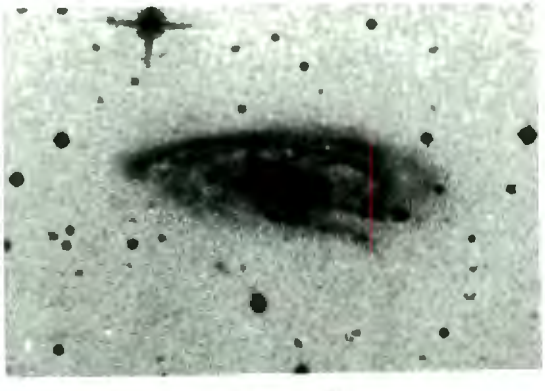

NGC 3312

NGC 2815

Plate 16

UNIFORM LINEAR SCALE

0 10 20 30 40 50 kpc

TYPE ab,b

MEDIUM ARMS

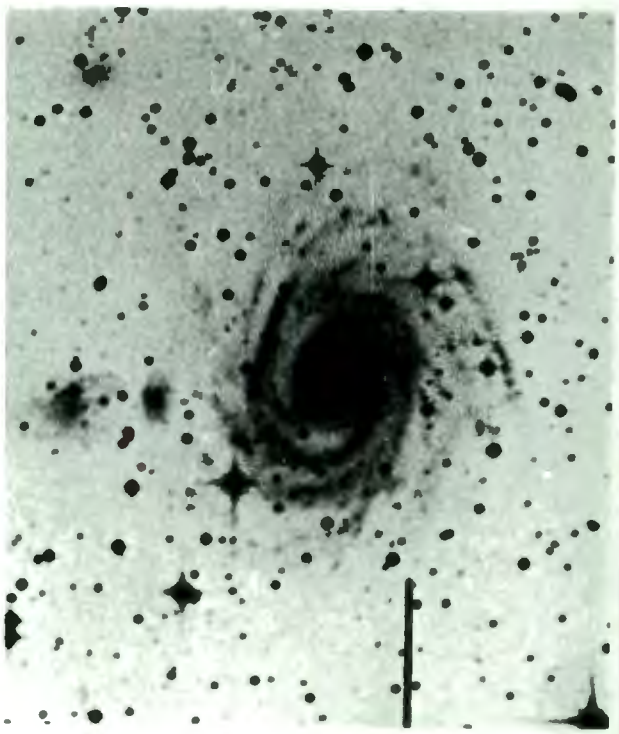

NGC 3261

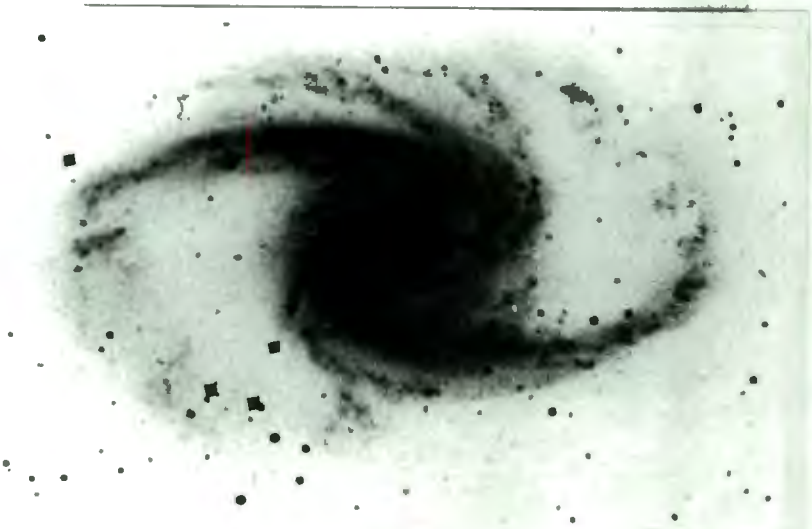

NGC 1365

Plate 17

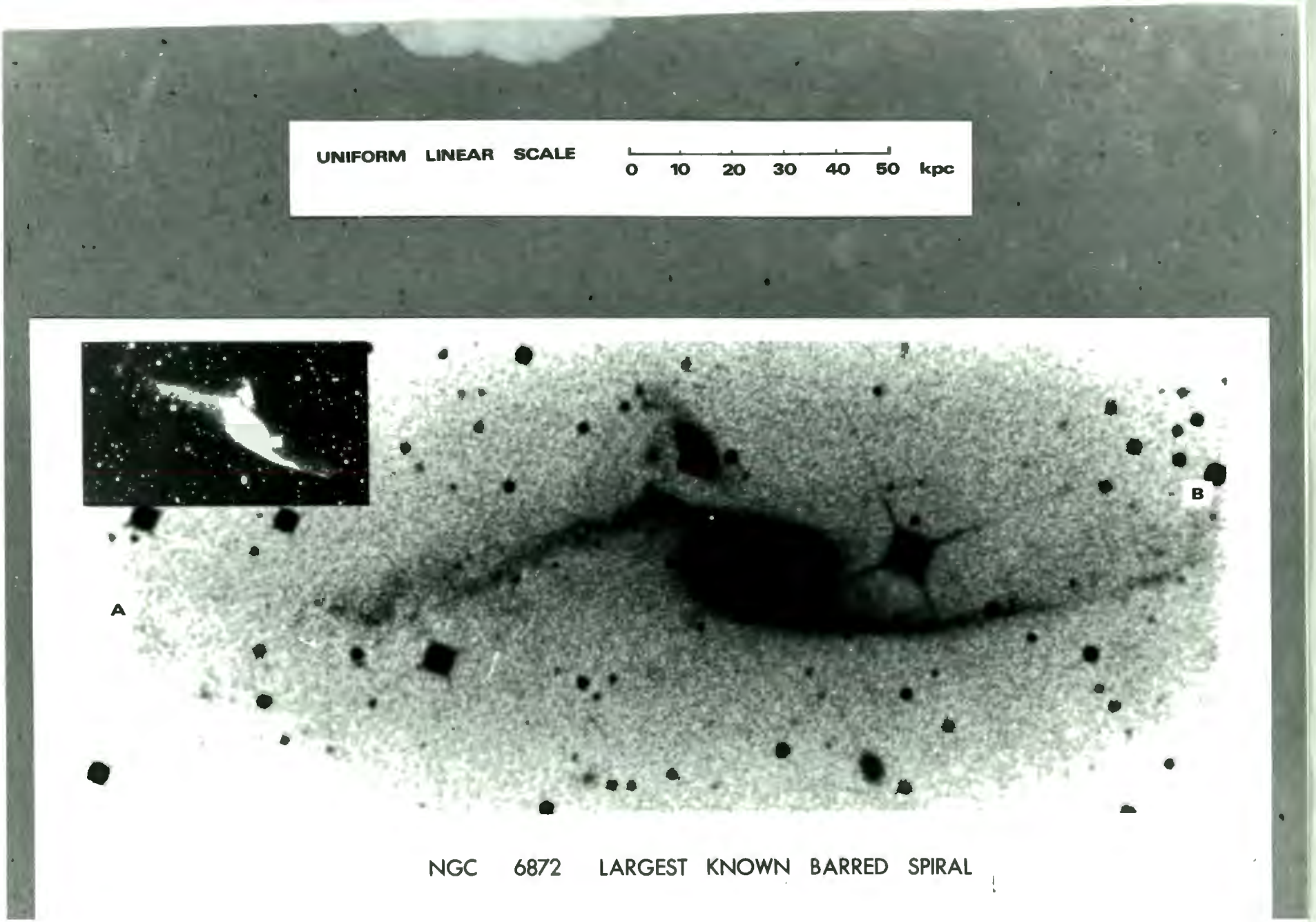

NGC 6872 LARGEST KNOWN BARRED SPIRAL

Plate 18

UNIFORM LINEAR SCALE

0 10 20 30 40 50 kpc

TYPE ab,b

WEAK ARMS

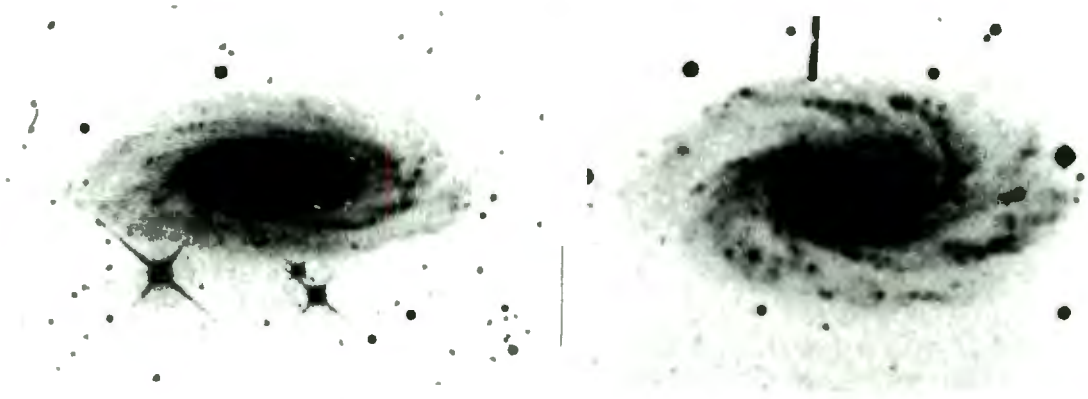

NGC 1425 NGC7083

EDGE–ON

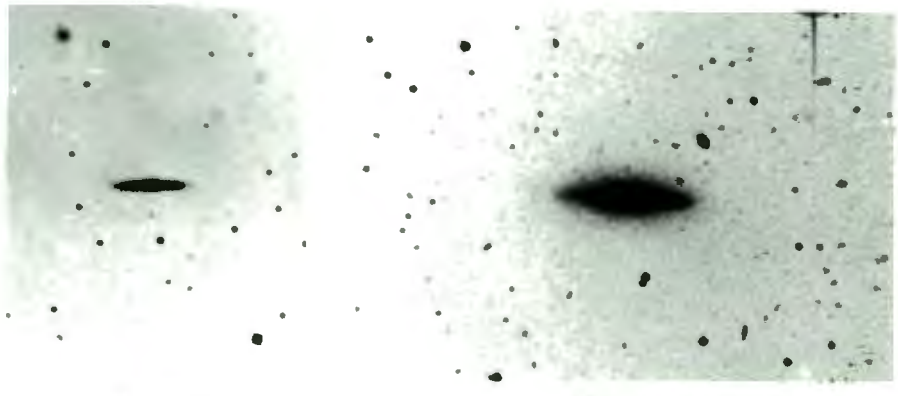

IC 1913 NGC 1380A

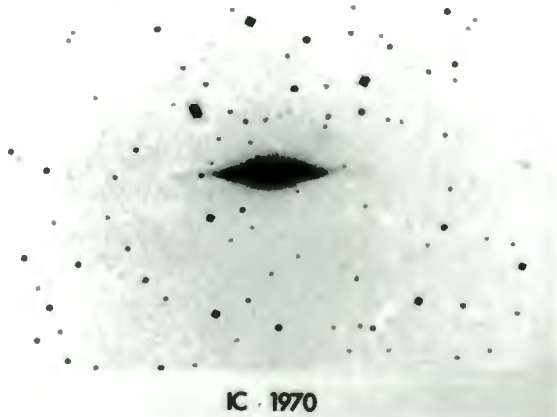

IC 1970

Plate 19

UNIFORM LINEAR SCALE

0 10 20 30 40 50 kpc

TYPE ab,b

EDGE–ON

IC 4351

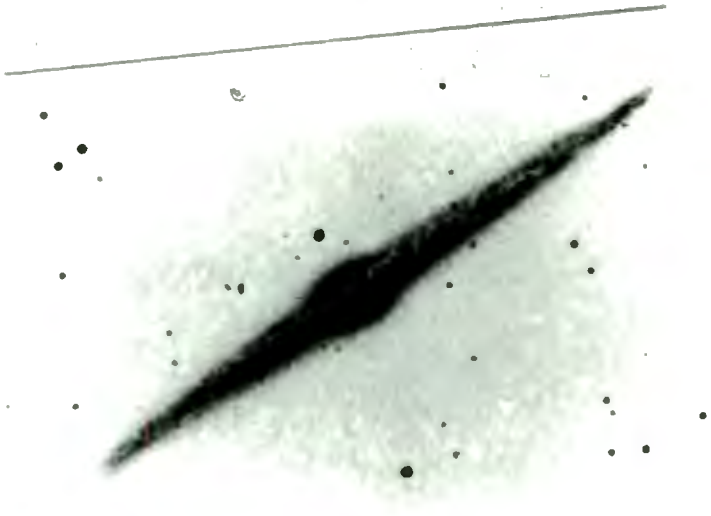

NGC 4565

Plate 20

The outer diameter of NGC 6782 is ∿44 kpc (projected); the saturated inner region ∿19 kpc (projected).

NGC 7172 is a curious galaxy; the prominent absorption bar - with a linear extent of some 17 kpc - is even more conspicuous on the ESO B film copy. The classification in the RC2 is Sab p? sp. It is interesting to note that outside the bar one has a region of such high surface brightness. NGC 7172 is a member of the NGC 7172/7173/7174/7176 chain of galaxies (fig. 1 in Rubin (1974); also fig. 2, where a 4-m telescope photograph of NGC 7172 is presented).*

A "problem case study" in galaxy classification is NGC 7232 (diameter ∿28 kpc); either an Sb galaxy seen almost edge-on, or an SO galaxy - type 3, ellipticity 7 i.e. $SO_3(7)$. [The SO_1 - SO_3 galaxies are illustrated in the "Hubble Atlas" (Sandage (1961))]. Whichever the case, one notes the completely saturated appearance on the IIIa-J photograph.

NGC 3318 (diameter ∿35 kpc), classified in the RSA as SBb(rs) II, presents somewhat irregular spiral arms, and we have chosen to include it here rather than in one of the preceeding sections.

NGC 6870 has a well-defined region of high surface brightness, surrounded by tenuous outer gaseous structure extending to ∿39 kpc. It is assigned type SA(r)ab in the RC2.

---

* Our photographs of NGC 7173/74/76 appear in chapter eight.

Type ab, b - Individually Discussed Examples

Galaxy NGC	Classification
782	SBb(r) I-II (RSA)
1350	(R')SB(r)ab
3318	SBb(rs) II
6782	SBab(s) (RSA) (R)SBO^{+}: (RC2)
6870	SA(r)ab
7172	Sabp? sp
7232	SO_3(7) or Sb (RSA) SB(rs)a: (RC2)
7582	SBab(rs) (RSA) (R')SB(s)ab (RC2)

UNIFORM LINEAR SCALE

0 10 20 30 40 50 kpc

TYPE ab,b

SOME INDIVIDUAL CASES

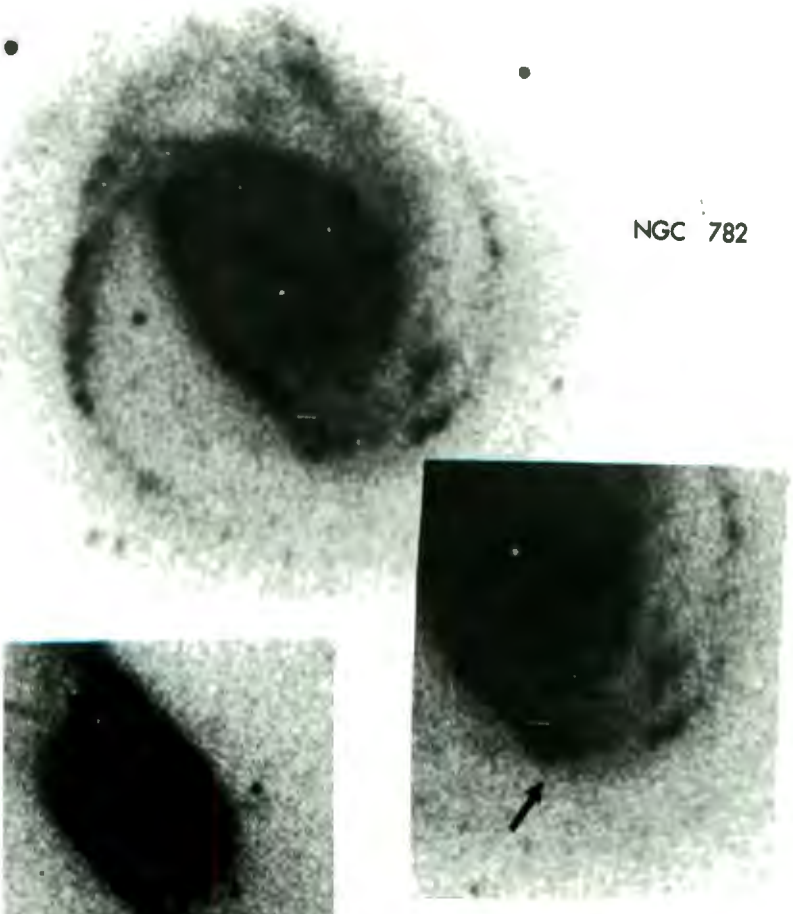

NGC 782

NGC 6872

NGC 7582

Plate 21

5.3 The Type O/a, a Spirals

The most striking example here - at least as surface brightness is concerned - is NGC 7213. It presents an almost completely saturated elliptical appearance on the IIIa-J photograph; (the uneven background in that photograph is due to the presence of a bright star). Sérsic (1968) in fact comments that

"NGC 7213 was classified by de Vaucouleurs (1963) as SA(s)a, but we think it is an E1 object with a light absorption band on the north-preceding side".

Inspection of the corresponding film copy of the 'Quick Blue' Survey, and the accompanying inset of NGC 7213 from the Radcliffe plate collection*, does however clearly reveal the (weak) spiral structure.**

Its surface brightness is very high - $\sim$21.6 mag arcsec^{-2} (table 6) - and is the second highest surface brightness galaxy in our entire sample [the highest SB value is for the Sc galaxy NGC 6215; table 6 and figure 11]. Coupled with a diameter of $\sim$18 kpc†, we have an absolute magnitude of -21.2: almost identical to that of M101!

Once again, the spiral arms in NGC 7213 support our earlier proposition that spirals with saturated/predominantly

---

* There are 2 plates: A1270 and A102, but the 90 minute exposure A102 shows the arms best. [The inset - not to scale - is from that plate].

** The situation is somewhat analogous to NGC 3928, classified as type E0 in the RC2 (1976), but shown to be a miniature spiral on a large scale IIIa-J plate (van den Bergh (1980)).

† The value of log R_{25} (from the RC2) for NGC 7213 is 0.02, so that the above diameter and absolute magnitude can be treated as that for face-on orientation.

saturated images on the J-survey preferentially do not (on an absolute scale) have impressive [and well developed] arms.

NGC 1341 is another example where the optical image is virtually saturated; as in the case of some other such spirals in previous sections, a faint, featureless outer envelope is detectable. This feature, when present, thus extends through the Hubble sequence, from type a and later. The overall diameter of NGC 1341, including the envelope, is ∿15 kpc.

NGC 7233 is a spiral of very early type; assigned SAB(s)O/a in the RC2. Its diameter - from the tip of the one spiral arm to the other - is ∿15 kpc.

Two other spirals assigned O/a are NGC 1316C and NGC 3314. In NGC 1316C, there is only a meagre hint of incipient spiral structure on the IIIa-J photograph; inspection of the ESO B film copy shows no spiral structure at all. The extent between the arrows indicated is ∿18 kpc. NGC 3314 is somewhat reminiscent of M82; the IIIa-J photograph shows a ring almost perpendicular to the major axis of the galaxy. It is classed in the RC2 as SB(s) O/a p, and has a diameter (from arrow to arrow) of ∿24 kpc.

Tightly wound spiral arms, characteristic of type a, are seen in NGC 3783 (diameter ∿26 kpc) and NGC 1317 (diameter ∿34 kpc); the arms surrounding the prominent central region gradually fade to the limiting surface brightness of the photograph.

IC 5240 (diameter ∿25 kpc) is an interesting spiral; a magnificent central inner ring, some 10 kpc in diameter, is seen; the galaxy is well described by the de Vaucouleurs classification SB(r) a. Also present are hints of a surrounding envelope.

Finally, we include IC 4299 (diameter ∿40 kpc) - a curious image is seen on the IIIa-J photograph, and the galaxy is appropriately assigned type a: (uncertain) in the RC2.

Spirals of Type O/a, a

Galaxy NGC	Classification (RC2)
7233	SAB(s)O/a
1341	SB(s)a
1316C	SO/a:
7213	SA(s)a:
3314	SB(s) O/a p
IC 5240	SB(r)a
3783	SB(r)a
1317	(R')SAB(rs)a
IC 4299	SAB(s)a:

UNIFORM LINEAR SCALE

0 10 20 30 40 50 kpc

THE TYPE O/a,a SPIRALS

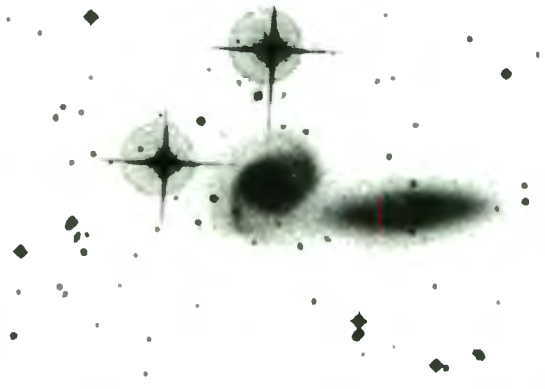

NGC 7233

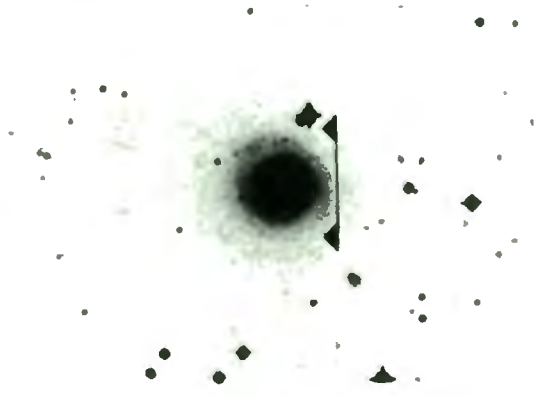

NGC 1341

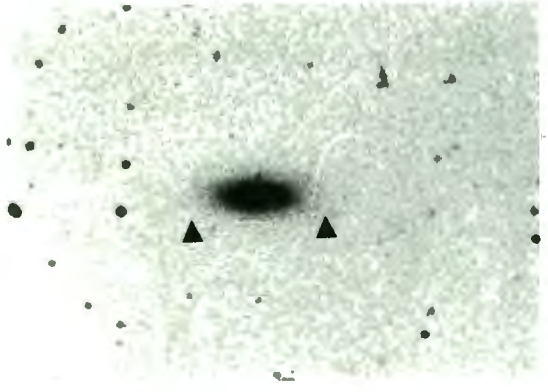

NGC 1316C

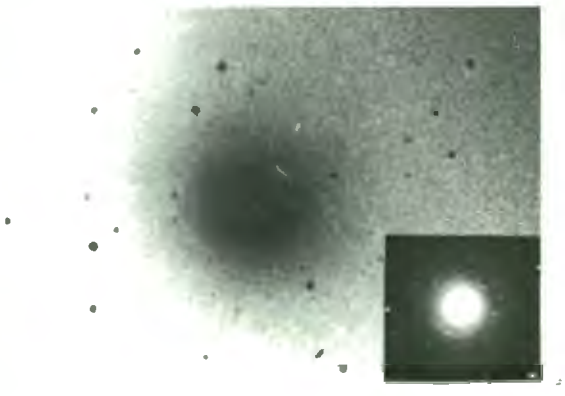

NGC 7213

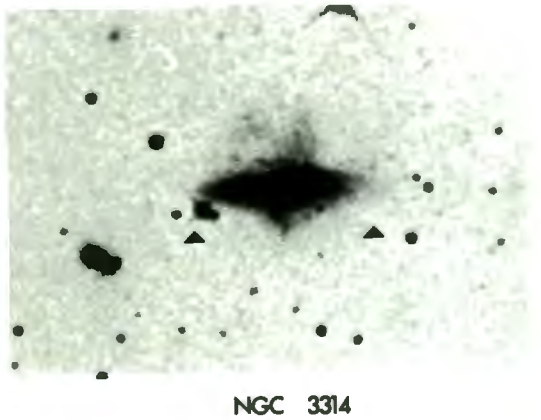

NGC 3314

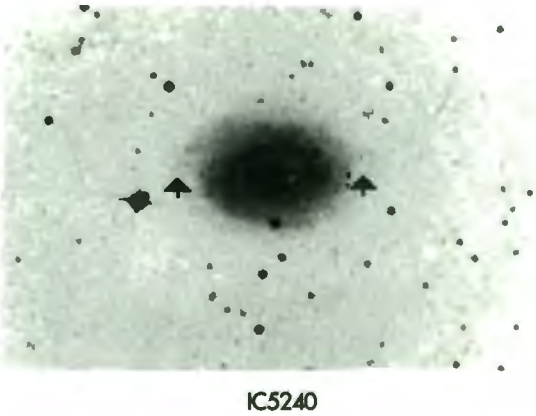

IC5240

Plate 23

UNIFORM LINEAR SCALE

0 10 20 30 40 50 kpc

THE TYPE 0/a,a SPIRALS

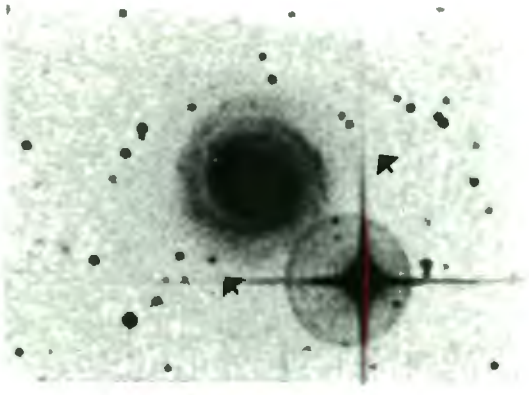

NGC 3783

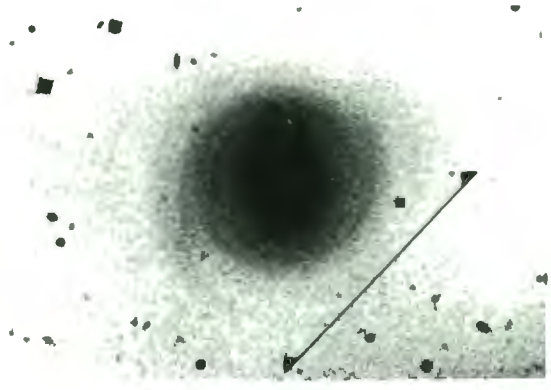

NGC 1317

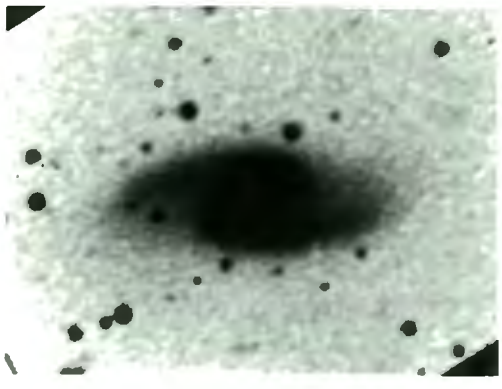

IC 4299

Plate 24

CHAPTER SIX

GALAXIES OF TYPE cd AND LATER

In 1959, de Vaucouleurs reintroduced Lundmark's (1926, 1927) very late-type systems into the formal spiral sequence via the Sd, Sm, SBm, and Im types; once again, we perform - for type cd, d spirals - a subdivision into our previous categories: predominantly saturated image, massive arms, medium or weak arms.

Of particular interest in this chapter is the high surface brightness magellanic spiral NGC 7764, as discussed in section 6.2.

6.1 Type cd, d

The overall range in spiral arm texture within this group is impressive; from the weak arms of NGC 5556 and IC 5201, to the massive spiral arms of A1427-34, and especially NGC 6806. The diameters of the type cd, d spirals within our sample range from 14 kpc (A2015-39) to 96 kpc (IC 5201).

As in the previous sections, we first consider

6.1.1 Type cd, d - Saturated Image

The only galaxy included here is A2015-39; it is intrinsically small (~14 kpc), and has an overall surface brightness which is relatively high. The spiral structure can nevertheless still be traced in the saturated region of the IIIa-J photograph. There are hints of a faint, featureless surrounding envelope. A2015-39 is assigned type SA(rs)d: in the RC2.

6.1.2 Type cd, d - Massive Arms

In this category, the outstanding example is NGC 6806; also A1427-34. The diameter of NGC 6806 is ∿35 kpc; that of A1427-34, ∿47 kpc*. In NGC 6806, the surface brightness along the spiral arms tends to decrease rather abruptly; while in A1427-34, the (inner) arms are patchy, and become very tenuous and fuzzy in the outer regions.

It is interesting to compare the morphology of these massive spiral armed galaxies to those in the other cd, d sections (e.g. NGC 5556 and IC 5201).

6.1.3 Type cd, d - Medium Arms

When inspecting the photograph of A0113-32 [SA(rs)d:], one is reminded of the spiral arm texture seen in A0253-27 (type bc, c section - medium arms). A0113-32 presents a well defined, regular and symmetric appearance; its diameter is ~44 kpc.

A0305-31, another example of a spiral with "medium" arms, shows a curious outer morphological appearance, which could be indicative of warping. Spiral arms A and B in the photograph do not appear to lie in the same plane - the situation might well be analogous to that in M33 (Sandage and Humphreys (1980). As with some of the warped galaxies studied

---

* This includes the faint outer arms; our limits for this diameter are marked on the photograph by arrows. One also sees the prominent central region occupies about half the total extent.

by Sancisi* (1976, 1977), A0305-31 has no close companions. [This problem has presented interesting theoretical challenges (e.g. Tubbs and Sanders (1979)]. From arrow to arrow in the photograph, A0305-31 has a diameter of ~80 kpc.

A totally different morphology is seen in A1829-41; the arms have the characteristic 'S shape' of the de Vaucouleurs scheme, and tend to form "a seashell". Most important, they do not originate at the nucleus. The diameter of A1829-41 is of the order of 65 kpc.

6.1.4 Type cd, d - Weak Arms

The need for extending the Hubble classification for spirals of type later than c is particularly well illustrated in NGC 5556, classified as SBcd in the RSA, and SABd in the RC2. With its faint outer spiral arms, this galaxy bears much likeness to the morphology seen in NGC 3059 [type bc, c section - weak arms]. The overall diameter of NGC 5556 is 33 kpc.

Another magnificent cd spiral is IC 5201, with a diameter as noted above of ~96 kpc. The RSA classification for IC 5201 is SBcdII; that in the RC2 SB(rs)cd. The point to be emphasized here is once again how one can have 2 galaxies, NGC 5556 and IC 5201, both cd, with marked differences in linear size.

---

* Sancisi found the HI disks of 4 out of the 5 edge-on galaxies he studied [using the Westerbork Synthesis Radio Telescope] to be warped. Of these, NGC 5907 showed the most pronounced warp - the HI layer bends away from the optical plane of that galaxy by more than 8 kpc at a distance of 40 kpc from the centre. Furthermore, NGC 5907 has no close companions.

6.2 Type: Magellanic

The earliest type example here is IC 1558, classified in the RC2 as SABdm. Its diameter on the photograph is of the order of 28 kpc.

Among the pure magellanic types in our sample, the most interesting galaxy is NGC 7764, which could appropriately be called "The Footprint". Its intrinsically small size - some 20 kpc - coupled with a high surface brightness - points to a high absolute magnitude: indeed, with H_o = 55 km s^{-1} Mpc^{-1}, we have a value from the RSA of $M^{o,i}_{B_T}$ = -19.9. This then reiterates the emphasis placed on surface brightness considerations in chapter 3; one also notes here the well defined outer envelope. Pertaining to inner morphology, the saturated region nicely resolves on the ESO B film copy into a structure very similar to that seen in A0031-31.

NGC 5464 shows no distinct features on either the IIIa J photograph, or on the "Quick Blue" Survey. In the RC2, it is assigned type IB(s)m?

Finally, in NGC 1879, a relatively dark inner region is seen - the galaxy is a clear type Im.

Type cd, d Spirals

Predominantly Saturated Image

A2015-39	SA(rs)d:

Massive Arms

NGC 6806	SAB(rs)cd
A1427-34	SB(s)d:

Medium Arms

A0113-32	SA(rs)d:
A1829-41	SAB(s)cd
A0305-31	SAB(r)cd

Weak Arms

NGC 5556	SBcd(s)I-II	(RSA)
	SAB(rs)d	(RC2)
IC 5201	SBcdII	(RSA)
	SB(rs)cd	(RC2)

TYPE MAGELLANIC

NGC	
AOO31-31	Im:
1879	Im
5464	IB(s)m?
7764	SBmIII
1558*	SABdm

* = IC

UNIFORM LINEAR SCALE

0 10 20 30 40 50 kpc

TYPE cd,d

SATURATED/PREDOMINANTLY SATURATED IMAGES ON IIIa–J SURVEY

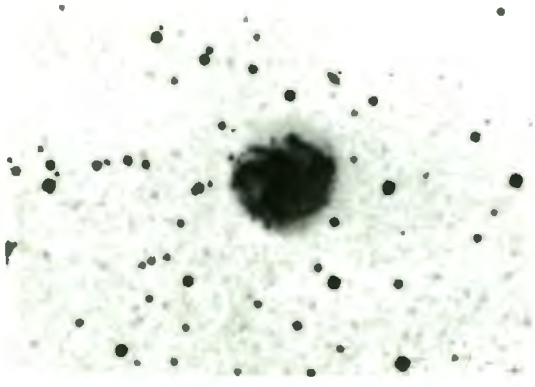

A2015–39

MASSIVE ARMS

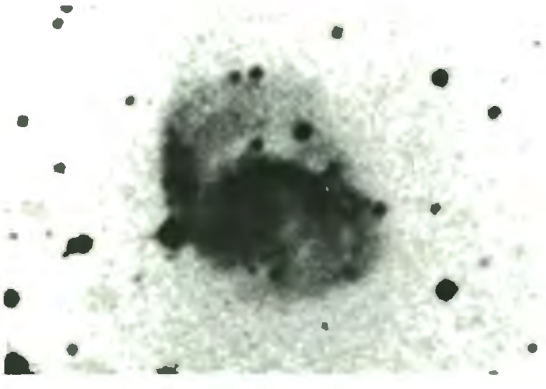

NGC 6806

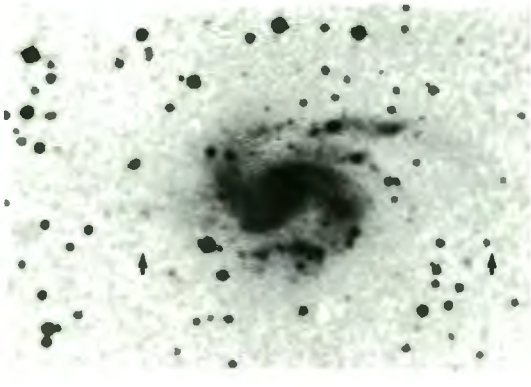

A1427–34

Plate 25

UNIFORM LINEAR SCALE

0 10 20 30 40 50 kpc

TYPE cd,d

MEDIUM ARMS

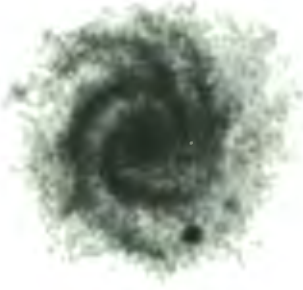

A0113–32

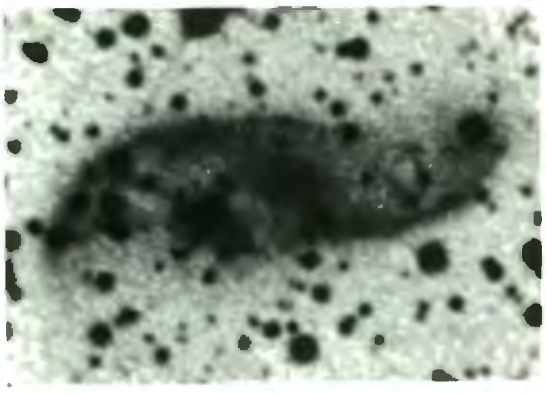

A1829–41

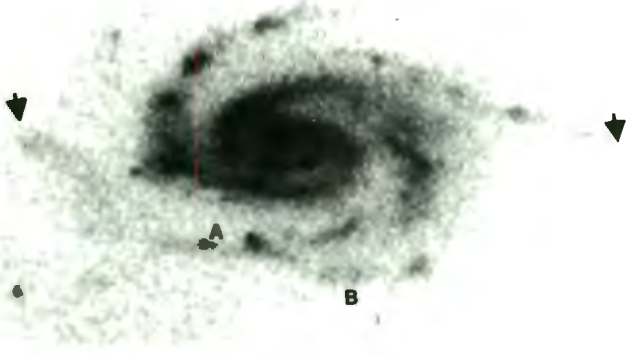

A0305–31

WEAK ARMS

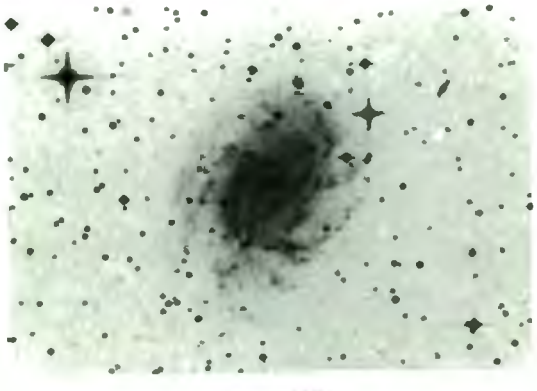

NGC 5556

Plate 26

UNIFORM LINEAR SCALE

0 10 20 30 40 50 kpc

TYPE cd,d

WEAK ARMS

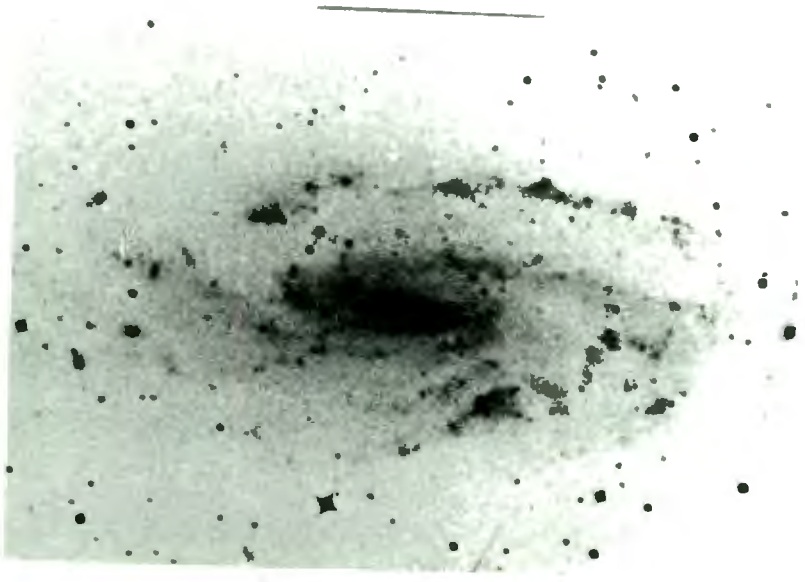

IC 5201

TYPE MAGELLANIC

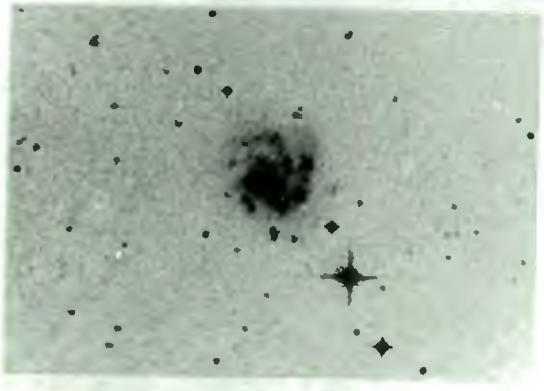

A0031–31

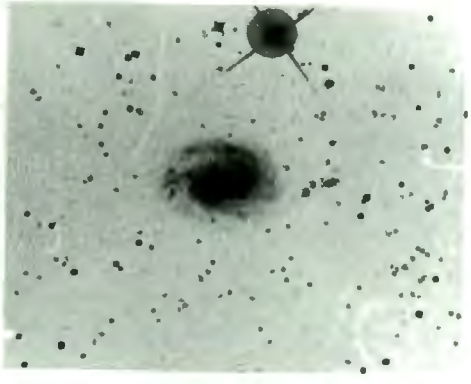

NGC 1879

Plate 27

UNIFORM LINEAR SCALE

0 10 20 30 40 50 kpc

TYPE MAGELLANIC

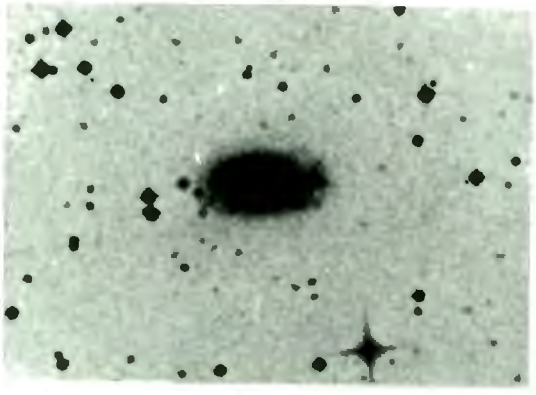

NGC 5464

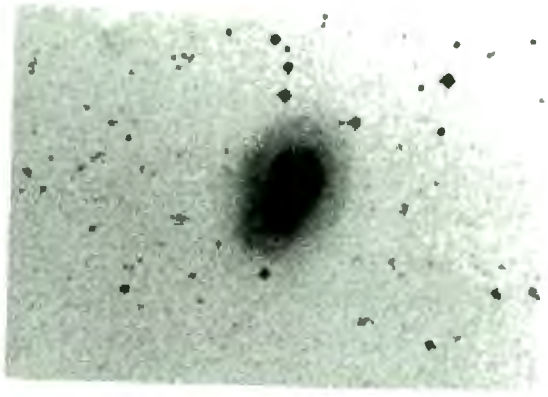

NGC 7764

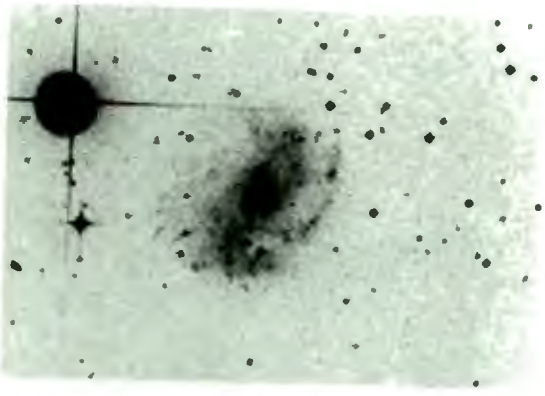

IC1558

Plate 28

CHAPTER SEVEN

THE ELLIPTICALS AND LENTICULARS

7.1 The Ellipticals

Of the ellipticals included in our sample, several are members of small groups, and a few of the Fornax cluster (as reflected in the list below). Only one (NGC 1531) is a close companion to a spiral galaxy.

We have arranged our montage in approximate order of increasing linear diameter - due to the presence of often extensive regions of decreasing surface brightness (such as in NGC 3136, NGC 2865, NGC 1427 and NGC 3706), it is difficult to visually assign any precise ordering.

The diameters of the inner (saturated) regions seen in plates 29 to 30 range from ~7 kpc (NGC 2434) to ~25 kpc (NGC 3557). The overall diameters are much larger; from NGC 2434, some 15 kpc*, to at least 60 kpc on the photograph for NGC 3557. [One can of course have much smaller and larger diameters (for types dE and cD respectively), but the photographs here serve to illustrate the point for ellipticals that one cannot on purely morphological grounds decide whether a galaxy is intrinsically large or small].

An elliptical with a ring

Of all the ellipticals presented, a fairly uniform appearance is seen. The one exception is NGC 2865 - an

---

* Including ellipticals from the cluster seen in chapter eleven (particularly galaxy no.18) sets the lower limit for ellipticals in our sample at ∿5 kpc.

elliptical with an encircling gaseous ring, approximately 30 kpc in diameter, and in a plane almost perpendicular to the major axis of the galaxy.

The Ellipticals

NGC (1)	Type (RC2) (2)	Comments (3)
2434	E0-1	
1339	E4	
1389	E4:	
1374	E0	In Fornax I cluster
3136	E4-5:	
5898	E0	
7097	E4*	
5304	E4:	In I4329 group
6851	E4:	
2865	E3-4	
1427	E3	Fornax I cluster
3250	E4	
5612	E2*	
6758	E1	In group
5903	E2	
1379	E0	In Fornax I cluster
6877	E6	In Pavo group
7029	E6:	In small group
4976	E4p:	Discussed by Sérsic (1968) p. 40.
IC 4889	E5-6	
6958	E1	
3706	E4*	
5357	E1	In I4329 group
7014	E0	
3309	E3	Brightest member in Hydra cluster
IC 4842	E5	In a group
6776	E2	
7796	E2	
6868	E2	
5330	-	Pair of ellipticals at 1'.7 separation
5328	E1:	
1404	E1	In Fornax I cluster
5419	E4	(=PKS 1400-33?)
6876	E3	Largest elliptical member in Pavo Group
3557	E3	In Klemola group number 18

Elliptical Companion to Spiral

1531	E6p?	Spiral galaxy is NGC 1532

Notes to the above list

1. An asterisk following the classification in column (2) indicates that the type is not from the RC2, but from Sandage (1978).

2. The comments in col. 3 are either from the RC2, or from the author.

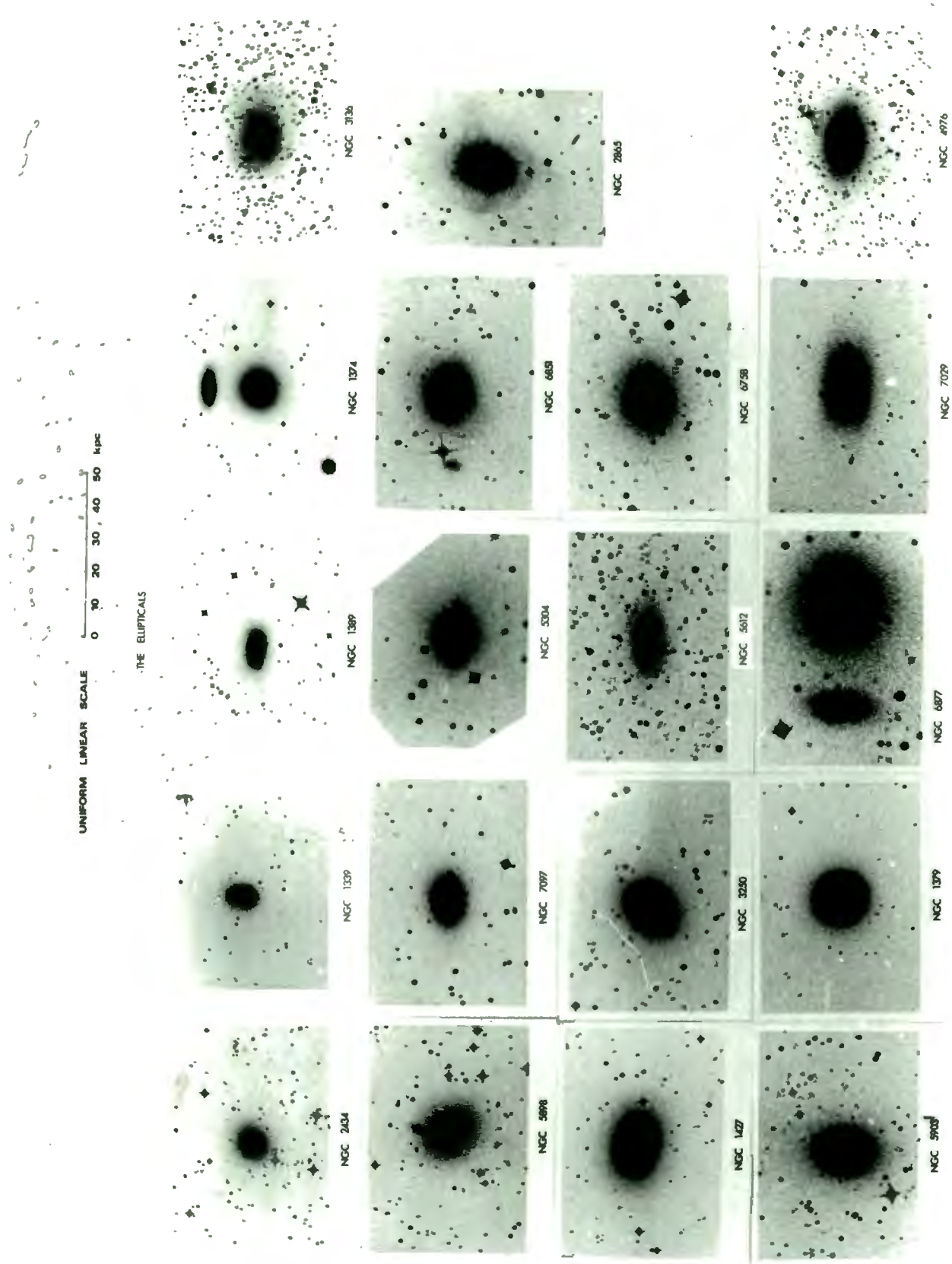
THE ELLIPTICALS
UNIFORM LINEAR SCALE
0 10 20 30 40 50 kpc
NGC 3136
NGC 2865
NGC 4976
NGC 1374
NGC 6861
NGC 6798
NGC 7029
NGC 1389
NGC 5304
NGC 5812
NGC 6877
NGC 1339
NGC 7097
NGC 3230
NGC 1379
NGC 2434
NGC 5898
NGC 1427
NGC 5903

Plate 29

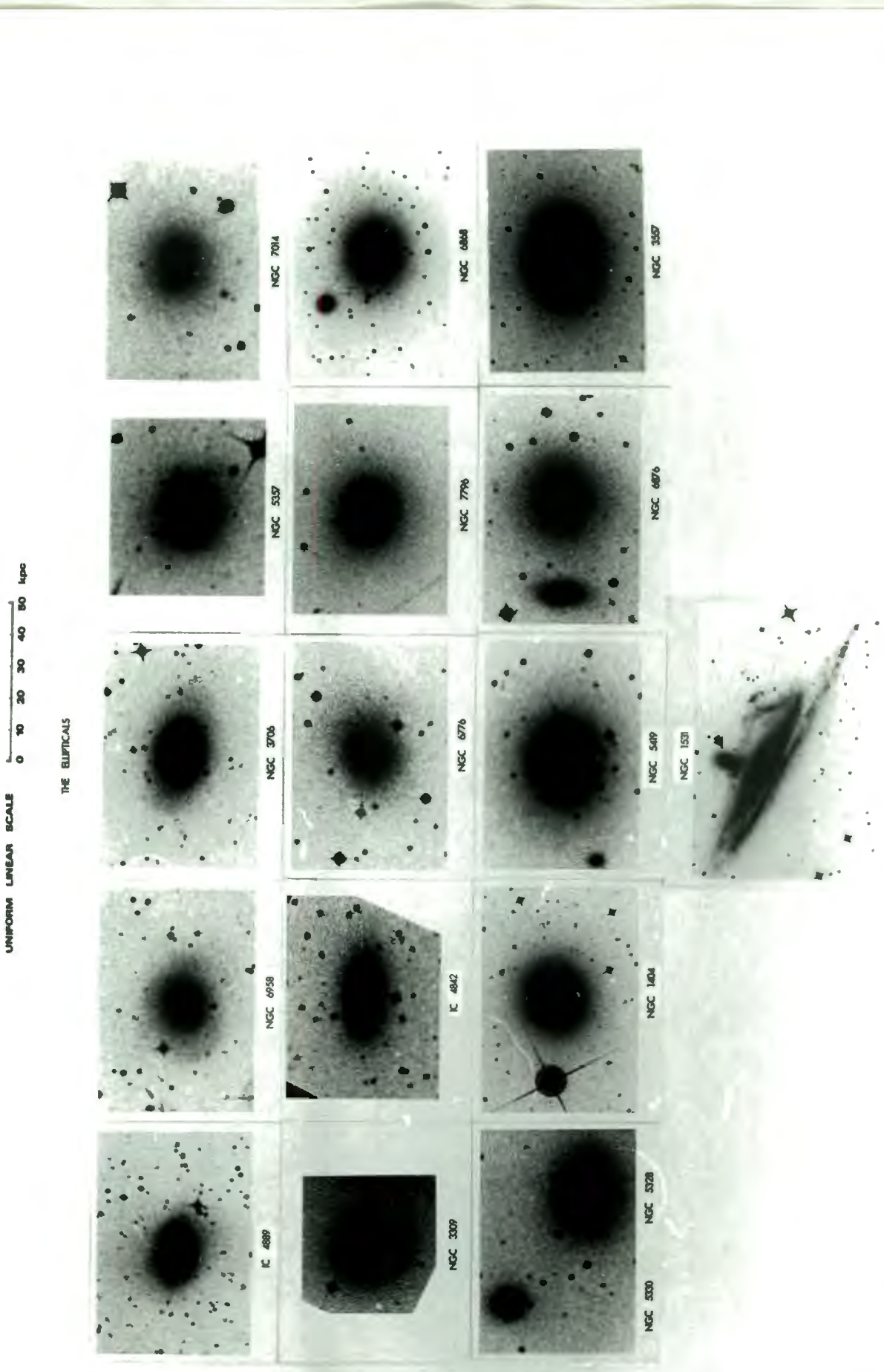
THE ELLIPTICALS
UNIFORM LINEAR SCALE
0 10 20 30 40 50 kpc
NGC 7014
NGC 6868
NGC 3557
NGC 5557
NGC 7796
NGC 6876
NGC 3706
NGC 6776
NGC 5419
NGC 1531
NGC 6958
IC 4842
NGC 1404
IC 4889
NGC 3309
NGC 5330
NGC 3328

Plate 30

7.2 The Lenticulars

The overall range in diameter for the lenticulars seen here is ~13 kpc (NGC 1380B), to about 60 kpc for NGC 6771 and ~64 kpc (from arrow to arrow) for IC 4329.

Several of the lenticulars in the montage have the appearance on the J-survey of some of our intrinsically small, high surface brightness spirals, with saturated IIIa-J images. This is particularly true of the lenticulars NGC 1411 and and NGC 5121.

With regard to interesting individual examples, one sees very prominent dust lanes in IC 5063 (diameter ~37 kpc) and NGC 612 (diameter ~55 kpc).

Clearly defined, extensive outer envelopes are visible in NGC 6893 and IC 4329.

NGC 7135 is a peculiar SO galaxy; a photograph also appears in Dressler and Sandage (1978) (fig. 2), who describe the system as a "*tidal jet with an unusual spherical cap in the opposite direction. Possible Toomre-like encounter* [cf. Toomre and Toomre (1972)] *with perturbing galaxy that may be visible in the cap*". Its cverall diameter, including the jet, in ~48 kpc.

Finally, IC 5267 (diameter ~58 kpc) shows faint outer spiral arms. [It is classified in the RC2 as an ordinary, intermediate stage, lenticular]. Spiral arms are also apparent in NGC 2601 [classified as SO: in the RC2].

The Lenticulars

Galaxy	Classification (RC2)
NGC	
1380B	SO^{+}:
1411	$S(r)O^{-}$:
5121	SO_1 (4) (Sandage (1978))
148	SO^{+}:sp
3308	$SAB(s)O^{-}$:
2601	SO:
1387	SO^{-}
1351	SAO^{-}:
IC 4960	SO:sp
1543	$(R)SB(s)O^{o}$
6861D	$SA(s)O^{-}$:
3564	SOsp
7049	$SA(s)O^{o}$
IC 5181	SAOsp
1381	SAOsp
7041	$SABO^{-}$
5140	$SAB(rs)O^{o}$:
5302	$SB(s)O^{+}$:
1201	$SA(r)O^{o}$:
5193	SBO^{-}p
5193A	No classification in RC2
6861	$SA(s)O^{-}$:
6893	$SAB(s)O^{o}$
6880	$SAB(s)O^{+}$:
IC 5063	SAO^{-}: Prominent dust lane
1380	SAO
7135	SAO^{-}p (RC2) SO pec (Dressler and Sandage (1978))
612	SOp(sp) Prominent dust lane
7702	$(R)SA(r)O^{+}$
IC 5267	$SA(rs)O^{o}$:
6771	$SB(r)O^{+}$?sp
IC 4329	SO^{-}?

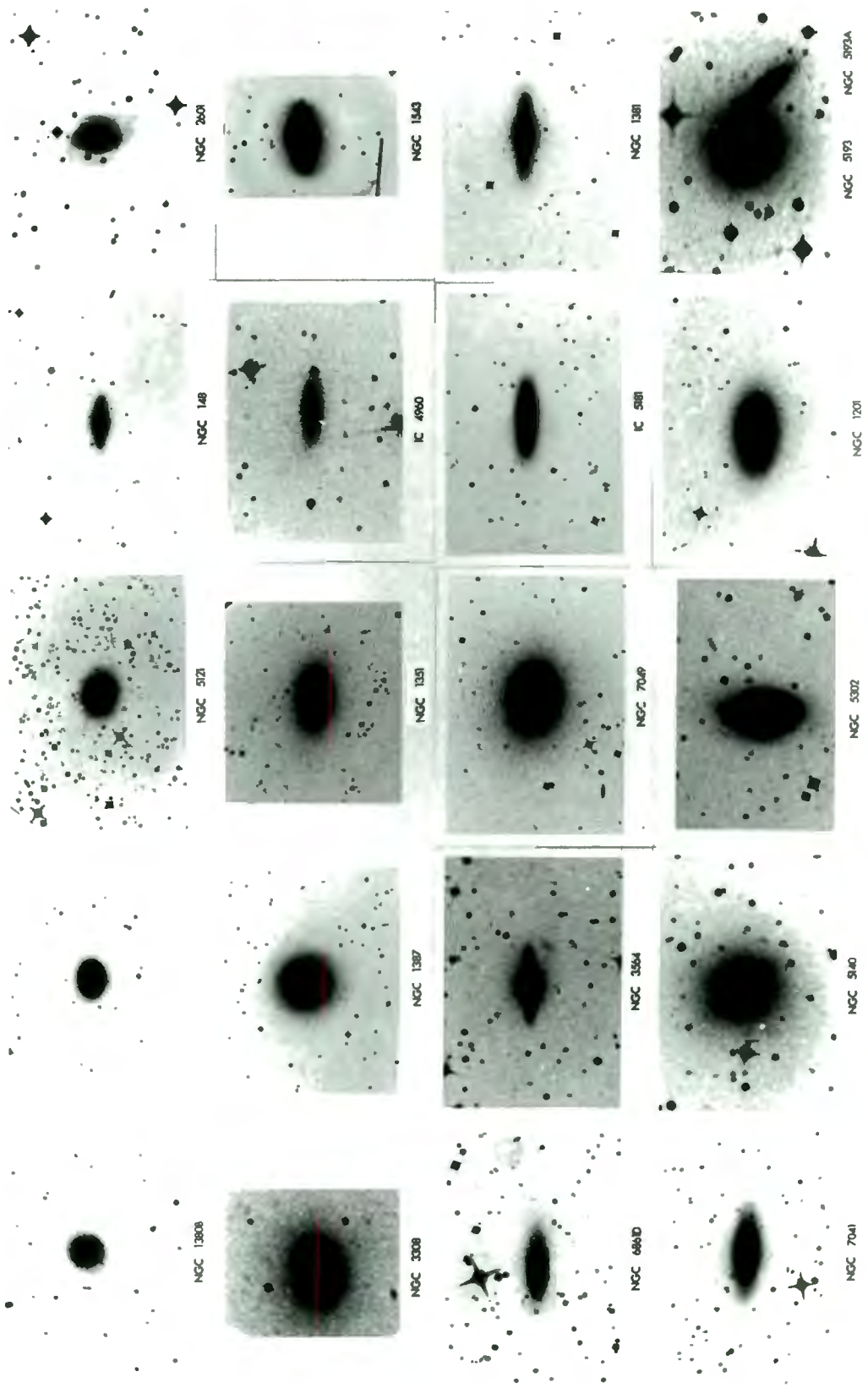
UNIFORM LINEAR SCALE
0 10 20 30 40 50 kpc
THE LENTICULARS
NGC 2681
NGC 1543
NGC 1381
NGC 5193
NGC 5993A
NGC 148
IC 4960
IC 5181
NGC 1201
NGC 5121
NGC 1351
NGC 7049
NGC 5302
NGC 1387
NGC 3384
NGC 5140
NGC 1808
NGC 3008
NGC 6861D
NGC 7041

Plate 31

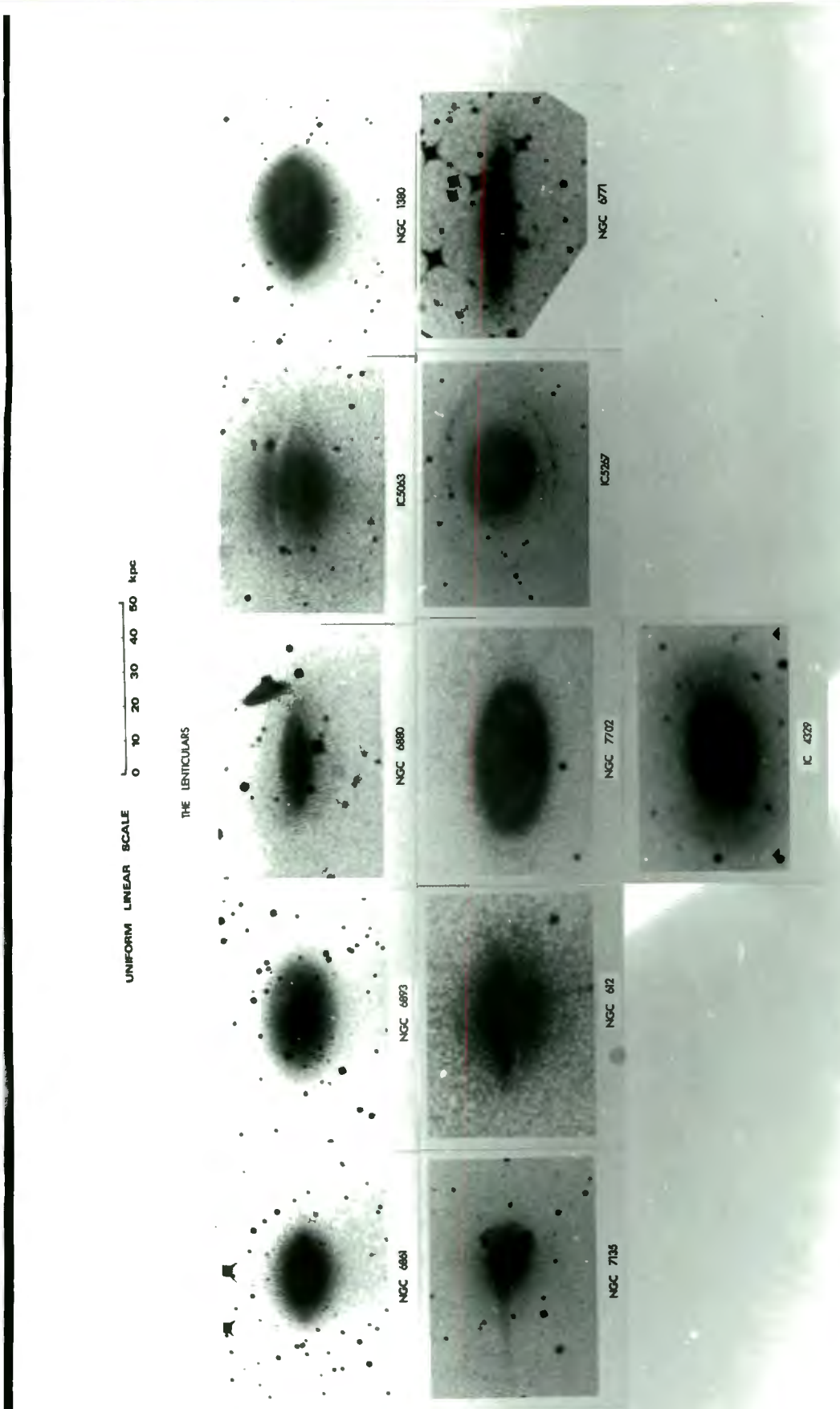
THE LENTICULARS
UNIFORM LINEAR SCALE
0 10 20 30 40 50 kpc
NGC 1380
NGC 6771
IC5083
IC5267
NGC 6880
NGC 7702
IC 4329
NGC 6873
NGC 612
NGC 6868
NGC 7135

Plate 32

CHAPTER EIGHT

8.1 Gravitationally Interacting Systems

A few of the galaxies photographed were gravitationally interacting pairs or systems; these are discussed below.

NGC 4105, classified in the RC2 as an elliptical [E3] shows clear signs of interaction with its companion NGC 4106 (to the left on the photograph). It is thus classed in the de Vaucouleurs (1959) type P(b). Neutral hydrogen emission from NGC 4105 has been detected by Huchtmeier, Tammann and Wendker (1977) and by Bottinelli and Gougenheim (1979).

Optical and HI observations of NGC 5291, and its companion, the Seashell, are presented in Longmore *et al.* (1979). Of particular interest is the remarkable series of small HII complexes (seen in plate 2 of their paper) extending to at least five galaxy diameters from NGC 5291, both to the north and south; with H_o = 55 km s^{-1} Mpc^{-1}, the total linear extent is ∿180 kpc. Longmore *et al.* classify NGC 5291 as a lenticular $SA0^+$; they also make the interesting observation that the knots discussed above are comparable in size to the Large Magellanic Cloud. The diameter of NGC 5291 on our photograph is ∿22 kpc; that of the Seashell is ∿15 kpc.

The interacting system NGC 6438 has been described by Sérsic (1966), and is illustrated in Sérsic (1968). Two separate components are distinguished; an S0 galaxy, and an "irregular component". Sérsic found the velocities of the two components to differ; contrary results were later reported by Burbidge and Burbidge (1972), who found a mean redshift velocity for both components of 2400 km s^{-1}. The diameter of the

irregular component is ∿30 kpc, and is well shown on the IIIa-J photograph.

NGC 6769 is classified in the RSA as SB(r)II, and appears to be tidally interacting with the neighbouring galaxy NGC 6770. A faint surrounding envelope enclosing the system is seen.

NGC 7173/4/6 forms part of the NGC 7172-7173-7174-7176 chain of galaxies. The classifications of NGC 7173/4/6 in the RC2 are E2:, Sbp?sp and EOp: respectively. The system was studied by Rubin (1974), who presented 4-m telescope photographs of these galaxies. In fig. 2 of that paper, one sees how the dust lane in (the tidally distorted spiral) NGC 7174 does not lie in only one plane, but [at the west end] turns abruptly upward to NGC 7173. The diameter of the interacting pair NGC 7176/NGC 7174 is ∿30 kpc from A to B in the photograph.

The interacting galaxy IC 5135 has the shape of a crab. The inner region is of high surface brightness, and faint outer arms extend to the companion seen at upper right. The diameter of IC 5135 is ∿40 kpc.

A1957-47A and A1957-47B form part of the interconnected Klemola 30 group of galaxies (Klemola (1969)). Spectroscopic observations of these two galaxies are contained in a paper by Graham and Rubin (1973). The overall diameter of the Klemola 30 group - including the faint extensions from the one arm of A1957-47A (marked by an arrow) - is some 130 kpc. [The photograph is printed at a 2 times reduction].

Both IC 5250 and F-157 are described by Fairall (1979b). The latter is an emission line galaxy; the diameter from B to C is ∿26 kpc; in the direction A to C, ∿43 kpc. The thickness

of the prominent "massive" arm is ∿3 kpc (those in NGC 309 are ∿7 kpc). F-157 has a close companion (also an emission line object). IC 5250 resolves into three separate nuclei on the ESO B Survey; an apparent redshift anomaly for this system has been reported by Fairall.

Pertaining to the question as to whether there is some general characteristic separation between interacting pairs, it is curious to note the following (projected) separations:

NGC 4105/6	∿13 kpc
The Seashell and NGC 5291	∿15 kpc
NGC 6438 and companion	∿ 8 kpc

This gives an arithmetric mean of 12 kpc, which, if we multiply by √2 (assuming random orientations in these different systems) gives a true separation of ∿17 kpc. There are of course exceptions (particularly NGC 6769/NGC 6770), but the trend is worthy of note.

Interacting Systems

Galaxy

NGC 4105/6

NGC 5291 and the Seashell

NGC 6438

NGC 6769/6770

NGC 7173/74/76

IC 5135

IC 5250

A1957 - 47A

A1957 - 47B

F-157

UNIFORM LINEAR SCALE

0 10 20 30 40 50 kpc

GRAVITATIONALLY INTERACTING SYSTEMS

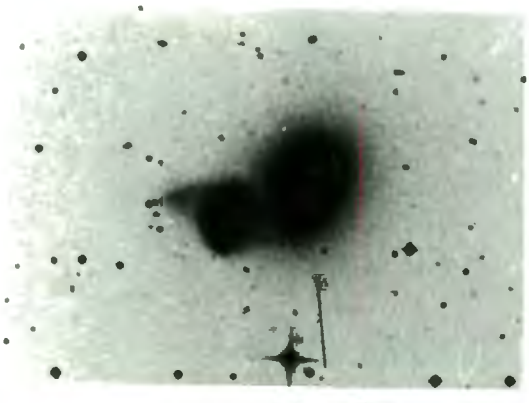

NGC 4105

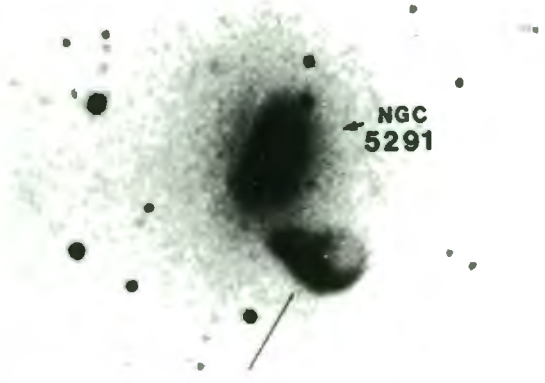

THE SEASHELL

NGC 6438

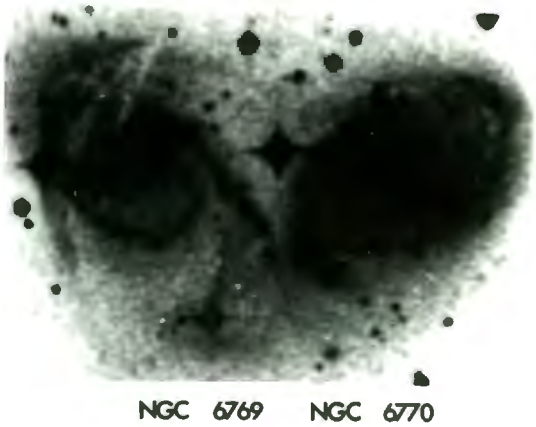

NGC 6769 NGC 6770

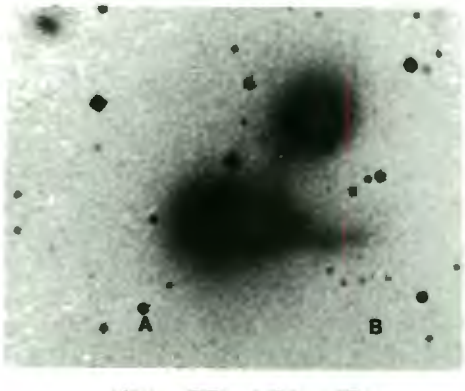

NGC 7176 NGC 7174

NGC 7173

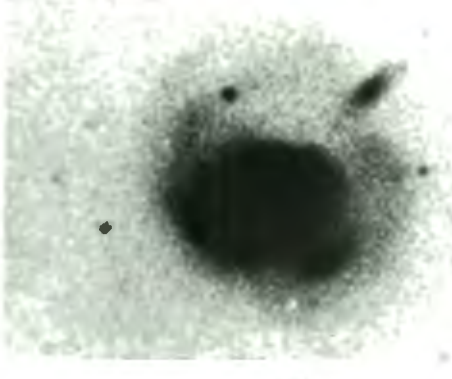

IC 5135

Plate 33

UNIFORM LINEAR SCALE

0 10 20 30 40 50 kpc

GRAVITATIONALLY INTERACTING SYSTEMS

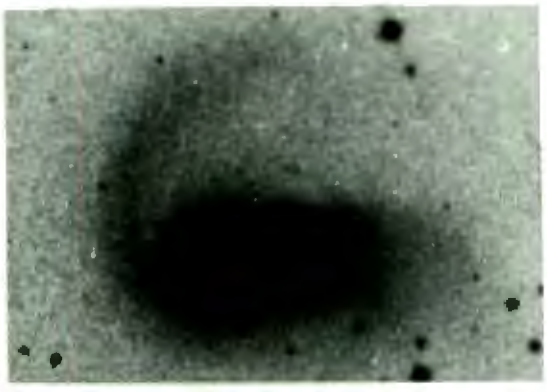

IC 5250

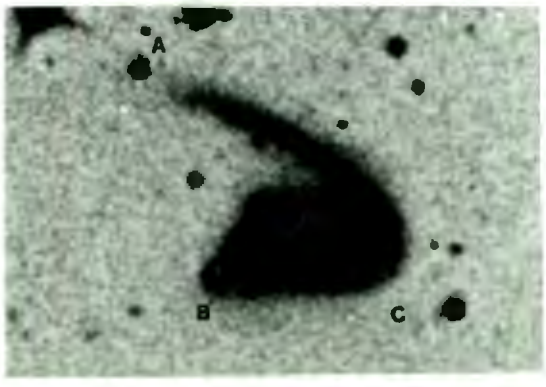

F 157

Plate 34

UNIFORM LINEAR SCALE

0 100

kpc

THE KLEMOLA 30 GROUP: 2× REDUCTION

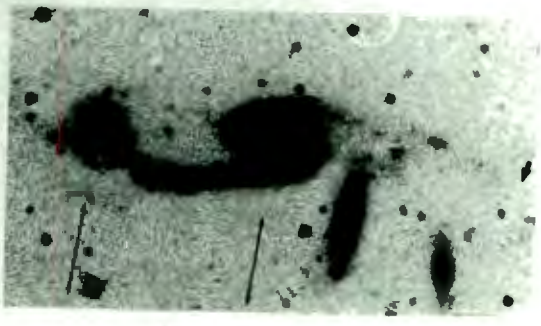

A1957–47B A1957–47A

Plate 35

8.2 Galaxies with Uncertain Classifications/No RC2 Classification

Of the galaxies photographed from shipments 1-6 of the J-Survey, the ones illustrated here have no classification in the RC2. Exceptions are

(i) IC 2554, designated SB(s)cp:, with rather chaotic spiral arms; the classification is uncertain.

(ii) NGC 2788 and IC 4845, assigned S:sp and SB(r)? respectively.

Pertaining to interesting (unclassified) individual cases, NGC 5292 and IC 4845 clearly show spiral arms; on their appearance here, a classification of type b is appropriate.

A1903-61 and IC 4831 are good examples of lenticulars, with well defined outer envelopes.

A2207-46 is a spiral galaxy well inclined to the line of sight; in the absence of other plate material, the galaxy could be of type b; one notices that its arms are (relatively) tightly wound, with no resolution into HII regions.

The montage is arranged in order of increasing right ascension for the Anonymous objects, and increasing IC number. Only two of the galaxies have an NGC designation: NGC 2788 and NGC 5292.

Galaxy

NGC 2788
NGC 5292
A1034-27A
A1234-72
A1332-33
A1335-33
A1345-30
A1515-23
A1903-61
A2100-48
A2101-48

Galaxy (cont.)

A2102-47
A2103-47
A2152-69
A2207-46
IC 1876
IC 2554
IC 4827
IC 4831 (photographed both on J and ESO(B) Surveys)
IC 4845
IC 4967

UNIFORM LINEAR SCALE

0 10 20 30 40 50 kpc

GALAXIES WITH NO RC2 CLASSIFICATION/UNCERTAIN CLASSIFICATIONS

NGC 2788

NGC 5292

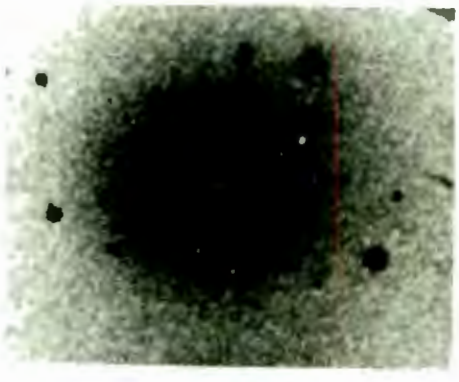

A1034–27A

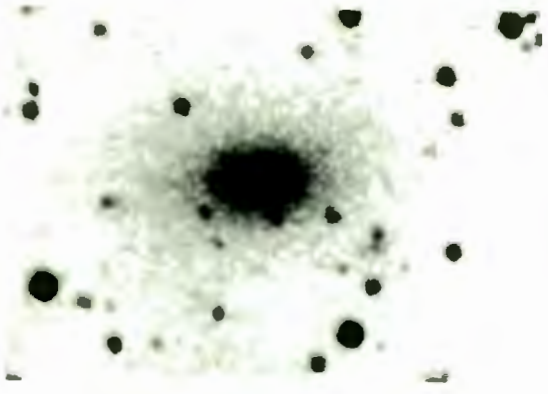

A1234–72

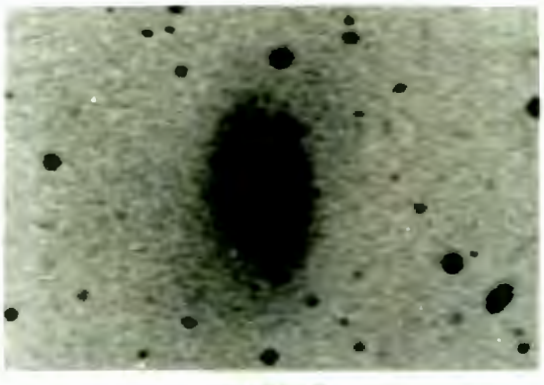

A1332–33

A1335–33

Plate 36

UNIFORM LINEAR SCALE

0 10 20 30 40 50 kpc

GALAXIES WITH NO RC2 CLASSIFICATION/UNCERTAIN CLASSIFICATIONS

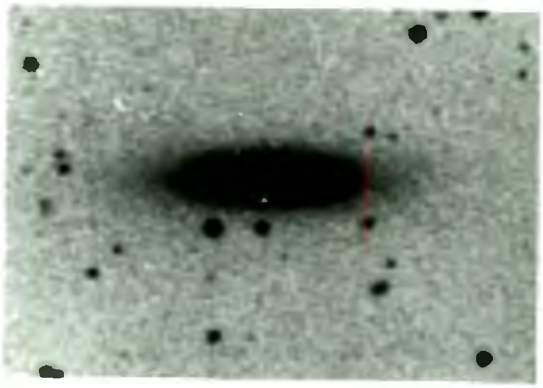

A1345–30

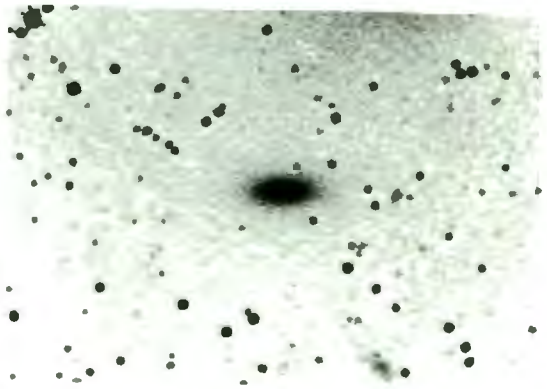

A1515–23

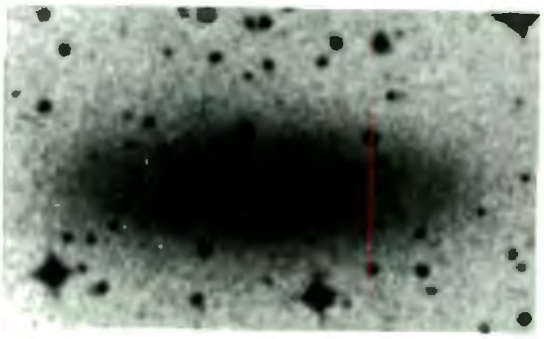

A1903–61

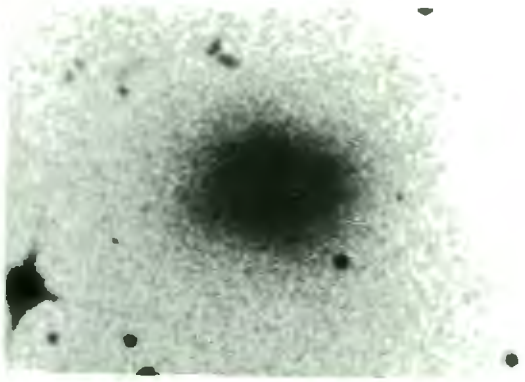

A2100–48

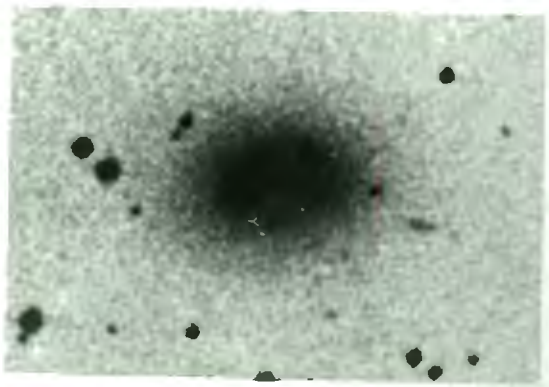

A2101–48

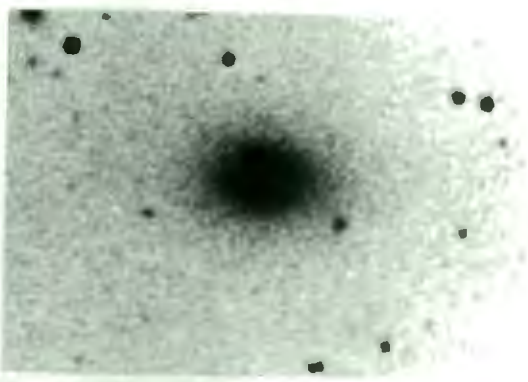

A2102–47

Plate 37

UNIFORM LINEAR SCALE

0 10 20 30 40 50 kpc

GALAXIES WITH NO RC2 CLASSIFICATION/UNCERTAIN CLASSIFICATIONS

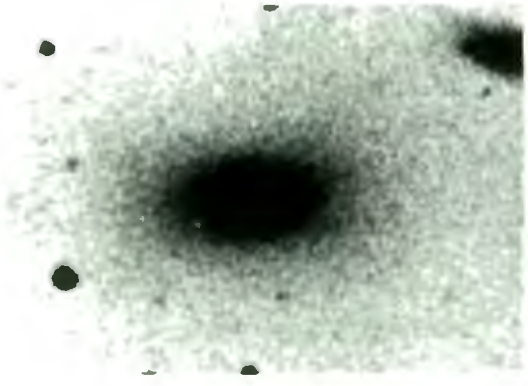

A2103–47

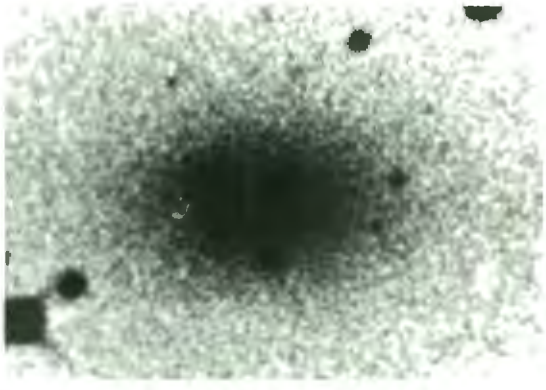

A2152–69

A2207–46

IC 1876

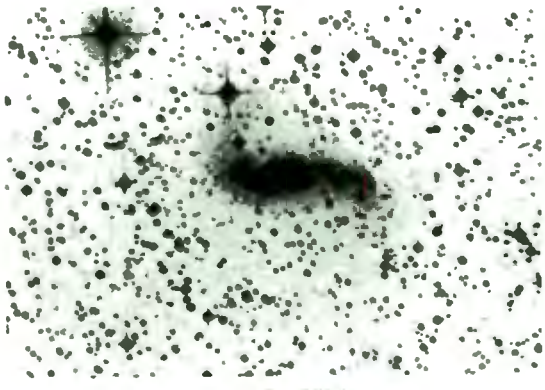

IC 2554

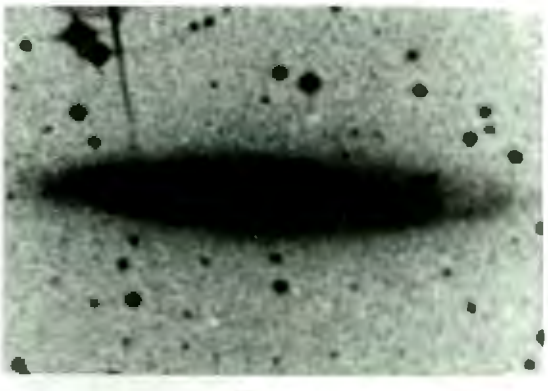

IC 4827

Plate 38

UNIFORM LINEAR SCALE

0 10 20 30 40 50 kpc

GALAXIES WITH NO RC2 CLASSIFICATION/UNCERTAIN CLASSIFICATIONS

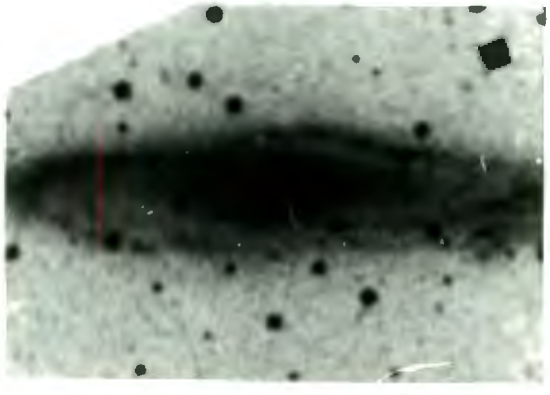

IC 4831

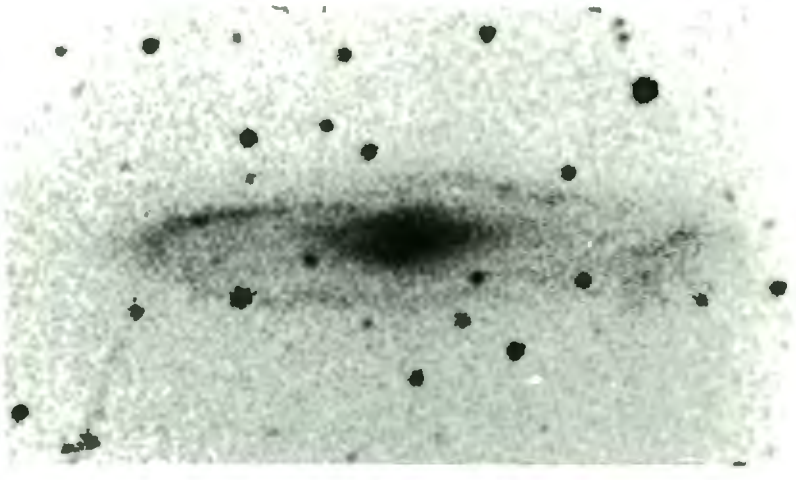

IC 4831 (B)

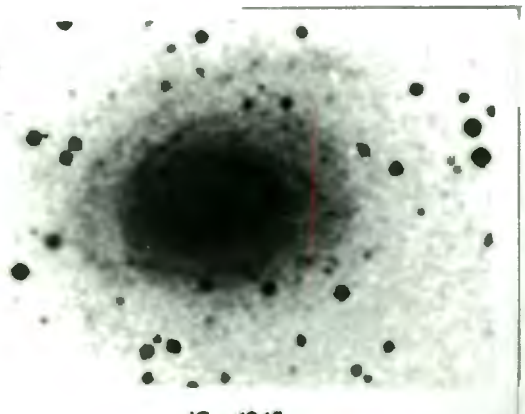

IC 4845

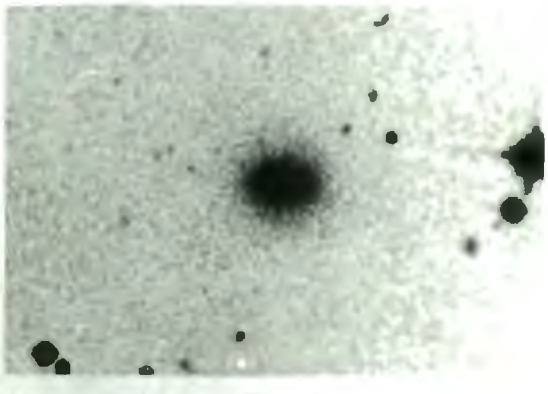

IC 4967

Plate 39

similar morphology.* It has a diameter of ∿35 kpc.

NGC 7496, classified in the RSA as SBc(s), only shows one faint outer arm instead of a pair, which almost encircles the galaxy. The major diameter is of the order of 30 kpc.

The dynamical effect of galaxies with ovally distorted disks is the same as that of a bar [e.g. the numerical hydrodynamical work of Sanders and Huntley (1976)].

---

* In this galaxy, the important difference is that the outer arms do not form a distinct component, but are a continuation of the brighter inner spiral arms.

Galaxies in Section 8.3

Galaxy NGC	Classification (RSA)
7496	SBc(s) II.8
7552	SBbc(s) I-II
7412	Sc(rs) I-II
986	SBb(rs) I-II
5135	SBb (I)

UNIFORM LINEAR SCALE

0 10 20 30 40 50 kpc

GALAXIES WITH A HIGH SURFACE BRIGHTNESS DISK, AND FAINT OUTER SPIRAL ARMS

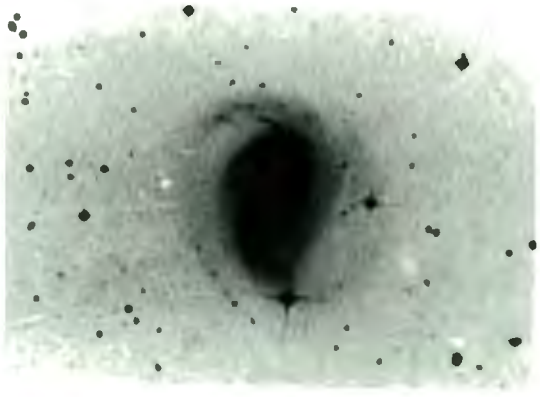

NGC 7496

NGC 7552

NGC 7412

NGC 986

Plate 40

UNIFORM LINEAR SCALE

0 10 20 30 40 50 kpc

GALAXIES WITH A HIGH SURFACE BRIGHTNESS DISK, AND FAINT OUTER SPIRAL ARMS

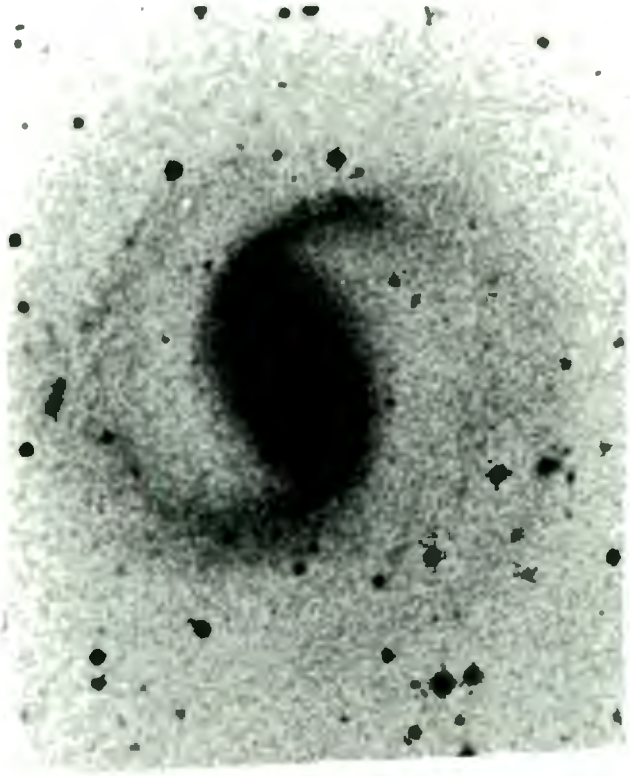

NGC 5135

Plate 41

UNIFORM LINEAR SCALE

0 10 20 30 40 50 kpc

TWO SOUTHERN GALAXIES WITH PREDOMINANT, ELLIPTICALLY SHAPED NUCLEI

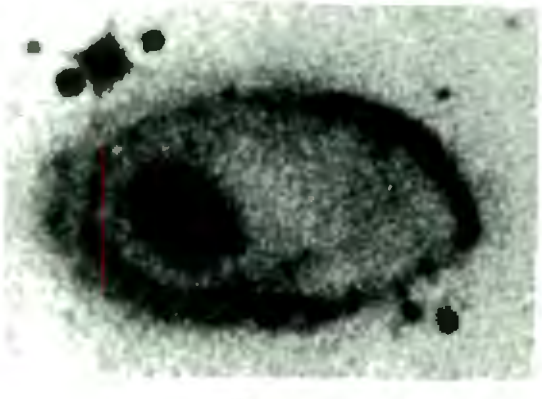

A0644–74

F 275

Plate 42

CHAPTER NINE

ScI Galaxies from the Palomar Observatory Sky Survey

The galaxies photographed here (from the POSS O = blue prints) were either classified as ScI by van den Bergh (1960a), or by Sandage and Tammann (1975b; table 1).

ScI's have been used as standard candles in mapping the global Hubble flow, and it is interesting to find such a great diversity in spiral arm texture within this group. *A priori*, one might well have expected to find a relatively similar morphology for this class - akin say to that of M101. The range, as seen on a linear scale, is indeed remarkable.

As with galaxies from the J-survey, the galaxies here can be grouped according to their appearance on the Palomar Observatory Sky Survey - (Blue Prints).

In viewing the montage (plates 43-48), one sees that several of the program ScI's included by Sandage and Tammann have saturated images [0145 + 12, NGC 644, IC 1743 and NGC 706]. Many have spiral arms of low surface brightness [such as IC 211, NGC 173, NGC 180 and NGC 521]. The outer arms sometimes become exceptionally tenuous (NGC 173, for example). Some can have massive arms, as in NGC 673.

Of those ScI's with medium arms, we discuss NGC 4254 and NGC 4321. Both are members of the Virgo cluster; Sandage and Tammann (1976) showed that their angular diameters were approximately $\frac{1}{3}$ that of M101 [fig. 6 of their paper], but that the galaxies had a corresponding velocity increase of $\sim$3. Thus, if these spirals were all of about the same intrinsic

size, one would have additional supportive evidence for the velocity ratio adopted by Sandage and Tammann of

$$v_o(\text{Virgo})/v_o(\text{M101}) = 2.7$$

and evidence against any smaller step.

It is thus interesting to see the analogue of their fig. 6 for M101, NGC 4321 and NGC 4254 on a uniform physical scale [M101 being illustrated in plate 55].

The range in intrinsic size for this illustrative sample is from some 30 kpc (for NGC 4254) to over 85 kpc for NGC 521.

ScI Galaxies

Saturated/Predominantly Saturated Images on POSS

0145 + 12

NGC 664

IC 1743

NGC 706

UNIFORM LINEAR SCALE

0 10 20 30 40 50 kpc

Scl GALAXIES FROM THE PALOMAR OBSERVATORY SKY SURVEY

SATURATED/PREDOMINANTLY SATURATED IMAGES

0145+12

NGC 664

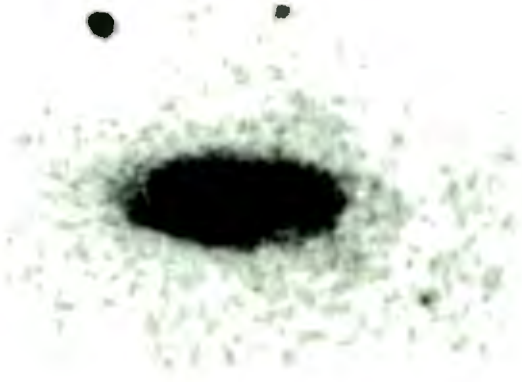

IC 1743

NGC 706

Plate 43

ScI Galaxies

Massive Arms

0037 + 02

NGC 673

UNIFORM LINEAR SCALE

0 10 20 30 40 50 kpc

Scl GALAXIES FROM THE PALOMAR OBSERVATORY SKY SURVEY

MASSIVE ARMS

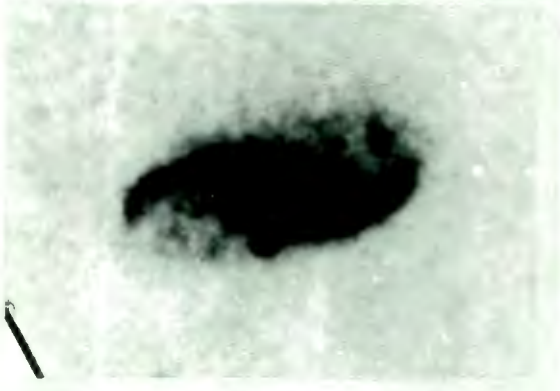

0037+02

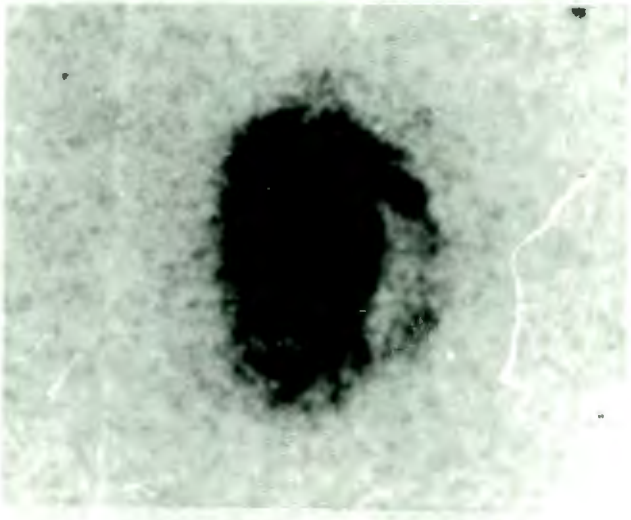

NGC 673

Plate 44

ScI Galaxies

Medium Arms

0152 + 06

NGC 4254

NGC 4321

NGC 257

NGC 7782

NGC 1232

UNIFORM LINEAR SCALE

0 10 20 30 40 50 kpc

Scl GALAXIES FROM THE PALOMAR OBSERVATORY SKY SURVEY

MEDIUM ARMS

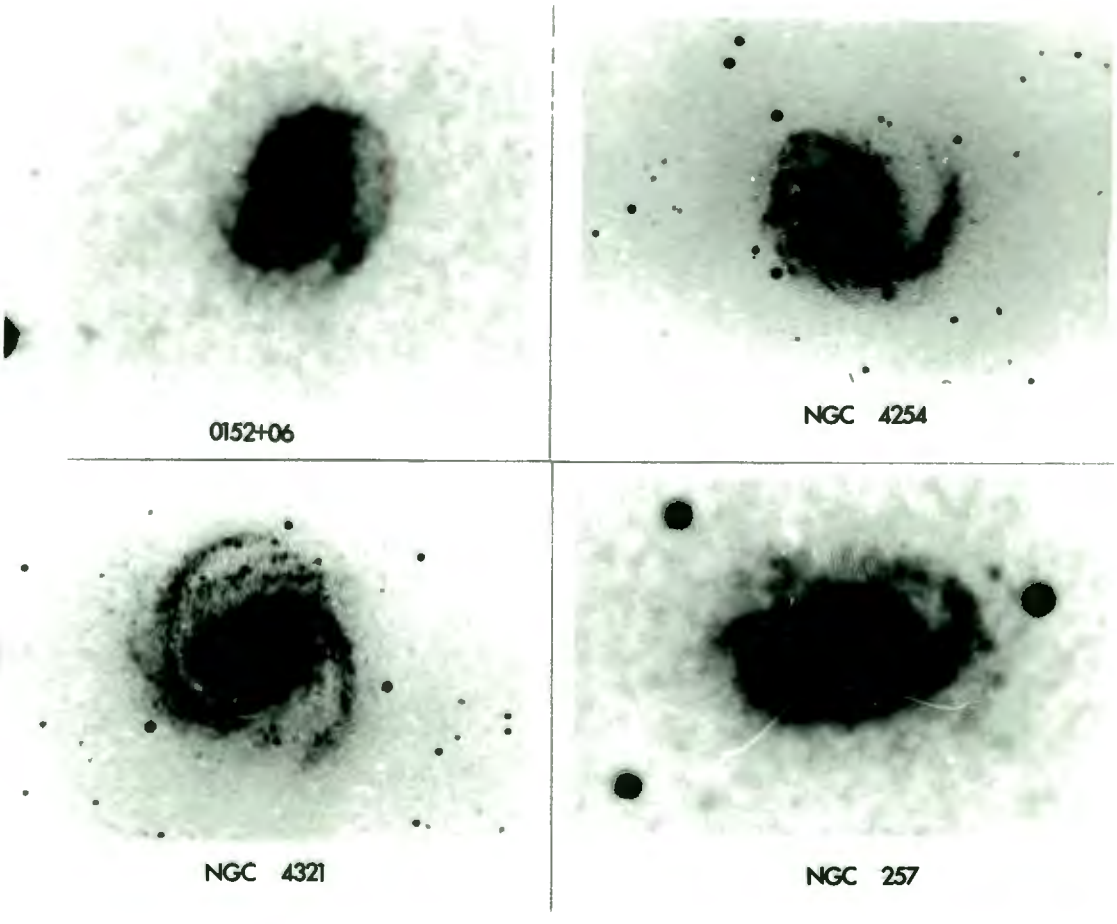

Plate 45

UNIFORM LINEAR SCALE

0 10 20 30 40 50 kpc

Scl GALAXIES FROM THE PALOMAR OBSERVATORY SKY SURVEY

MEDIUM ARMS

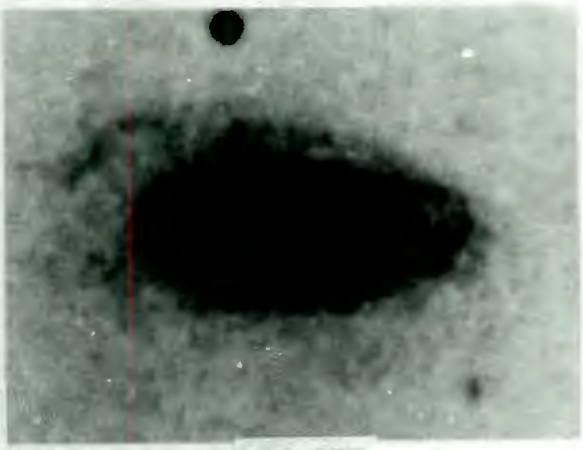

NGC 7782

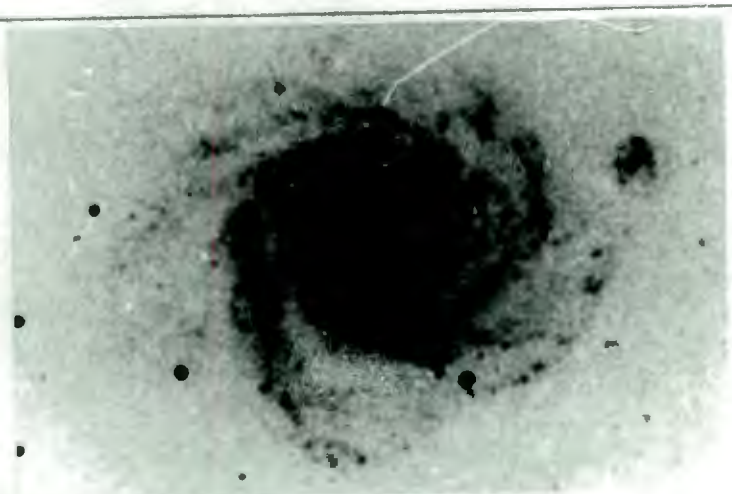

NGC 1232

Plate 46

ScI Galaxies

Weak Arms

IC 211

NGC 99

2255 + 02

NGC 7816

0115 + 11

NGC 173

NGC 180

NGC 182

NGC 521

UNIFORM LINEAR SCALE

0 10 20 30 40 50 kpc

Scl GALAXIES FROM THE PALOMAR OBSERVATORY SKY SURVEY

WEAK ARMS

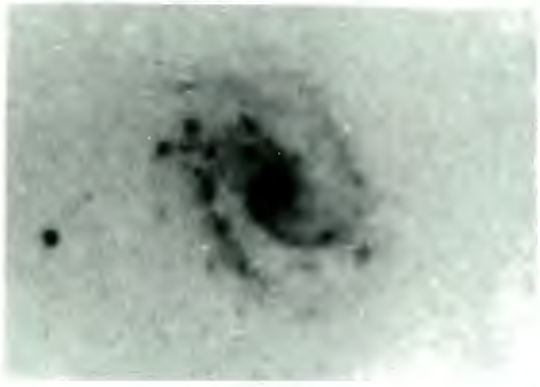

IC 211

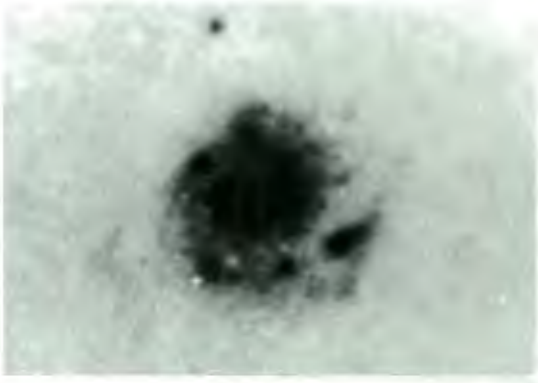

NGC 99

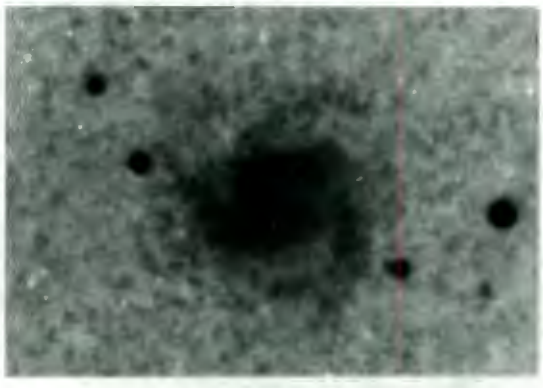

2255+02

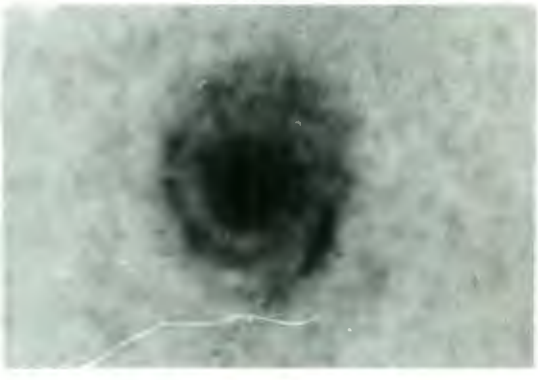

NGC 7816

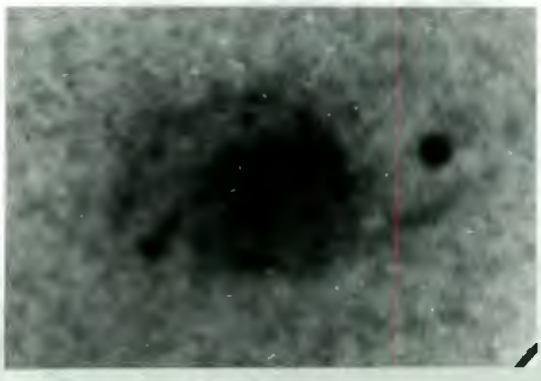

0115+11

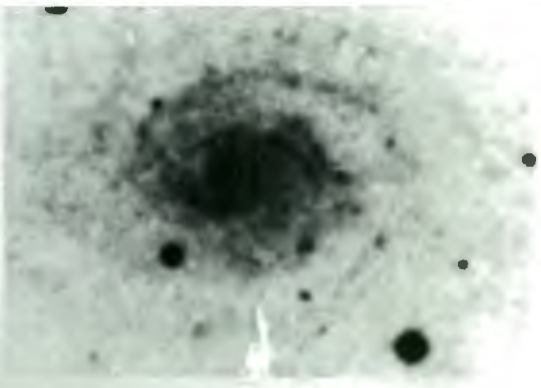

NGC 173

Plate 47

UNIFORM LINEAR SCALE

0 10 20 30 40 50 kpc

Scl GALAXIES FROM THE PALOMAR OBSERVATORY SKY SURVEY

WEAK ARMS

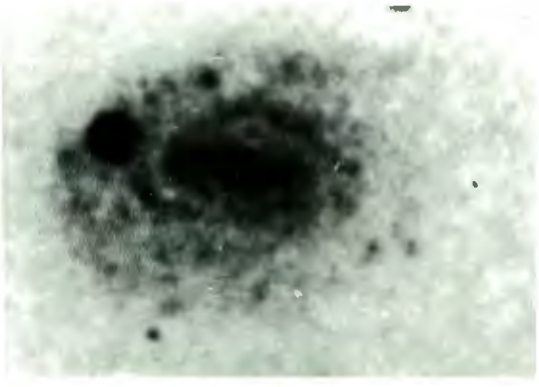

NGC 180

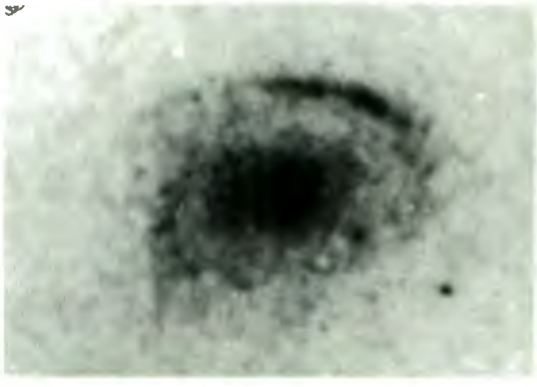

NGC 182

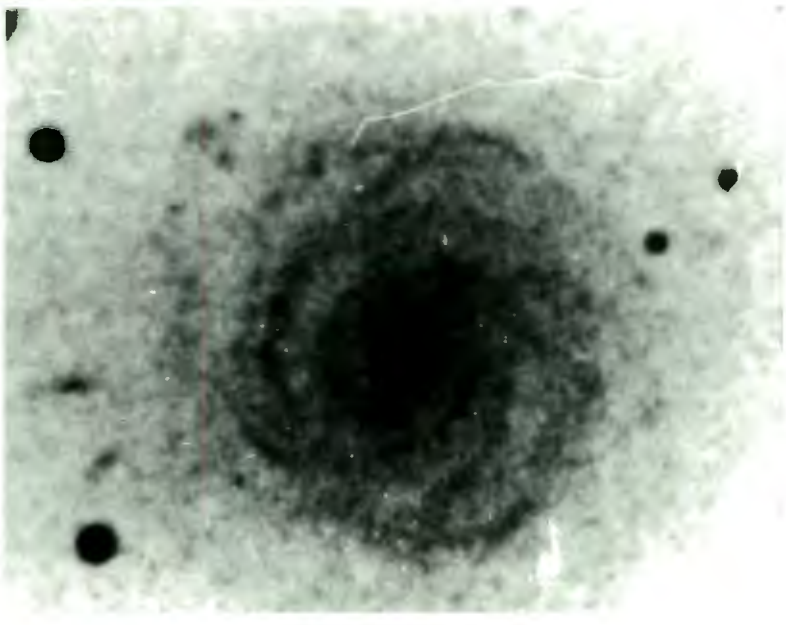

NGC 521

Plate 48

CHAPTER TEN

A MONTAGE OF IIIa-J AND "QUICK BLUE" SURVEY PHOTOGRAPHS

In this chapter, we present twenty-nine pairs of photographs, one set from the IIIa-J Survey, and a corresponding set from the ESO B Survey. The superior f-ratio of the U.K. Schmidt telescope, coupled with the sensitization of the IIIa-J emulsion, results in a far deeper survey than the "Quick Blue", and is especially well suited in revealing both massive, and faint outlying spiral arms.

Our principal observations from an intercomparison of the pairs may be enumerated as follows:

(I) Galaxies with predominantly saturated images on the IIIa-J Survey present an inner morphology which is generally not regular or global; moreover, particularly in the intrinsically small spirals NGC 2082, A2015-39 and NGC 6215, a rather distorted or ragged appearance is seen, indicative of [substantial] differential rotation effects.

(II) The proposed subdivision according to a galaxy's appearance on the J-Survey is not a property of that survey; a similar progression from massive to weak arms is seen on the ESO B Survey. In particular,

(a) Galaxies with massive arms on the J-Survey have corresponding well defined arms on the B-Survey (for example, IC 4366, A1213-34 and A1427-34).

(b) Thin and regular spiral arm features are seen in the medium arm category; this being well illustrated in A2125-38, NGC 6699 and A1517-36.

(c) In the weak arm subdivision, the arms on the J-Survey are barely discernable on the B-Survey; A1125-36 is a good example.

The groupings illustrate a fundamental inherent difference in spiral arm texture.

PAIRS OF IIIa-J AND ESO B PHOTOGRAPHS

IIIa-J Subdivision: Saturated/Predominantly Saturated Image

NGC

2082

A2015-39

6215

440

1511

7361

6221

5188

3568

434

Massive Arms

NGC 6753

IC 4366

A1213-34

A1427-34

Medium Arms

A2125-38

NGC 6699

IC 4852

A1517-36

NGC 3312

A1829-41

Weak Arms

NGC 5556

A1125-36

NGC 5161

Type O/a, a Spirals

NGC
3314
3783

Gravitationally Interacting Systems

NGC
4105
6769/6770

Other galaxies discussed separately

NGC
6782
5292

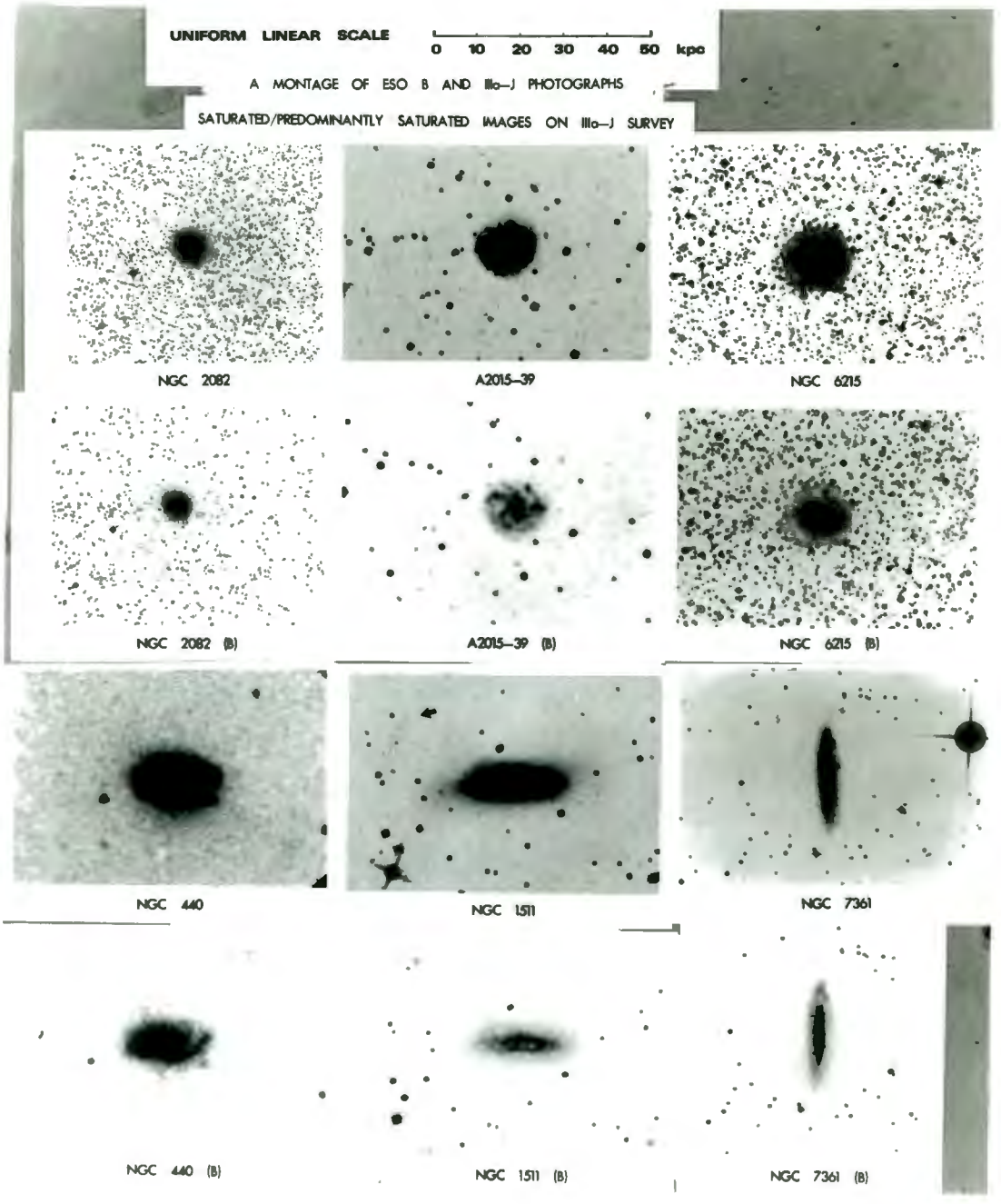
UNIFORM LINEAR SCALE
0 10 20 30 40 50 kpc
A MONTAGE OF ESO B AND IIIa–J PHOTOGRAPHS
SATURATED/PREDOMINANTLY SATURATED IMAGES ON IIIa–J SURVEY
NGC 2082
A2015–39
NGC 6215
NGC 2082 (B)
A2015–39 (B)
NGC 6215 (B)
NGC 440
NGC 1511
NGC 7361
NGC 440 (B)
NGC 1511 (B)
NGC 7361 (B)

Plate 49

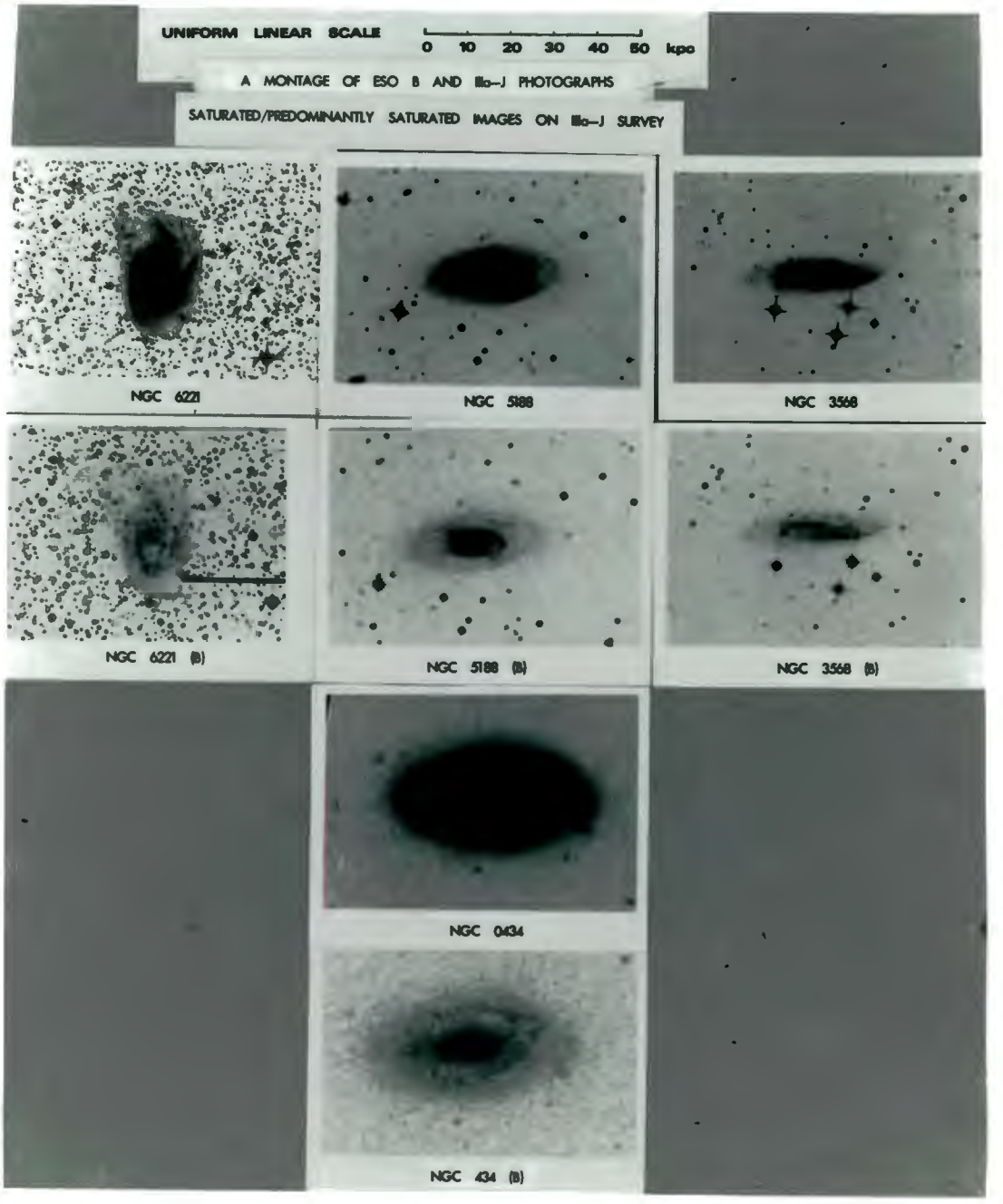
UNIFORM LINEAR SCALE
0 10 20 30 40 50 kpc
A MONTAGE OF ESO B AND IIIa–J PHOTOGRAPHS
SATURATED/PREDOMINANTLY SATURATED IMAGES ON IIIa–J SURVEY
NGC 6221
NGC 5188
NGC 3568
NGC 6221 (B)
NGC 5188 (B)
NGC 3568 (B)
NGC 0434
NGC 434 (B)

Plate 50

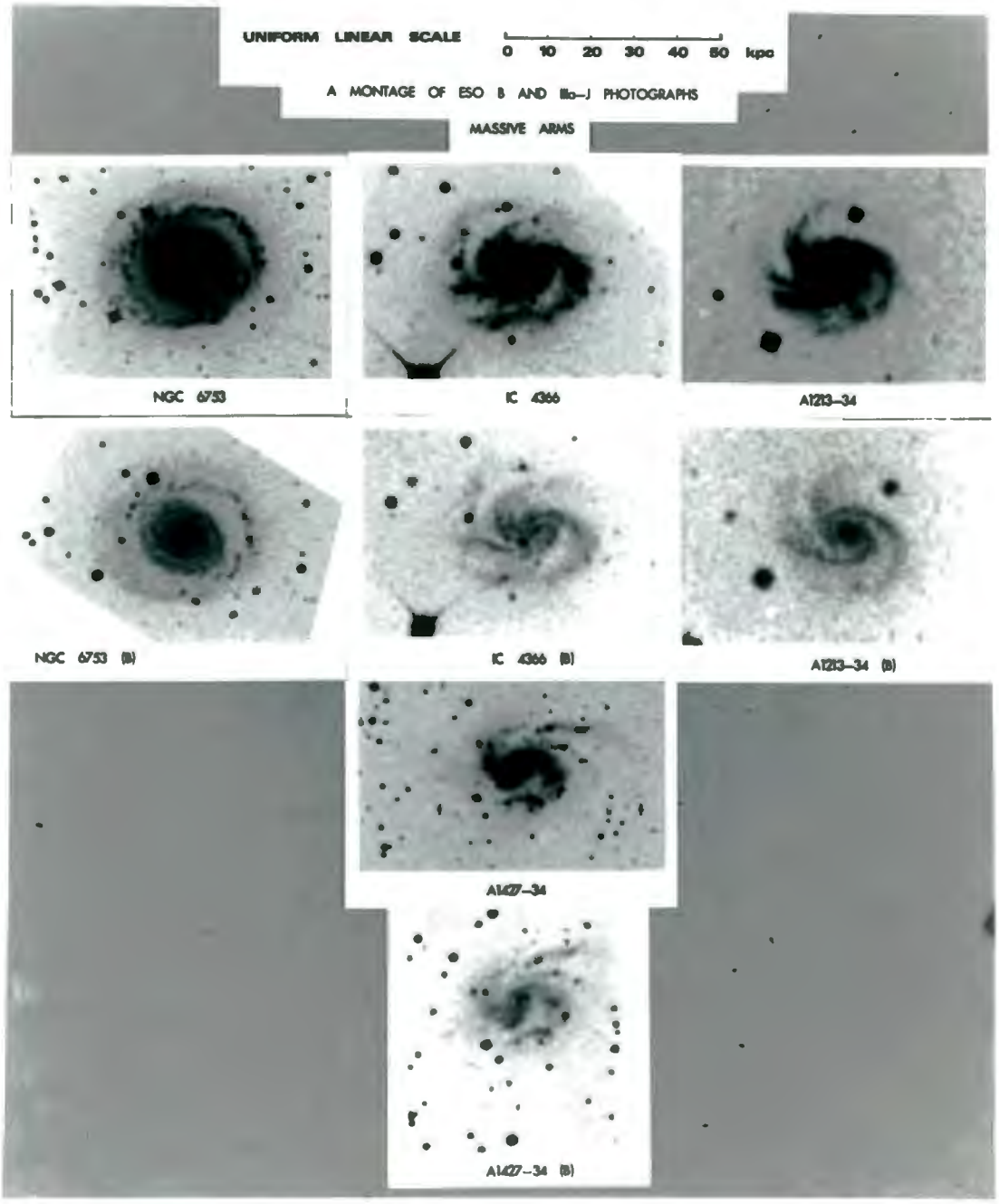
UNIFORM LINEAR SCALE
0 10 20 30 40 50 kpc
A MONTAGE OF ESO B AND IIIa-J PHOTOGRAPHS
MASSIVE ARMS
NGC 6753
IC 4366
A1213-34
NGC 6753 (B)
IC 4366 (B)
A1213-34 (B)
A1427-34
A1427-34 (B)

Plate 51

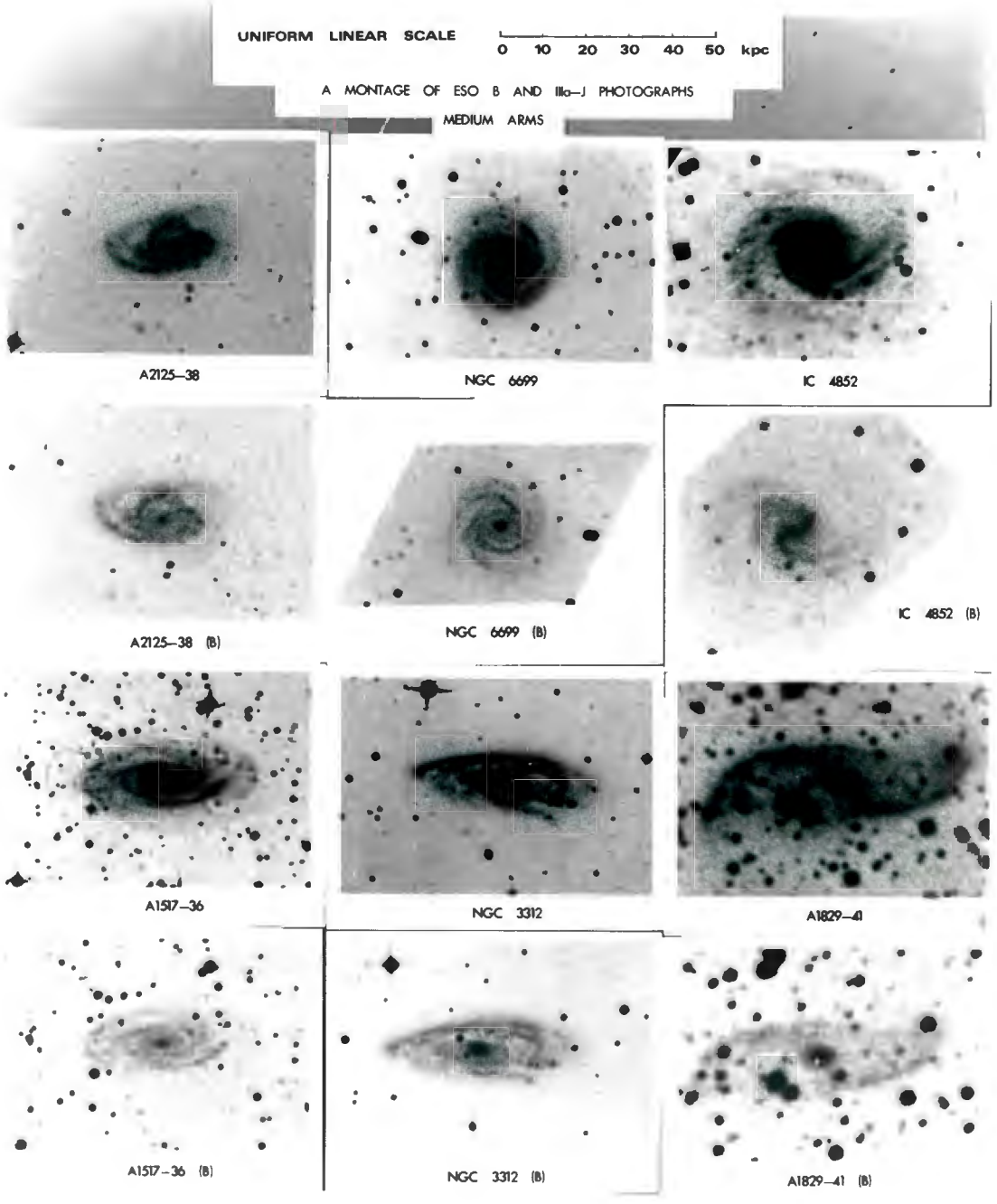
UNIFORM LINEAR SCALE
0 10 20 30 40 50 kpc
A MONTAGE OF ESO B AND IIIa–J PHOTOGRAPHS
MEDIUM ARMS
A2125–38
NGC 6699
IC 4852
A2125–38 (B)
NGC 6699 (B)
IC 4852 (B)
A1517–36
NGC 3312
A1829–41
A1517–36 (B)
NGC 3312 (B)
A1829–41 (B)

Plate 52

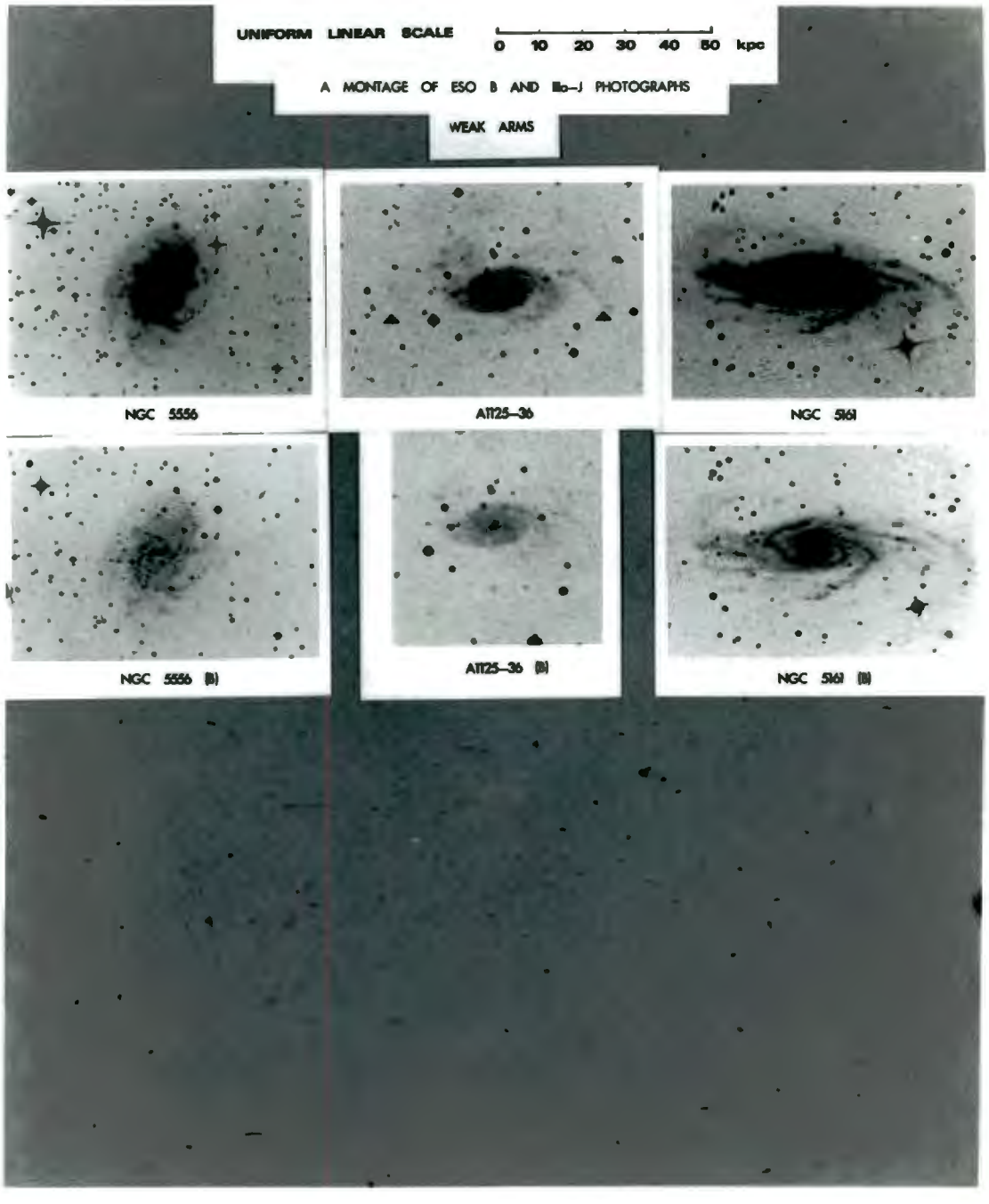
UNIFORM LINEAR SCALE
0 10 20 30 40 50 kpc
A MONTAGE OF ESO B AND IIIa-J PHOTOGRAPHS
WEAK ARMS
NGC 5556
AM125-36
NGC 5161
NGC 5556 (B)
AM125-36 (B)
NGC 5161 (B)

Plate 53

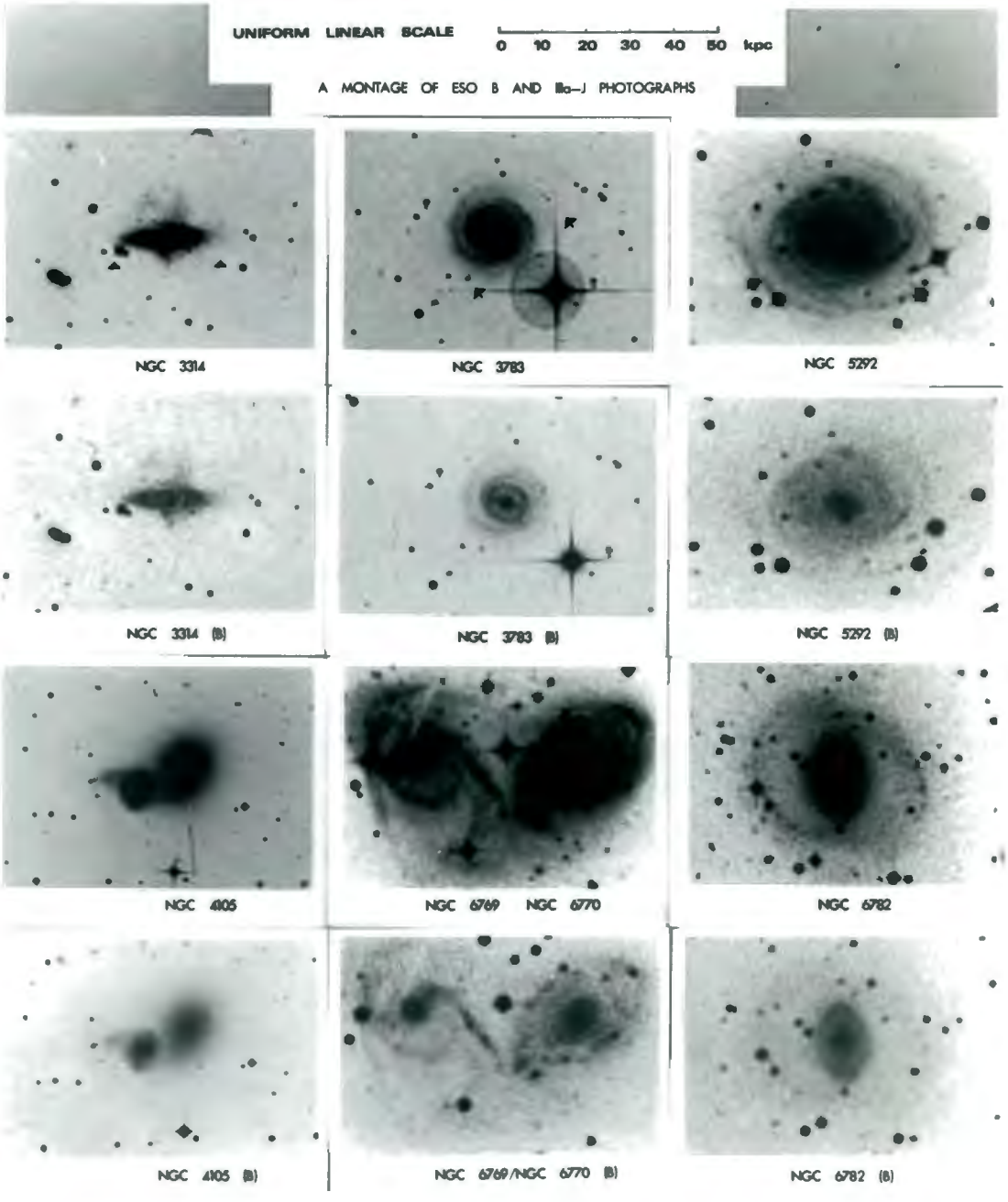
UNIFORM LINEAR SCALE
0 10 20 30 40 50 kpc
A MONTAGE OF ESO B AND IIIa–J PHOTOGRAPHS
NGC 3314
NGC 3783
NGC 5292
NGC 3314 (B)
NGC 3783 (B)
NGC 5292 (B)
NGC 4105
NGC 6769 NGC 6770
NGC 6782
NGC 4105 (B)
NGC 6769/NGC 6770 (B)
NGC 6782 (B)

Plate 54

CHAPTER ELEVEN

MISCELLANIA

11.1 The Danver Spirals: A Comparison

In this section, we compare the form of the absolute magnitude-diameter plot obtained for the sample of galaxies we photographed [i.e. all those galaxies with listed absolute magnitudes in table 6], to that obtained using the Danver sample of galaxies [table 8].

The results, illustrated in figures 9 and 10, show that the coefficient of correlation for our sample in the (M, log D) plane is $|\rho| = 0.795$, while the correlation for the Danver spirals is higher: $|\rho| = 0.88$. This re-asserts, once again, the very large range in surface brightness (for both spirals and ellipticals) within our sample. [The arrowed line in figure 9 has the slope dM/d(log D) = -5, and indicates the form of the graph one would obtain if all the galaxies were of constant surface brightness].

An interesting correlation is seen in figure 11; a diameter - surface brightness plot for all our galaxies with listed apparent magnitudes and de Vaucouleurs diameter D_{25} (in table 6). The coefficient of correlation is significant: $\rho = 0.62$, while for the Danver spirals the value is (considerably) lower: $\rho = 0.44$, (figure 12).

11.2 A Montage of Some Well Known Galaxies

The montage consists of M33, M31, M83, M101, NGC 5128 and NGC 4303 (Virgo cluster member), all on a uniform linear scale. M31, so often illustrated in textbooks on a large

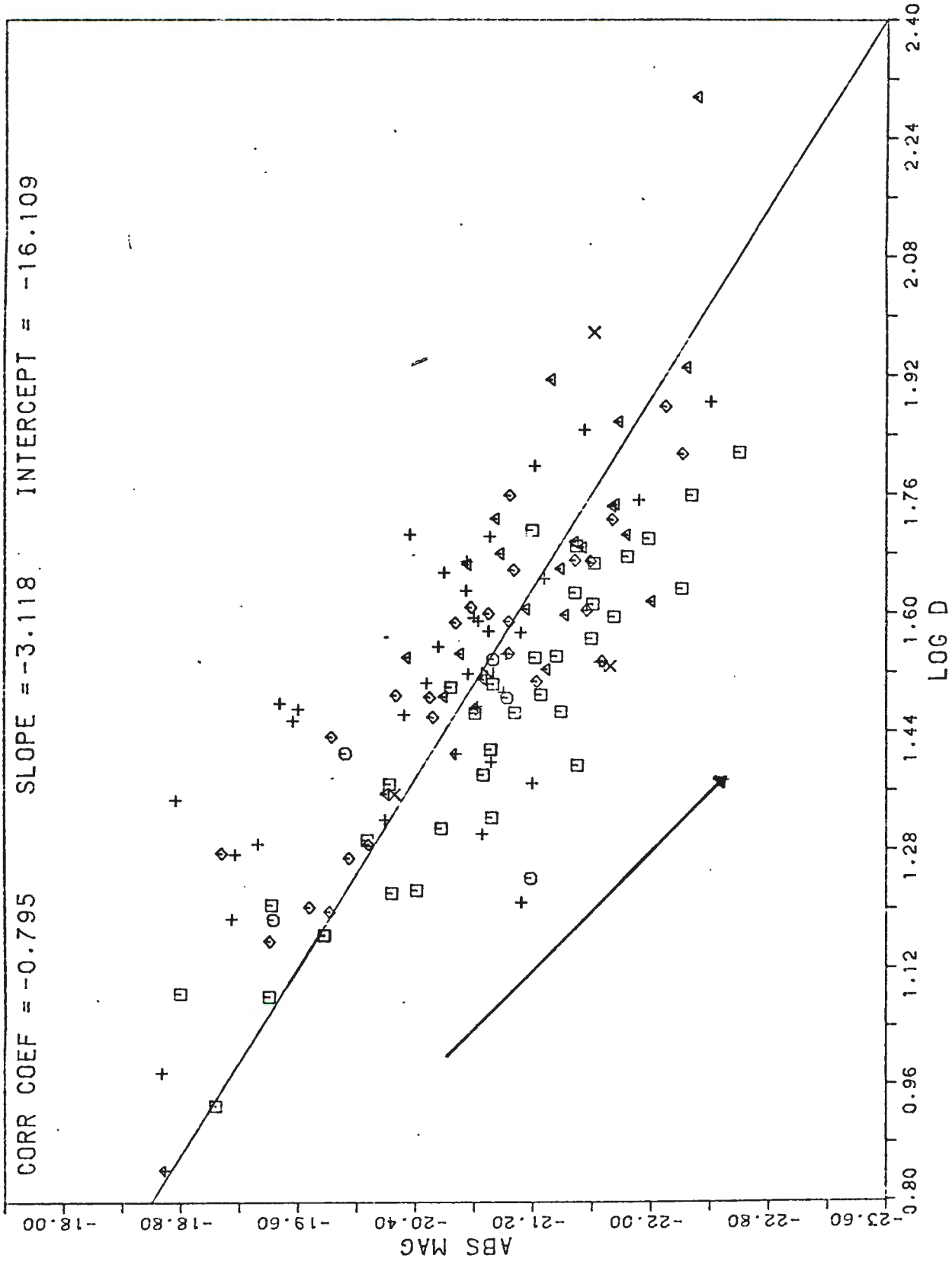

Figure 9. Absolute magnitude - log D plot for all galaxies photographed (listed in Table 6) with known apparent magnitudes. Different symbols denote different Hubble types. The solid line has the (theoretical) slope of -5.

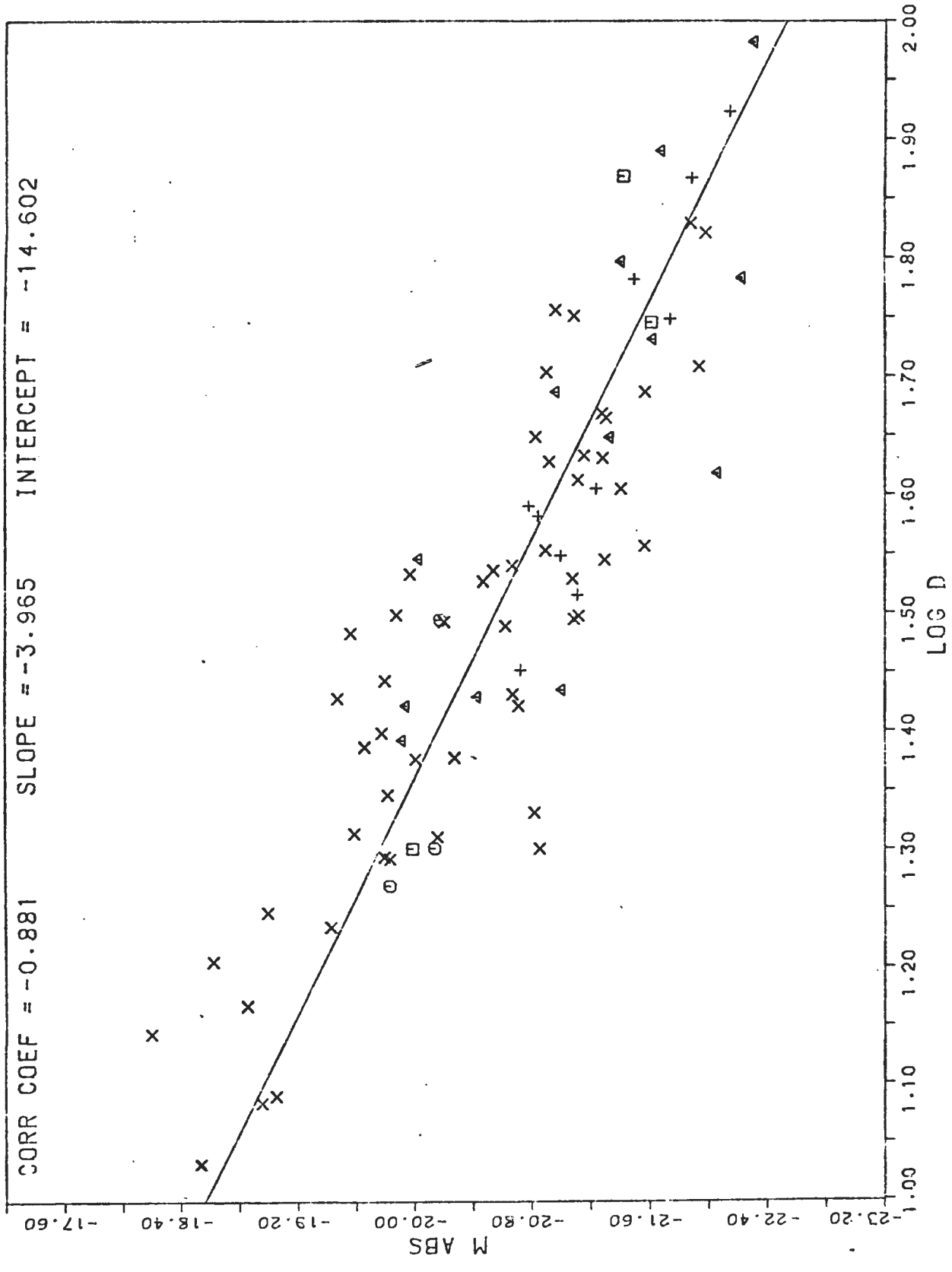

Figure 10. Corresponding to figure 9, we plot the Danver Spirals (table 8) in an absolute magnitude - log D diagram.

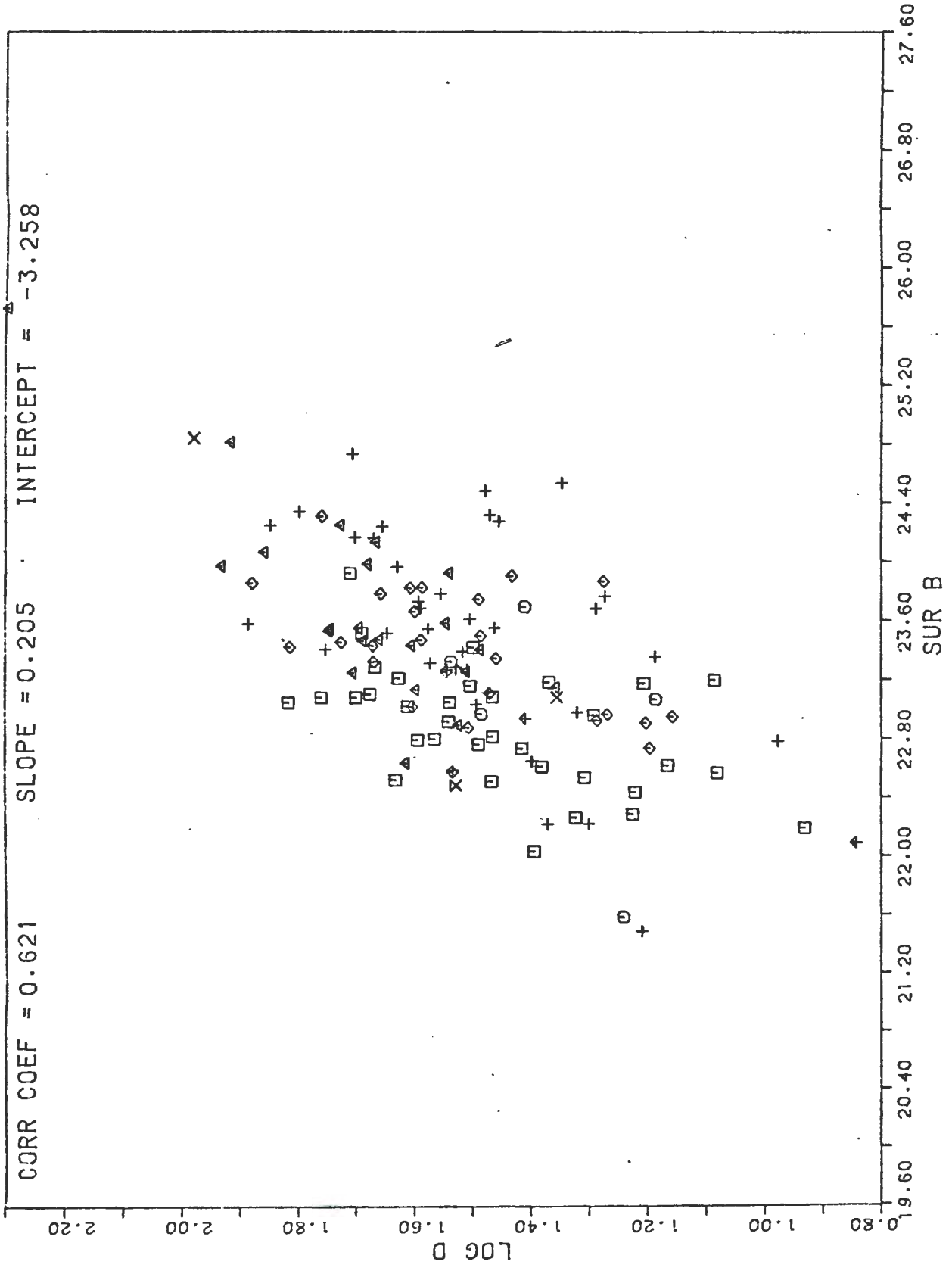

Figure 11. The diagram shows a general correlation of log diameter - surface brightness for galaxies in our sample. The correlation coefficient is $\rho = 0.6$.

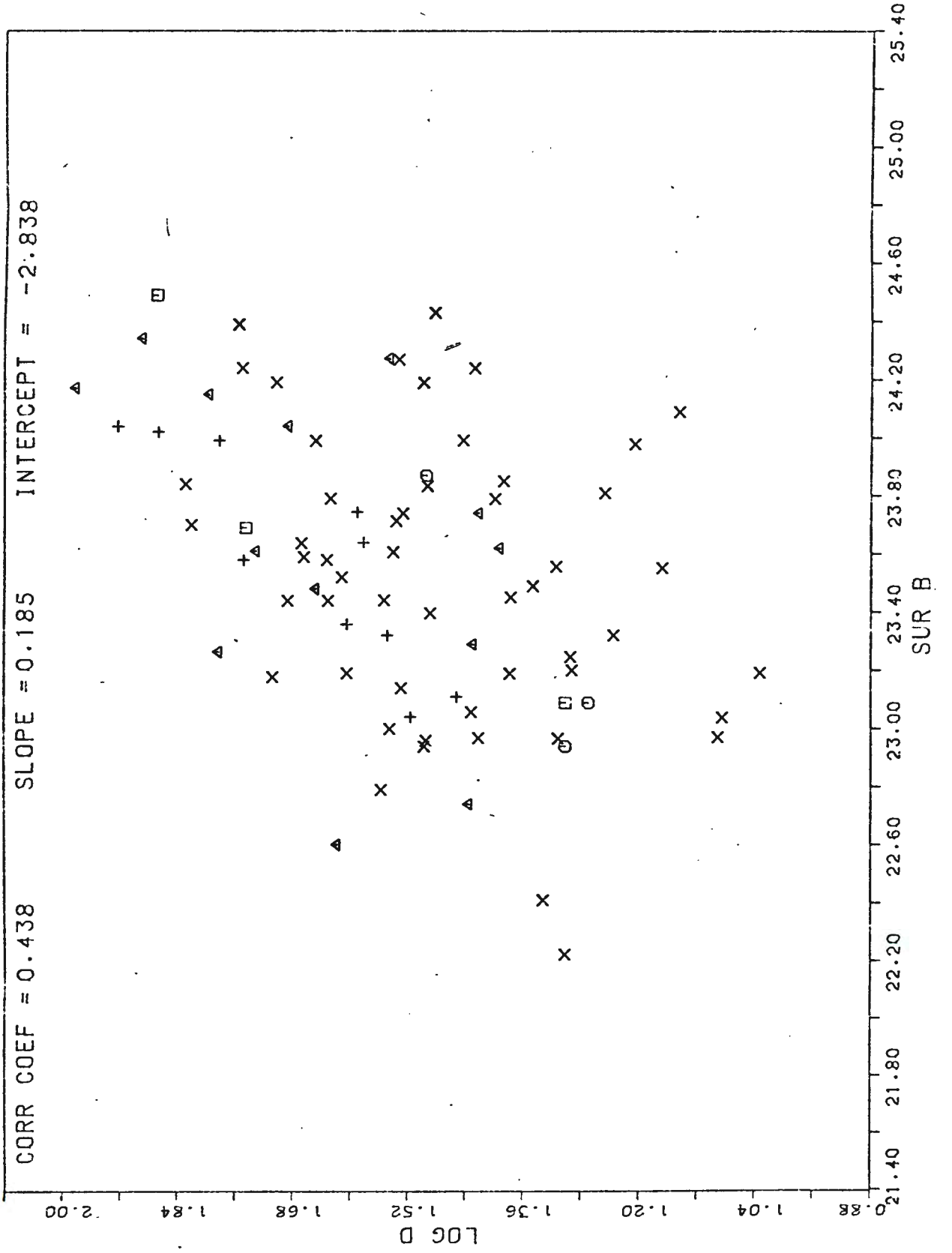

Figure 12. A less significant correlation is seen for the Danver Spirals [table 8] in this log diameter - surface brightness diagram.

angular scale, is truly 'scaled to size'; in printing that photograph, the RSA distance of 679 kpc has been adopted.

The saturated region of the elliptical component of NGC 5128 is not particularly large when compared to other ellipticals (chapter seven); of the order of 20 kpc. The overall extent is ∿52 kpc; a 6.5 Mpc distance has been assumed. Interestingly enough, NGC 5128 is not strikingly large at all; in their recent study, Dufour *et al.* (1979) note that the suggestion of a collision between an elliptical and a spiral [as proposed by Baade and Minkowski (1954)] *still cannot be ruled out.*

Adopting a 20 Mpc distance to the Virgo cluster, one obtains a diameter of one of its members, NGC 4303, nicely comparable to that of M101.

M83 and M33 have been discussed in chapter five.

11.3 Galaxies from the Fairall Survey

The cluster 1842-633 is included here as it contains both very small and very large ellipticals; Fairall (1979a) cites the dominant elliptical member IC 4765 as an undersized cD galaxy; only the central region is seen in our photograph. In contrast, the small ellipticals have diameters from ∿5 kpc upwards.

Also included in this section are galaxies selected and described by Fairall (1979b). Of these, F-51, F-156, F-158, F-166, F-177, F-182, IC4769, F-189, IC 5222, IC 5272 and and F-203 are emission line objects. The range in diameters of these galaxies is once again remarkable; and is well illustrated in the "spinal column" in plate 1 of Fairall (1980a). F-166 has a diameter of only ∿5 kpc, and looks like a small

elliptical; F-51 is much larger - diameter ∿40 kpc.

The galaxies photographed in each montage are listed below:

Cluster 1842 - 633

Members 1, 2, 3, 4, 5, 6, 8, 9, 10, 11, 12, 16, 17, 18, 21, 23, 25 have been photographed.

Galaxies from Fairall (1979b)

F51
F156
F158
F164
F165
F166
F177
F178
IC 4741
IC 4742
F182
IC 4751
IC 4753
IC 4754
NGC 6673
F187
IC 4769
F189
IC 5222
IC 5272
F203

A MONTAGE OF SOME WELL KNOWN GALAXIES

UNIFORM LINEAR SCALE

0 10 20 30 40 50 kpc

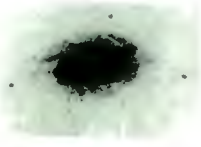

NGC 598 (M33)

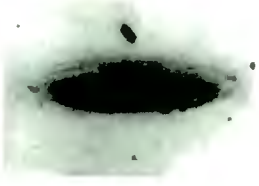

NGC 224=M31

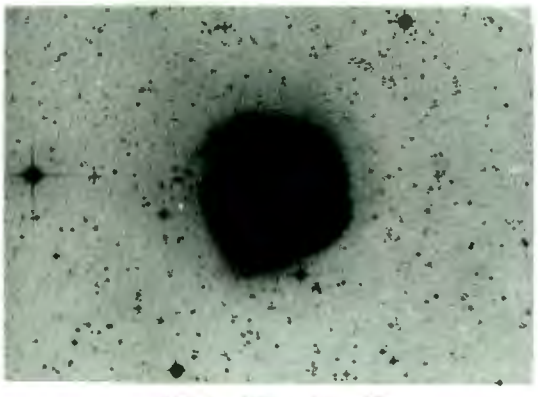

NGC 5236 (M 83)

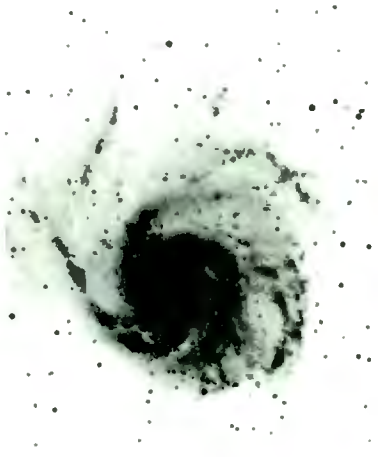

NGC 5457 (M 101)

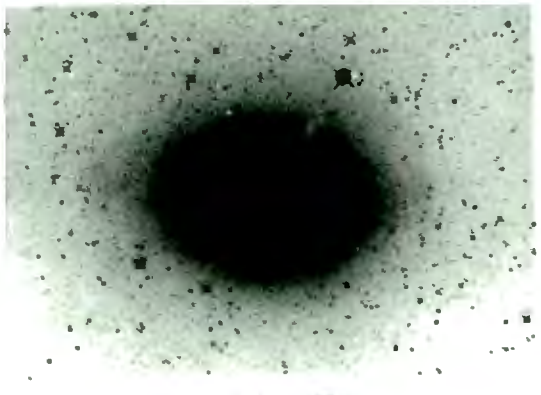

NGC 5128

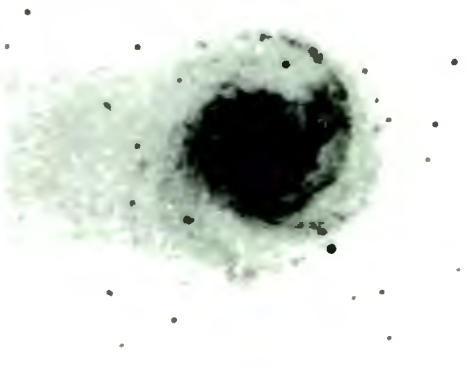

NGC 4303

Plate 55

UNIFORM LINEAR SCALE 0 10 20 30 40 50 kpc

GALAXIES FROM THE FAIRALL SURVEY

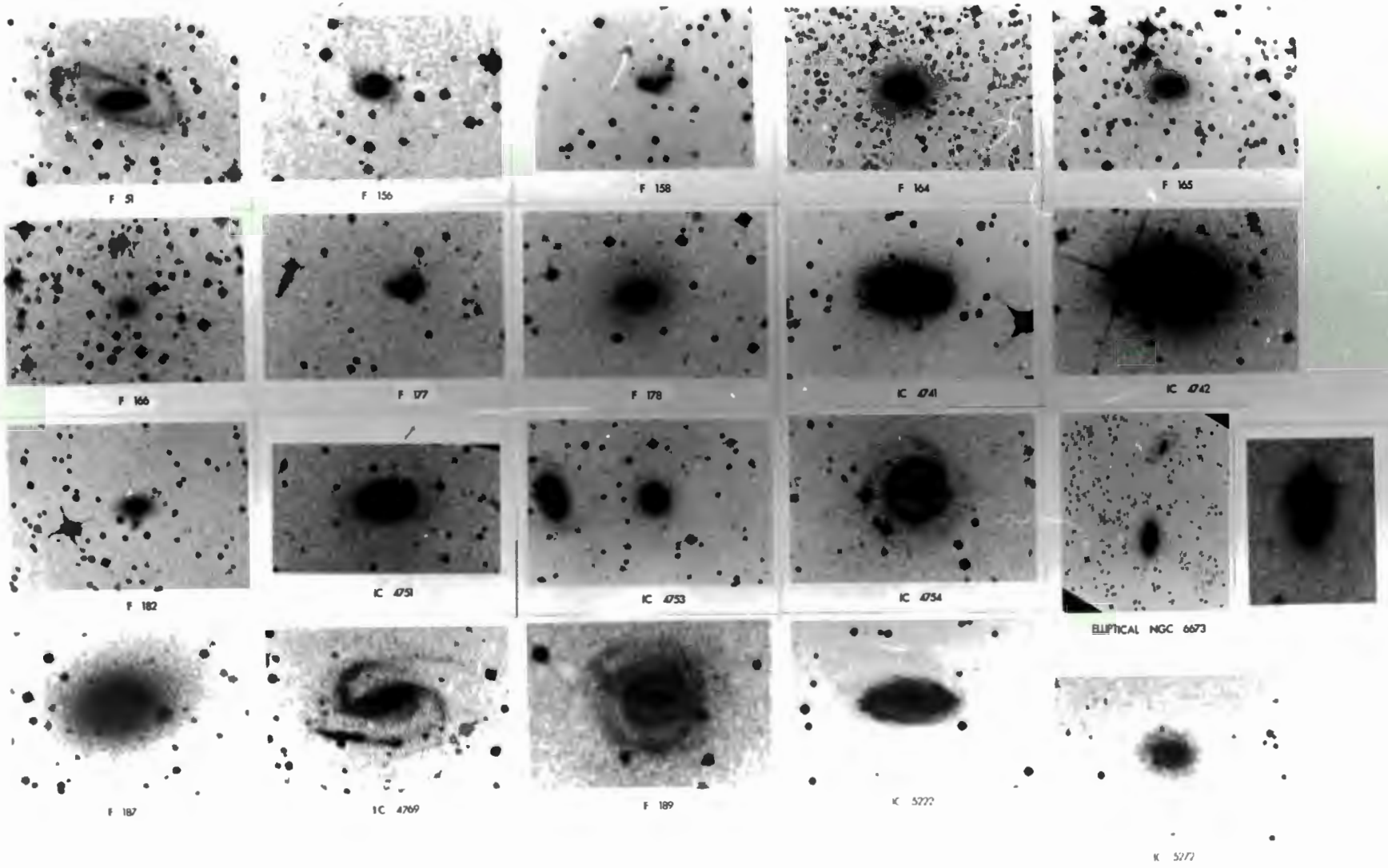

Plate 56

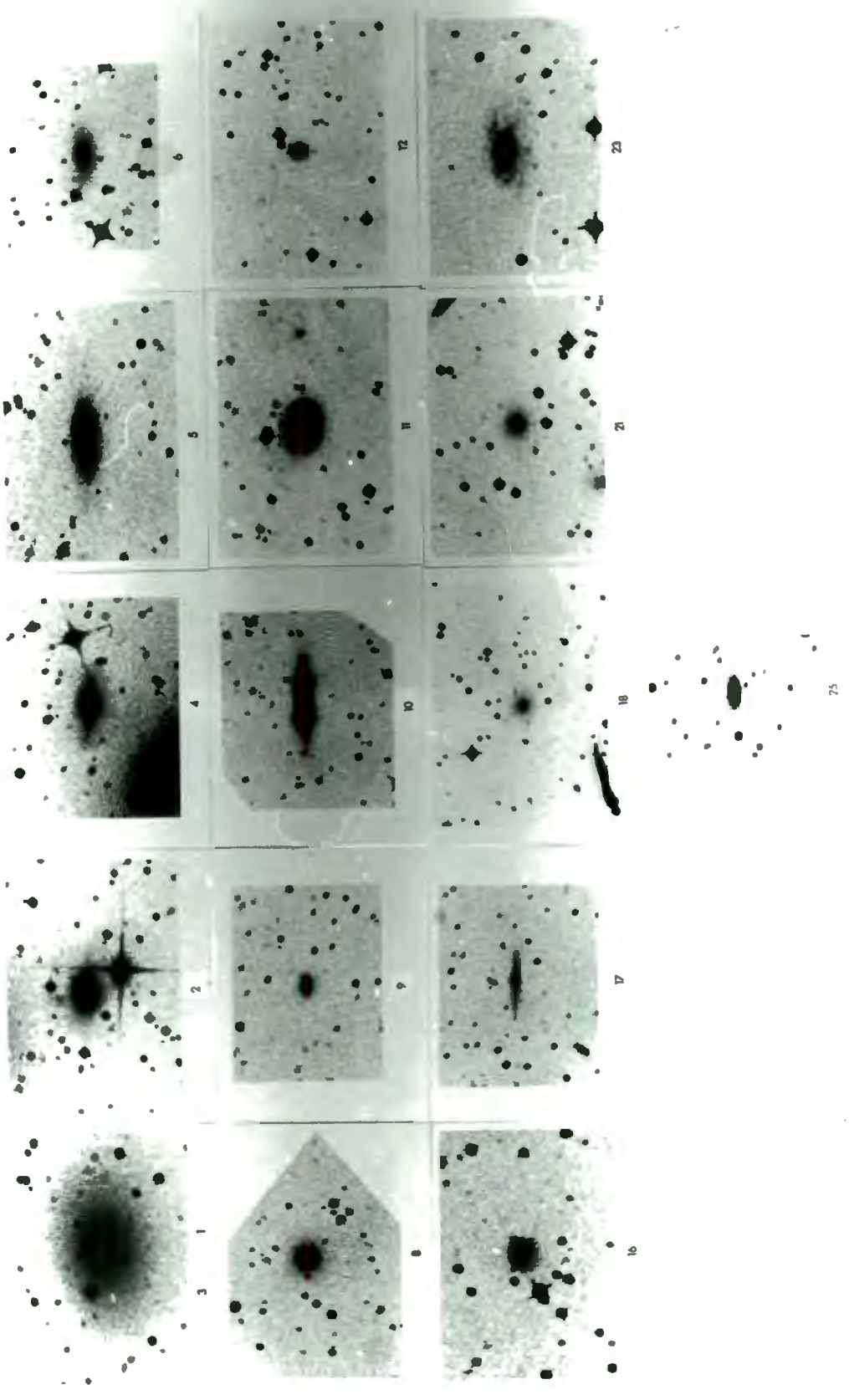
UNIFORM LINEAR SCALE
0 10 20 30 40 50 kpc
GALAXIES FROM THE FAIRALL SURVEY
GALAXIES FROM CLUSTER 1842 633
1
2
3
4
5
6
7
8
9
10
11
12
16
17
18
21
23
25

Plate 57

CHAPTER TWELVE

CONCLUSIONS

This is the first time to the author's knowledge that a major effort has been undertaken to produce a large sample of galaxy photographs of a uniform linear or physical scale.

Not only is the vast range in physical size immediately evident - for type b, from ~11 kpc (IC 1913) to over 200 kpc (NGC 6872) - but of special significance is the great diversity in spiral arm texture, which cannot be appreciated (or seen) on an angular scale. In a nutshell, a nearby galaxy such as M33 is often described as having "characteristically massive arms", but on a linear scale, we have noted (plate 5) that the arms are not massive at all. In contrast, an inspection of the (more distant) spiral NGC 309 in the Hubble Atlas (pg. 32) does not show any particularly massive spiral arms, while here that galaxy ranks as having some of the most massive and well developed arms of all our spirals.

There is a further point, namely that "filamentary" arms are not necessarily thin, as might be supposed; a good case in point is NGC 1232, seen on an angular scale on page 32 of the Hubble Atlas, and on a uniform physical scale in plate 46 of this investigation. It is our viewpoint that the classification scheme we have adopted should provide a far more accurate insight into the true range in spiral arm texture (cf. plate 5). If theoreticians are to meet the problem "head on", they should surely familiarise themselves with this diversity in spiral arm development.

As the situation currently stands, the gap between the observational and theoretical side is very wide; it would be true to say that most theoreticians (on spiral structure) have seldom - if ever - been to a telescope, or know what galaxies at varying redshifts look like. The problem has never been approached from the point of view of using the intrinsic size of a galaxy as a fundamental parameter. Even Professor Lin, whom I admire for his elegant mathematical formulation, writes that

*"Each galaxy is composed of about 10 billion stars. Our galaxy is among the largest"**

[Lin (1974)]

Secondly, and most important, we find the apparent lack of surface brightness considerations surprising; too often the viewpoint is emphasized that "*intrinsically large galaxies are bright; intrinsically small galaxies are faint*". While van den Bergh found that galaxies with long, well developed arms were (generally) much brighter than galaxies with ragged arms, he correctly never in fact wrote that the supergiants were intrinsically larger, but rather intrinsically brighter, than giants. The misunderstanding which has crept in is as a result of neglecting surface brightness. As emphasized in preceeding chapters, even physically small

---

* Interestingly enough, the density wave theory has only been applied to galaxies which are not intrinsically very large. Its success can rather be traced in the opposite direction: galaxies such as NGC 3031 = M81, NGC 5194 = M51, NGC 224 = M31 and NGC 598 = M33 [Roberts, Roberts, and Shu (1975)], with diameters - as listed in table 8 - of 25 kpc, 33 kpc, 35 kpc, and 16 kpc, respectively.

magellanic types - such as NGC 7764 - can be bright. We also have in mind other small, high surface brightness spirals: NGC 7213, for example, with an absolute magnitude comparable to M101, but with a ratio in (projected) diameters of ~55 kpc/ 18 kpc = 3.06.

Moreover, we find that these spirals, with saturated or predominantly saturated images on the IIIa-J Survey, present an inner morphological appearance (chapter ten and accompanying plates) which is generally indicative of substantial differential rotation effects.

Such galaxies have presumably undergone many very differential (and not solid body) rotations; as stressed by Rubin, Ford and Thonnard, any deviation from linearity in the initial rising $V \alpha r$ section of a rotation curve has important ramifications. In the case of M101, for example, one finds a deviation from solid body rotation of $\Delta V \sim 50$ km/s within 2 arc min , or ~4 kpc, from the nucleus*. The time for this differential effect to completely wind round through 360^{o} is $\frac{2\pi r}{\Delta V}$, which here amounts significantly to ~5 x 10^{8} years. This is an order of magnitude calculation, but serves to illustrate the point. It is thus unfortunate that the rotation curves available and used by Kormendy and Norman in their analysis were generally not accurate enough to show how much they did in fact deviate from linearity in this region.

Thirdly, we mention the extensive and featureless outer envelopes often seen in some of our intrinsically

---

* cf. Figure 3 in Kormendy and Norman (1979). We adopt as before a 7.2 Mpc distance to M101.

smaller galaxies. Massive halos are not only *a priori* to be expected if the mass does not converge to a limiting value at the last detected point of optical emission, but rather are required in maintaining warps, as in those edge-on galaxies studied by Sancisi and which do not have bright, close companions.

Warps indeed seem to be present in many galaxies, as shown by empirical rectification or HI observations. In our sample, we refer specifically to A0305-31 (plate 26), whose spiral arms present a most unusual form, which almost certainly do not lie in the same plane. This places further doubts on assigning a unique inclination angle to many well studied galaxies, such as M83 and M33, and hence in the problem of finding diameters corresponding to "face-on" orientation.

Some interesting morphological features are seen on the plates, such as faint outer spiral arms with a completely different pitch angle to those of the bulk of the galaxy. This would necessitate a re-think on the underlying spiral potential needed in the density wave theory.

Another particularly interesting feature is how the surface brightness in a spiral arm can drop so suddenly [cf. NGC 782], with a corresponding change in pitch angle.

Having found no common morphological features on a uniform linear scale, we proceeded to inquire whether the diameter of a galaxy would in any way be correlated to the pitch angle of its spiral arms [in the sense that intrinsically large Sc's, for example, might have a more open spiral pattern, with a corresponding lower value of $\langle\mu\rangle$], or in the number of times the arms wound round the nucleus. Our

conclusion was that [for logarithmic spirals] the difference in intrinsic size was simply reflected in a difference in the scaling factor r_o.

Perhaps the only feature which observationally can be said to be common to the spiral arms rectified by Danver is the tendency for logarithmic spirals to have a pitch angle close to 73^o. To the author's surprise, no mention of this is made in current theoretical studies.

Whenever an arm "forces its way" past 73^o, there appears to be a restoration effect by it "giving birth" to secondary arms whose pitch angles are of the order of 73^o. This is particularly well seen in NGC 4304.

A variation on this theme is where the restoration consists of fragmentation of the arm into small segments, each of which shows an alignment toward $\approx 73^o$; NGC 6753 , for example.

In contrast, in the spiral density wave theory, there is no prediction of a favoured 73^o; both the pitch angle of the arms, and the degree of nonuniform rotation of the disk of a galaxy, are governed by the degree of central mass concentration toward the galactic centre. For $\tilde{\omega}_{0.5M}/\tilde{\omega}_c$ large*, much of the total mass is distributed outside the corotation radius; the arms are predicted to be loosely wound and open. On the other hand, if $\tilde{\omega}_{0.5M}/\tilde{\omega}_c$ is small, the degree of mass concentration inside the corotation radius is high, and the galaxy is expected to have tightly wound arms [cf. Roberts, Roberts and Shu (1975)].

---

* Here, $\tilde{\omega}_c$ denotes the radius where the matter corotates with the spiral wave, while $\tilde{\omega}_{0.5M}$ is the half-mass radius.

A fundamental step in this direction is the classification scheme proposed by van den Bergh (1976), and which is based entirely on disk-to-bulge ratios. Thus, NGC 4866, one of those Sa spirals not having a large nuclear bulge, finds its home in class b, as its disk to bulge ratio is larger than 3†.

While the major *tour de force* of the density wave theory is to alleviate the winding dilemma, there are problems in explaining the persistence of such features for more than a few rotations of the galaxy [cf. the review by Toomre (1977)].

Another interesting theoretical attempt at explaining observed spiral forms is that of Gerola and Seiden (1978, 1979), where aggregates of stars, produced by a chain reaction mechanism, are strung out by a differentially rotating disk. Of particular note is the way the density of stars become greater for earlier Hubble types. While the model attempts to generate multiarmed configurations, these stochastic star formation models have problems with two-armed spirals, and also with spirals which are intrinsically very large.

Yet a third direction has been impressive hydrodynamical calculations of the response of a two dimensional gaseous disk to barlike perturbations. Sanders and Huntley (1976) - also Sørensen, Matsuda and Fujimoto (1976) - showed that this response would be trailing spiral waves, rotating with the same angular speed as that of the central perturbation. It is also possible to simulate the dust lanes seen in the inner regions

---

† Those galaxies with apparent disk-to-bulge ratios in the range 1 to 3 are classed as Sa; those in the range 3 to 10 as Sb, and larger than 10 as Sc.

of barred spirals [Roberts, Huntley and van Albada (1979)].

While the Hubble scheme has very likely a deep cosmogonic meaning [cf. Lequeux (1969)], the author increasingly feels that one of the few parameters which can be measured for a galaxy has, particularly on the theoretical side, been sadly overlooked. It is our hope that in developing future theories on spiral structure, a new recognition and appreciation of the range in intrinsic diameter will be made.

Table 6

List of Southern Galaxies Photographed from Film Copies of the U.K. Schmidt IIIa-J Survey*

	NGC (1)	m (2)	A_B (3)	m^0 (4)	log D_{25} (5)	SB (6)	v (7)	M^0 (8)	D (kpc) (9)
1	148	13.08	0.00	13.08	1.38	23.87	1486	-19.08	18.85
2	406	12.58	0.05	12.53	1.58	24.32	1468	-19.60	29.52
3	418						5684		
4	434	13.13	0.00	13.13	1.29	23.47	4725	-21.54	48.73
5	440						5014		
6	612						9115		
7	613	10.79	0.00	10.79	1.76	23.48	1500	-21.39	45.65
8	646						8230		
9	782						5975		
10	1187	10.93	0.00	10.93	1.70	23.32	1413	-21.12	37.45
11	1201	11.58	0.00	11.58	1.64	23.67	1722	-20.90	39.76
12	1288	12.80	0.00	12.80	1.37	23.54	4495	-21.76	55.73
13	1310						1715		
14	1316C						2065		
15	1317	11.94	0.00	11.94	1.50	23.33	2060	-20.93	34.45
16	1339	12.49	0.00	12.49	1.36	23.18	1326	-19.42	16.07
17	1341	13.18	0.00	13.18	1.20	23.07	1830	-19.43	15.34
18	1350	11.40	0.00	11.40	1.63	23.44	1786	-21.16	40.29
19	1351	12.76	0.00	12.76	1.26	22.95	1491	-19.41	14.35
20	1365	10.14	0.00	10.14	1.99	23.98	1649	-22.24	85.23
21	1374	12.38	0.00	12.38	1.26	22.57	1251	-19.40	12.04
22	1379	12.23	0.00	12.23	1.30	22.62	1386	-19.78	14.63
23	1380	11.10	0.00	11.10	1.69	23.44	1809	-21.49	46.86
24	1380A						1616		
25	1380B						1925		
26	1381	12.72	0.00	12.72	1.46	23.91	1776	-19.83	27.09
27	1387	11.95	0.00	11.95	1.38	22.74	1239	-19.81	15.72
28	1389	12.66	0.00	12.66	1.33	23.20	1076	-18.80	12.17
29	1404	11.20	0.00	11.20	1.39	22.04	1908	-21.50	24.77
30	1411	11.77	0.00	11.77	1.45	22.91	1070	-19.68	15.95
31	1425	11.60	0.00	11.60	1.73	24.14	1628	-20.76	46.24
32	1427	12.05	0.00	12.05	1.45	23.19	1567	-20.22	23.36
33	1437	12.58	0.00	12.58	1.46	23.77	1231	-19.17	18.78
34	1448	11.30	0.00	11.30	1.91	24.74	1182	-20.36	50.81
35	1511	12.20	0.07	12.13	1.52	23.62	1827	-20.48	32.00
36	1531	12.80	0.05	12.75	1.11	22.19	1253	-19.04	8.54
37	1543	11.57	0.06	11.51	1.59	23.35	1400	-20.52	28.81
38	1792	10.85	0.09	10.76	1.60	22.65	1189	-20.91	25.03
39	1879						1248		
40	2082	12.96	0.12	12.84	1.21	22.78	1104	-18.67	9.47
41	2090	11.99	0.15	11.84	1.65	23.98	1805	-20.75	42.64
42	2196	12.10	0.29	11.81	1.44	22.90	2294	-21.29	33.42
43	2397	12.93	0.21	12.72	1.35	23.36	1299	-19.15	15.38
44	2434	12.30	0.23	12.07	1.40	22.96	1477	-20.07	19.62
45	2466						5161		
46	2601						3234		
47	2788						1538		
48	2815	12.66	0.31	12.35	1.55	23.99	2550	-20.98	47.85
49	2865	12.35	0.27	12.08	1.31	22.52	2714	-21.39	29.31
50	3059	11.91	0.37	11.54	1.51	22.98	1223	-20.19	20.93
51	3175	12.20	0.21	11.99	1.68	24.28	1125	-19.57	28.48
52	3241	13.60	0.24	13.36	1.18	23.15	2834	-20.20	22.69
53	3250	12.10	0.38	11.72	1.50	23.11	2833	-21.84	47.38
54	3261	12.16	0.55	11.61	1.61	23.55	2572	-21.74	55.42
55	3308	13.25	0.16	13.09	1.30	23.48	3674	-21.04	38.77

	NGC (1)	m (2)	A_B (3)	m^0 (4)	log D_{25} (5)	SB (6)	v (7)	M^0 (8)	D (kpc) (9)
56	3309	12.90	0.16	12.74	1.28	23.03	4057	-21.60	40.89
57	3312	12.73	0.16	12.57	1.56	24.26	2774	-20.95	53.27
58	3314						3031		
59	3318	12.59	0.39	12.20	1.41	23.14	2910	-21.42	39.56
60	3557	11.40	0.23	11.17	1.60	23.06	3111	-22.60	65.50
61	3564	13.25	0.23	13.02	1.32	23.51	2771	-20.50	30.62
62	3568						2436		
63	3706	12.30	0.20	12.10	1.46	23.29	3045	-21.61	46.45
64	3783	12.89	0.21	12.68	1.28	22.97	3033	-21.02	30.57
65	4105	11.94	0.12	11.82	1.38	22.61	1895	-20.86	24.04
66	4219	12.30	0.27	12.03	1.65	24.17	1978	-20.75	46.73
67	4304	12.75	0.14	12.61	1.38	23.40	2595	-20.76	32.92
68	4835	12.53	0.33	12.20	1.53	23.74	2188	-20.80	39.21
69	4976	11.17	0.44	10.73	1.63	22.77	1369	-21.25	30.89
70	5121	12.46	0.18	12.28	1.36	22.97	1532	-19.95	18.56
71	5140						3728		
72	5161	11.95	0.14	11.81	1.73	24.35	2212	-21.21	62.83
73	5188						2326		
74	5193A						3519		
75	5193	12.58	0.14	12.44	1.25	22.58	3644	-21.67	34.27
76	5236	8.20	0.12	8.08	2.05	22.22	337(☉)**	-20.85	20.00
77	5291						4326		
78	5292						4442		
79	5302	13.20	0.13	13.07	1.23	23.11	3289	-20.81	29.54
80	5304						3683		
81	5328	12.60	0.11	12.49	1.23	22.53	4776	-22.21	42.90
82	5330						4870		
83	5357						4975		
84	5398	12.65	0.15	12.50	1.46	23.69	1272	-19.32	19.40
85	5419						4268		
86	5464						2686		
87	5483	12.09	0.31	11.78	1.49	23.12	1820	-20.82	29.75
88	5556	11.88	0.13	11.75	1.49	23.09	1385	-20.26	22.64
89	5612	13.03	0.33	12.70	1.30	23.09	2764	-20.81	29.17
90	5898	12.60	0.15	12.45	1.24	22.54	2214	-20.58	20.35
91	5903	12.50	0.15	12.35	1.30	22.74	2468	-20.91	26.04
92	5967	12.67	0.33	12.34	1.46	23.53	2904	-21.28	44.30
93	6215	11.79	0.69	11.10	1.30	21.49	1532	-21.12	16.17
94	6221	11.50	0.66	10.84	1.50	22.23	1403	-21.20	23.47
95	6300	11.13	0.41	10.72	1.73	23.26	1140	-20.86	32.38
96	6438	12.50	0.16	12.34	1.41	23.28	2431	-20.89	33.05
97	6699	12.56	0.21	12.35	1.27	22.59	3473	-21.65	34.20
98	6753	11.93	0.18	11.75	1.40	22.64	3103	-22.01	41.22
99	6754	13.16	0.20	12.96	1.34	23.55	3257	-20.90	37.69
100	6758	12.49	0.18	12.31	1.32	22.80	3327	-21.60	36.76
101	6769	12.58	0.16	12.42	1.39	23.26	3903	-21.84	50.67
102	6770	12.88	0.16	12.72	1.39	23.56	3813	-21.49	49.50
103	6771	13.54	0.16	13.38	1.41	24.32	4216	-21.04	57.31
104	6776	12.95	0.15	12.80	1.28	23.09	5696	-22.28	57.40
105	6780	13.15	0.16	12.99	1.28	23.28	3476	-21.02	35.03
106	6782	12.58	0.16	12.42	1.43	23.46	3736	-21.74	53.18
107	6806						5717		
108	6851	12.75	0.12	12.63	1.26	22.82	3034	-21.08	29.20
109	6861	12.10	0.12	11.98	1.43	23.03	2819	-21.56	40.13
110	6861D						2493		
111	6868	11.87	0.11	11.76	1.43	22.80	2763	-21.75	39.33
112	6870	13.15	0.11	13.04	1.40	23.93	2610	-20.34	34.67
113	6872	12.45	0.11	12.34	1.90††	25.73	4701†	-22.32	197.49
114	6876	12.41	0.11	12.30	1.38	23.09	3951	-21.90	50.13
115	6877	13.85	0.11	13.74	1.16	23.43	4132	-20.64	31.59
116	6880						3929		
117	6893	12.29	0.10	12.19	1.45	23.33	3135	-21.59	46.73
118	6907	12.00	0.13	11.87	1.53	23.42	3155	-21.92	56.54

	NGC (1)	m (2)	A_B (3)	m^0 (4)	log D_{25} (5)	SB (6)	v (7)	M^0 (8)	D (kpc) (9)
119	6958	12.21	0.08	12.13	1.38	22.92	2742	-21.36	34.79
120	7014	13.25	0.06	13.19	1.29	23.53	4750	-21.50	48.98
121	7029	12.69	0.06	12.63	1.15	22.27	2818	-20.92	21.05
122	7038	12.36	0.06	12.30	1.48	23.59	4802	-22.40	76.70
123	7041	12.05	0.06	11.99	1.59	23.83	1877	-20.67	38.62
124	7049	11.80	0.06	11.74	1.45	22.88	2158	-21.23	32.17
125	7059	13.16	0.06	13.10	1.50	24.49	1797	-19.47	30.05
126	7083	12.00	0.07	11.93	1.65	24.07	3049	-21.78	72.03
127	7097	12.32	0.04	12.28	1.40	23.17	2404	-20.93	31.94
128	7125	12.84	0.06	12.78	1.50	24.17	3012	-20.91	50.38
129	7126						3009		
130	7135	12.69	0.00	12.69	1.45	23.83	2718	-20.78	40.51
131	7172	12.82	0.00	12.82	1.34	23.41	2651	-20.60	30.67
132	7173	13.05	0.00	13.05	1.10	22.44	2501	-20.24	16.65
133	7174						2778		
134	7176	12.90	0.00	12.90	1.10	22.29	2525	-20.41	16.81
135	7213	11.35	0.00	11.35	1.27	21.59	1769	-21.19	17.42
136	7232						2010		
137	7233						1841		
138	7329	12.32	0.05	12.27	1.62	24.26	3189	-21.55	70.31
139	7361	12.95	0.00	12.95	1.54	24.54	1212	-18.77	22.23
140	7412	11.90	0.00	11.90	1.60	23.79	1705	-20.56	35.90
141	7496						1470		
142	7531	11.97	0.00	11.97	1.54	23.56	1580	-20.32	28.97
143	7552	11.40	0.00	11.40	1.55	23.04	1661	-21.00	31.17
144	7582	11.40	0.00	11.40	1.66	23.59	1452	-20.71	35.10
145	7702	13.14	0.00	13.14	1.28	23.43	6471	-22.21	65.21
146	7796	12.53	0.00	12.53	1.36	23.22	3496	-21.49	42.36
147	1558*						1556		
148	1637*						6002		
149	1876*	14.70	0.00	14.70	0.87	22.94	6546	-20.68	25.66
150	1913*						1287		
151	1970*						1074		
152	2580*						3137		
153	4219*						3647		
154	4299*						4028		
155	4329*	12.55	0.12	12.43	1.51	23.87	4416	-22.10	75.58
156	4351*	12.30	0.12	12.18	1.75	24.82	2761	-21.33	82.12
157	4366*						4609		
158	4721*	12.55	0.24	12.31	1.61	24.25	2095	-20.59	45.14
159	4827*						4301		
160	4831*						4271		
161	4837*	12.78	0.18	12.60	1.44	23.69	2668	-20.83	38.86
162	4842*	13.30	0.16	13.14	1.38	23.93	4049	-21.20	51.37
163	4845*						3823		
164	4852*						4498		
165	4889*	12.20	0.14	12.06	1.42	23.05	2491	-21.22	34.65
166	4960*						3479		
167	4967*						4112		
168	4970*	14.70	0.11	14.59	0.89	22.93	4715	-20.08	19.36
169	5063*	13.05	0.08	12.97	1.28	23.26	3485	-21.04	35.12
170	5135*	13.00	0.00	13.00	1.12	22.49	4842	-21.72	33.76
171	5181*	12.61	0.00	12.61	1.45	23.75	2070	-20.27	30.86
172	5201*	11.31	0.00	11.31	1.93	24.85	2112	-21.61	95.07
173	5240*	12.26	0.00	12.26	1.51	23.70	1503	-19.92	25.72
174	5267*	11.40	0.00	11.40	1.70	23.79	1715	-21.07	45.46
	Anonymous								
175	A0031-31						1586		
176	A0112-32						5262		
177	A0113-32						6041		
178	A0253-27						5272		

NGC (1)	m (2)	A_B (3)	m^0 (4)	log D_{25} (5)	SB (6)	v (7)	M^0 (8)	D (kpc) (9)
Anonymous								
179 A0305-31						4907		
180 A0644-74						6466		
181 A0922-24						2413		
182 A1018-37						7633		
183 A1034-27A						4698		
184 A1125-36						2976		
185 A1213-34						7741		
186 A1234-72						7125		
187 A1332-33						3834		
188 A1335-33						3826		
189 A1345-30						5235		
190 A1427-34						3014		
191 A1515-23	14.60	0.15	14.45	0.75	22.09	2340	-18.70	6.96
192 A1517-36						3069		
193 A1829-41						5794		
194 A1903-61						4219		
195 A1957-47A						6410		
196 A1957-47B						6760		
197 A2004-29						6986		
198 A2015-39						2719		
199 A2100-48						5260		
200 A2101-48						4812		
201 A2102-47						4944		
202 A2103-47						5163		
203 A2125-38						2567		
204 A2152-69						8225		
205 A2207-46						2692		

Notes to Table

Col. 1 contains the galaxy's NGC, IC or A designation. Arranged in order of increasing NGC number, and IC number. * = IC.

Col. 2 lists the B_T (or m_c) apparent magnitude [when available from the RC2 (1976)].

Col. 3 contains the correction for foreground galactic absorption [cf. chapter 3, section 2, eqn. (3.9)], with the corrected apparent magnitude m^0 listed in *Col. 4*.

Col. 5 is from the RC2 (1976) [for those galaxies which have listed B_T (or m_c) apparent magnitudes]. Units are 0.1. The surface brightness SB, in mag arc sec^{-2}, follows using columns 4 and 5, and is given in *Col. 6*.

Col. 7 The velocity (heliocentric) used in printing each photograph is listed; these are from the RC2 (1976), or from Sandage (1978). For a discussion of the velocities, see chapter 2, section 4.

Col. 8 contains the absolute magnitude, corrected for foreground galactic absorption but not for inclination effects. The values, computed using columns 4 and 7 in equation (3.12), are based on H_o = 55 km s^{-1} Mpc^{-1}.

Col. 9 Finally, in we present the de Vaucouleurs diameter - in kpc [using columns 5 and 7 and equation (3.14)]. The exception is NGC 6872 (no. 113), where the diameter corresponds to a limiting surface brightness of ∿25.5 B mag $arcsec^{-2}$.

Remarks

** For NGC 5236 = M83, we use the RC2 v_0 value of 337 km s^{-1}. This then yields a distance to the NGC 5128 group of ∿6 Mpc, in agreement with Tammann (1977).

† This is the RC2 value; Sandage (1978) gives an almost identical velocity of v = 4737 km s^{-1}.

†† The value here is strictly log $D_{25.5}$, and not log D_{25}. We adopt a value of 8 arc min for NGC 6872 on the J-survey.

* SHIPMENTS 1-5, and preliminary shipment.

Table 7

Galaxies Photographed Primarily from Shipment 6

(not included in table 6)

	Galaxy NGC (1)	v (2)
1	986	2058
2	2369	3296
3	3136	1691
4	5135	4157
5	7764	1704
6	2554*	1367
7	F-275	6330†

Notes to Table 7

* = IC

† Redshift from Fairall (1980b)

Table 8

Denver Spirals* with known Apparent Magnitudes and Distance Moduli (or v_o)

	NGC (1)	m (2)	A_B (3)	m^o (4)	log D_{25} (5)	SB (6)	v_o (7)	M^o (8)	D (kpc) (9)
1	151	12.28	0.00	12.28	1.57	24.02	3746	-21.89	73.61
2	224=M31	4.36	0.23	4.13	3.25	24.27	679kpc†	-20.03	35.13
3	300	8.70	0.00	8.70	2.30	24.09	μ=26.9†	-18.20	13.92
4	578	11.50	0.00	11.50	1.68	23.79	1675†	-20.92	42.40
5	598=M33	6.26	0.12	6.14	2.79	23.98	μ=24.76†	-18.62	16.05
6	613	10.79	0.00	10.79	1.76	23.48	1462	-21.33	44.49
7	628	9.75	0.05	9.70	2.01	23.64	861†	-21.28	46.60
8	772	11.10	0.07	11.03	1.85	24.17	2562	-22.31	95.93
9	877	12.50	0.06	12.44	1.37	23.18	4117	-21.93	51.04
10	895	12.30	0.00	12.30	1.56	23.99	2319	-20.82	44.53
11	908	10.85	0.00	10.85	1.74	23.44	1470	-21.28	42.72
12	958	12.95	0.00	12.95	1.44	24.04	5756	-22.15	83.85
13	1022	12.20	0.00	12.20	1.40	23.09	1505	-19.99	19.99
14	1042	11.50	0.00	11.50	1.67	23.74	1360	-20.47	33.64
15	1058	12.15	0.25	11.90	1.48	23.19	674	-18.54	10.77
16	1068	9.51	0.00	9.51	1.84	22.60	1134	-22.06	41.49
17	1084	11.22	0.00	11.22	1.46	22.41	1406	-20.82	21.45
18	1087	11.55	0.00	11.55	1.54	23.14	1844	-21.08	33.82
19	1090	12.60	0.00	12.60	1.58	24.39	2835+	-20.96	57.01
20	1097	10.25	0.00	10.25	1.97	23.99	1227	-21.49	60.56
21	1177	10.93	0.00	10.93	1.70	23.32	1334	-20.99	35.36
22	1232	10.50	0.00	10.50	1.89	23.84	1644	-21.88	67.49
23	1300	11.10	0.00	11.10	1.81	24.04	1422	-20.96	48.56
24	1309	12.00	0.00	12.00	1.37	22.74	2195	-21.01	27.21
25	1385	11.65	0.00	11.65	1.48	22.94	1968†	-21.12	31.43
26	2403	8.85	0.14	8.71	2.25	23.85	259	-19.65	24.36
27	2835	10.95	0.28	10.67	1.80	23.56	617	-19.58	20.59
28	2903	9.50	0.06	9.44	2.10	23.83	467	-20.20	31.09
29	2964	12.05	0.04	12.01	1.47	23.25	1261	-19.79	19.68
30	2997	10.60	0.33	10.27	1.91	23.72	799†	-20.54	34.35
31	3031=M81	7.75	0.07	7.68	2.41	23.62	3.3Mpc†	-19.91	24.67
32	3147	11.45	0.08	11.37	1.60	23.27	2881	-22.22	60.66
33	3184	10.40	0.00	10.40	1.84	23.49	607†	-19.81	22.21
34	3198	10.94	0.00	10.94	1.92	24.43	691	-19.56	30.40
35	3351	10.50	0.00	10.50	1.87	23.74	673	-19.94	26.39
36	3367	12.05	0.00	12.05	1.37	22.79	2906†	-21.56	36.03
37	3511	11.56	0.11	11.45	1.73	23.99	976	-19.79	27.72
38	3512	13.00	0.00	13.00	1.23	23.04	1352	-18.95	12.14
39	3513	11.99	0.11	11.88	1.44	22.97	845†	-19.05	12.31
40	3627	9.70	0.00	9.70	1.94	23.29	583	-20.43	26.86
41	3756	12.15	0.00	12.15	1.64	24.24	1159	-19.47	26.76
42	3893	11.10	0.00	11.10	1.64	23.19	1034	-20.27	23.87
43	3938	10.91	0.00	10.91	1.73	23.45	838	-20.00	23.80
44	4030	11.07	0.00	11.07	1.63	23.11	1255	-20.72	28.31
45	4088	11.10	0.00	11.10	1.76	23.79	822	-19.77	25.02
46	4145	11.50	0.00	11.50	1.76	24.19	1035	-19.87	31.50
47	4151	11.13	0.00	11.13	1.77	23.87	1002	-20.17	31.21
48	4156	13.85	0.00	13.85	1.19	23.69	6797	-21.61	55.68
49	4254	10.42	0.00	10.42	1.73	22.96	1100†	-21.09	31.24
50	4303	10.21	0.00	10.21	1.78	23.00	1100†	-21.30	35.06
51	4321=M100	10.10	0.00	10.10	1.84	23.19	1100†	-21.41	40.25
52	4501	10.27	0.00	10.27	1.84	23.36	1100†	-21.24	40.25
53	4504	11.92	0.00	11.92	1.60	23.81	939	-19.00	17.67
54	4535	10.66	0.00	10.66	1.83	23.70	1853	-21.98	66.26
55	4567	12.08	0.00	12.08	1.47	23.32	1100†	-19.43	17.17
56	4593	11.72	0.00	11.72	1.60	23.61	2560	-21.62	53.90
57	4736	8.85	0.00	8.85	2.04	22.94	345†	-20.14	20.01
58	4826	9.35	0.00	9.35	1.97	23.09	377	-19.83	18.61
59	4899	12.61	0.04	12.57	1.43	23.61	2437†	-20.67	34.69
60	5055	9.30	0.00	9.30	2.09	23.64	587	-20.84	38.19
61	5068	10.53	0.07	10.46	1.84	23.55	402	-18.86	14.71
62	5085	11.94	0.08	11.86	1.53	23.40	1720†	-20.62	30.82
63	5194=M51	8.95	0.00	8.95	2.04	23.04	565	-21.11	32.77
64	5236=M83	8.20	0.12	8.08	2.05	22.22	337	-20.85	20.00
65	5247	11.10	0.06	11.04	1.73	23.58	1511	-21.15	42.92

Table 8 (cont.)

	NGC (1)	m (2)	A_B (3)	m^o (4)	log D_{25} (5)	SB (6)	v_o (7)	M^o (8)	D (kpc) (9)
66	5364	11.05	0.00	11.05	1.85	24.19	1349	-20.90	50.51
67	5457=M101	8.20	0.00	8.20	2.43	24.24	396	-21.09	56.37
68	5595	12.69	0.07	12.62	1.31	23.06	2501†	-20.67	27.01
69	5597	12.60	0.07	12.53	1.31	22.97	2444†	-20.71	26.39
70	5676	11.60	0.00	11.60	1.59	23.44	2363	-21.57	48.62
71	5678	12.08	0.00	12.08	1.51	23.52	2391	-21.11	40.92
72	5859	13.25	0.00	13.25	1.47	24.49	4735	-21.42	73.91
73	5921	11.45	0.05	11.40	1.69	23.75	1503	-20.78	38.93
74	5985	11.80	0.05	11.75	1.74	24.34	2671	-21.68	77.63
75	6412	12.35	0.12	12.23	1.37	22.97	1650	-20.16	20.46
76	6643	11.75	0.15	11.60	1.59	23.44	1736	-20.89	35.72
77	6946	9.63	0.52	9.11	2.04	23.20	338	-19.83	19.60
78	7309	13.05	0.00	13.05	1.33	23.59	4086	-21.30	46.20
79	7331	10.35	0.24	10.11	2.03	24.15	1105	-21.41	62.62
80	7424	10.98	0.00	10.98	1.88	24.27	850	-19.97	34.10
81	7479	11.70	0.06	11.64	1.61	23.58	2604	-21.74	56.11

Remarks to Table 8

Columns (1) - (9) are as in table 6, expect that here col. (7) contains v_o and not v. The author is indebted to Prof. Tammann for providing all velocities marked by a †, and for the RSA distance moduli μ.

* All those galaxies with measured pitch angles and winding angles as listed in appendix III of Danver (1942).

REFERENCES

Allen, R.J., and Shu, F.H.: 1979, *Ap. J., 227*, 67.

Arp, H.: 1973, in "The Redshift Controversy" (ed. Field, G.B.) W.A. Benjamin Inc., London, p. 38.

Baade, W.: 1944, *Ap. J., 100*, 137.

Baade, W.: 1951, *Publ. Obs. Univ. Michigan, 10*, 7.

Baade, W., and Minkowski, R.: 1954, *Ap. J., 119*, 215.

Baade, W., 1963, "Evolution of Stars and Galaxies" (ed. C. Payne-Gaposchkin), Harvard University Press.

Balkowski, C., Bottinelli, L., Chameraux, P., Gougouenheim, L., and Heidmann, J.: 1974, *Astron. Astrophys. 34*, 43.

Biometrika Tables for Statisticians.

Block, D.L.: 1974, *Quart. J. Roy. Astron. Soc., 15*, 264.

Block, D.L.: 1979, *Astron. Astrophys. 79*, L22.

Bottinelli, L., and Gougouenhein, L.: *Astron. Astrophys. 74*, 172.

Brosche, P.: 1971, *Astron. Astrophys. 13*, 293.

Bunner, A.N., and Sanders, W.T.: 1978, *Bull. AAS., 10*, 663.

Burbidge, E.M., and Burbidge, G.R.: 1972, *Ap. J. 171*, 253.

Burnstein, D., and Heiles, C.: 1979, unpublished.

Cannon, R.D.: 1976, in "The Galaxy and the Local Group" (RGO Bulletin No. 182), p. 283.

Capaccioli, M., and Fasano, G.: 1980, *Astron. Astrophys. 83*, 354.

Danver, C.G.: 1942, Lund Obs. Ann. *10*.

Demarque, P., and McClure, R.D.: 1977, "The Evolution of Galaxies and Stellar Populations" (ed. Tinsley, B.M. and Larson, R.B.), p. 199.

Dressler, A., and Sandage, A.: 1978, *P.A.S.P., 90*, 5.

Dufour, R.J., van den Bergh, S., Harvel, C.A., Martins, D.H., Schiffer, F.H., Talbot, R.J., Talent, D.L., and Wells, D.C.: 1979, *Astron. J. 84*, 284.

Dzigvashvili, R.M., and Borchkhadze, T.M.: "The Spiral Structure of our Galaxy" (ed. Becker, W. and Contopoulos, G.), D. Reidel, Dordrecht, p. 41.

Eddington, A.S.: 1914, "Stellar Movements and the Structure of the Universe", MacMillan, London, p. 172.

Ellis, G.F.R.: 1971, "Relativistic Cosmology" in "General Relativity and Cosmology", ed. Sachs, R.K. Rendiconti Scuolo Enrico Fermi, XLVIII Corso, Academic Press, New York.

Ellis, G.F.R.: 1979, *Gen. Rel. and Gravitation, 11*, 281.

Ellis, G.F.R.: 1980, *Annals N.Y. Acad. Sci., 336*, 130.

Evans, D.S.: 1957, "Cape Photographic Atlas of Southern Galaxies" [Royal (Cape) Observatory]

Fairall, A.P.: 1979a, *Mon. Not. Roy. Astron. Soc., 188*, 343.

Fairall, A.P.: 1979b, *Mon. Not. Roy. Astron. Soc., 188*, 349.

Fairall, A.P.: 1980a, *Mon. Not. Roy. Astron. Soc., 191*, 391.

Fairall, A.P.: 1980b, *Mon. Not. Roy. Astron. Soc.*, in press.

Fisher, J.R., and Tully, R.B.: 1975, *Astron. Astrophys. 44*, 151.

Freeman, K.C.: 1970, *Ap. J., 160*, 811.

Freund, J.E.: 1971, "Mathematical Statistics", Prentice-Hall.

Gerola, H., and Seiden, P.E.: 1978, *Ap. J., 223*, 129.

Graham, J.A., and Rubin, V.C.: 1973, *Ap. J., 183*, 19.

Graham, J.A.: 1974, *Observatory, 94*, 290.

Hainebach, K.L., and Schramm, D.N.: 1976, *Ap. J. Lett., 207*, L79.

Hawarden, T.G.: 1979, private communication.

Hawkins, G.S.: 1962, *Nature, 194*, 563.

Heidmann, J.: 1967, *C.R. Acad. Sci. 265B*, 866.

Heidmann, J.: 1969a, *Astrophys. Lett. 3*, 19.

Heidmann, J.: 1969b, *C.R. Acad. Sci. 268B*, 1782.

Heidmann, J.: 1970, *C.R. Acad. Sci. 271B*, 658.

Heidmann, J., Heidmann, N., and de Vaucouleurs, G.: 1972, *Mem. Roy. Astron. Soc. 76*, 85, 105, 121.

Holmberg, E.: 1946, *Medd. Lund. Obs. Ser. 2*, No. 117.

Holmberg, E.: 1958, *Medd. Lund. Obs. Ser. 2*, No. 136.

Holmberg, E.: 1964, *Ark. Astr. 3*, 387.

Holmberg, E.: 1975, in "Galaxies and the Universe" (ed. Sandage, A., Sandage, M., and Kristian, J.), Univ. Chicago Press, Chicago.

Hubble, E.: 1926, *Ap. J., 64*, 321.

Hubble, E.: 1936, "The Realm of the Nebulae", Yale University Press.

Huchtmeier, W.K., Tammann, G.A., and Wendker, H.J.: 1977, *Astron. Astrophys. 57*, 313.

Huchtmeier, W.K., and Witzel, A.: 1979, *Astron. Astrophys. 74*, 138.

Humason, M.L., and Wahlquist, H.D.: 1955, *Astron. J. 60*, 254.

Jones, J.E., and Jones, B.J.T.: 1980, *Mon. Not. Roy. Astron. Soc. 191*, 685.

Kennicutt, R.C.: 1979, *Ap. J. 228*, 696.

Klemola, A.R.: 1969, *Astron. J. 74*, 804.

Kormendy, J.: 1979, *Ap. J., 227*, 714.

Kormendy, J., and Norman, C.A.: 1979, *Ap. J., 233*, 539.

Lequeux, J.: 1969, "Structure and Evolution of Galaxies", Gordon and Breach, New York.

Lewis, B.M.: 1968, *Proc. Astr. Soc. Australia, 1*, 104.

Liller, M.: 1960, *Ap. J. 132*, 306.

Liller, M.: 1966, *Ap. J. 146*, 28.

Lin, C.C.: 1974 in "Mathematics Applied to Deterministic Problems in the Natural Sciences" (ed. Lin, C.C. and Segel, L.A.), MacMillan, New York.

Lin, C.C., and Shu, F.H.: 1964, *Ap. J. 140*, 646.

Longmore, A.J., Hawarden, T.G., Cannon, R.D., Allen, D.A., Mebold, U., Goss, W.M., and Reif, K.: 1979: *Mon Not. Roy. Astron. Soc., 188*, 285.

Lundmark, K.: 1926, *Ark. Mat. Astron. Fys., Ser. B., 19*, No. 8.

Lundmark, K.: 1927, *Medd. Astron. Obs. Uppsala*, No. 30.

Malmquist, K.G.: 1920, *Medd. Lund Obs. Ser. 2*, No. 22.

Matthews, T.A., Morgan, W.W., and Schmidt, M.: 1964, *Ap. J., 140*, 35.

Moore, P.: 1970, "Atlas of the Universe", Mitchell Beazley, London.

Oemler, A.: 1976, *Ap. J., 209*, 693.

Phillips, M.M., and Frogel, J.A.: 1980, *Ap. J., 235*, 761.

Reiz, A.: 1941, *Ann. Lund. Obs., 9*, 48.

Reynolds, J.H.: 1927, *Observatory, 50*, 185.

Roberts, M.S.: 1978, *Astron. J., 83*, 1026.

Roberts, W.W., Roberts, M.S., and Shu, F.H.: 1975, *Ap. J., 196*, 381.

Roberts, W.W., Huntley, J.M., and van Albada, G.D.: 1979, *Ap. J. 233*, 67.

Rogstad, D.H., Lockhart, I.A., and Wright, M.C.H.: 1974, *Ap. J., 193*, 309.

Rubin, V.C.: 1974, *Ap. J., 191,* 645.

Rubin, V.C., Ford, W.K., and Thonnard, N.: 1978, *Ap. J. Lett. 225,* L107.

Rubin, V.C., Ford, W.K., and Thonnard, N.: 1980, preprint. [*Ap. J.* (in press)].

Sancisi, R.: 1976, *Astron. Astrophys. 53,* 159.

Sancisi, R.: 1977, "Topics in Interstellar Matter" (ed. van Woerden, H.) - Dordrecht: D. Reidel.

Sandage, A.: 1961, "Hubble Atlas of Galaxies" (Carnegie Institution of Washington), Publication 618.

Sandage, A.: 1972, *Ap. J. 173,* 485.

Sandage, A.: 1973, *Ap. J. 183,* 711.

Sandage, A.: 1975a, in "Galaxies and the Universe" (ed. Sandage, A., Sandage, M., and Kristian, J.), University of Chicago Press, Chicago.

Sandage, A.: 1975b, *Ap. J., 202,* 563.

Sandage, A.: 1978, *Astron. J. 83,* 904.

Sandage, A. and Dressler, A.: 1978, see Dressler and Sandage (1978).

Sandage, A. and Humphreys, R.M.: 1980, *Ap. J. Lett., 236,* L1.

Sandage, A., and Tammann, G.A.: 1974a, *Ap. J. 190,* 525 (Paper I).

Sandage, A., and Tammann, G.A.: 1974b, *Ap. J., 191,* 603 (Paper II).

Sandage, A., and Tammann, G.A.: 1974c, *Ap. J., 194,* 223 (Paper III).

Sandage, A., and Tammann, G.A.: 1974d, *Ap. J., 194,* 559 (Paper IV).

Sandage, A., and Tammann, G.A.: 1975a, *Ap. J., 196,* 313, (Paper V).

Sandage, A., and Tammann, G.A.: 1975b, *Ap. J., 197,* 265, (Paper VI).

Sandage, A., and Tammann, G.A.: 1976, *Ap. J., 210,* 7 (Paper VII).

Sandage, A., and Tammann, G.A.: 1980, "Revised Shapley Ames Catalogue" (Carnegie Institute of Washington, in press).

Sandage, A., and Visvanathan, N.: 1978, *Ap. J. 223,* 707.

Sandage, A., Tammann, G.A., and Yahil, A.: 1979a, *Ap. J. 232,* 352.

Sanders, R.H., and Huntley, J.M.: 1976, *Ap. J. 209,* 53.

Schechter, P.: 1976, *Ap. J., 203,* 297.

Segal, I.: 1975, *Proc. Nat. Acad. Sci., 72,* 2473.

Seiden, P.E., and Gerola, H.: 1979, *Ap. J. 233,* 56.

Sérsic, J.L.: 1966, *Z.f. Astrophys. 64,* 202.

Sérsic, J.L.: 1968, "Atlas de Galaxias Australes" - Observatorio Astronómico Universidad Nacional de Córdoba, Córdoba, Argentina.

Sérsic, J.L.: 1979, *Observatory, 99,* 48.

Sérsic, J.L., and Pastoriza, M.: 1965, *P.A.S.P. 77,* 287.

Sérsic, J.L., and Pastoriza, M.: 1967, *P.A.S.P. 79,* 152.

Sørenson, S.A., Matsuda, T., and Fujimoto, M.: 1976, *Astrophys. Sp. Sci. 43,* 491.

Sulentic, J.W.: 1977, *Ap. J. Lett.* L59.

Talbot, R.J., Jensen, E.B., and Dufour, R.J.: 1979, *Ap. J., 229,* 91.

Tammann, G.A.: 1976, in "The Galaxy and the Local Group" (ed. Dickens, R.J. and Perry, J.E.), RGO Bulletin No. 182, p. 135.

Tammann, G.A.: 1977, *Mitt. Astron. Gesell.* Nr. 42, 42.

Tammann, G.A.: 1980, Lectures delivered at the South African Astronomical Observatory.

Tammann, G.A., Yahil, A., and Sandage, A.: *Ap. J. 234*, 775.

Tammann, G.A., Sandage, A., and Yahil, A.: 1979c, "The Determination of Cosmological Parameters", preprint of the Astron. Institute of the Univ. of Basel, No. 1.

Tammann, G.A., Sandage, A., and Yahil, A.: 1980, *Physica Scripta, 21*, 630.

Tinsley, B.M.: 1975, *P.A.S.P., 87*, 837.

Toomre, A., and Toomre, J.: 1972, *Ap. J. 178*, 623.

Toomre, A.: 1977, *Ann. Rev. Astr. Ap. 15*, 437.

Tritton, S.B.: 1978, *Proc. Astronomical Soc. Australia, 3*, Nr. 3, 206.

Tubbs, A.D., and Sanders, R.H.: 1979, in "Photometry, Kinematics and Dynamics of Galaxies" (ed. Evans, D.S., University of Texas).

Tully, R.B.: 1972, *Mon. Not. Roy. Astron. Soc. 159*, 35P.

Tully, R.B., and Fisher, J.R.: 1977, *Astron. Astrophys. 54*, 661.

van den Bergh, S.: 1960a, *Ap. J. 131*, 215.

van den Bergh, S.: 1960b, *Ap. J. 131*, 558.

van den Bergh, S.: 1966, *Astron. J. 71*, 922.

van den Bergh, S.: 1976, *Ap. J. 206*, 883.

van den Bergh, S.: 1980, preprint.

de Vaucouleurs, G.: 1959, "Handbuch der Physik" (Springer Verlag: Berlin), *53*, 275.

de Vaucouleurs, G.: 1963, *Ap. J. Supp. 8*, No. 74, 31.

de Vaucouleurs, G.: 1979a, *Ap. J. 227*, 380.

de Vaucouleurs, G.: 1979b, *Ap. J. 227*, 729.

de Vaucouleurs, G., and de Vaucouleurs, A.: 1964, "Reference Catalogue of Bright Galaxies" [RC1] (University Texas Press: Austin).

de Vaucouleurs, G., de Vaucouleurs, A., and Corwin, H.G.: 1976, "Second Reference Catalogue of Bright Galaxies" [RC2], (University Texas: Austin).

de Vaucouleurs, G., and Bollinger, G.: 1979, *Ap. J. 233*, 433.

Wilson, A.G.: 1955, *P.A.S.P., 67*, 27.

Wood, R., and Andrews, P.J.: 1974, *Mon. Not. Roy. Astron. Soc. 167*, 28.

Yahil, A., Tammann, G.A., and Sandage, A.: 1977, *Ap. J., 217*, 903.